DESIGN AND IMPLEMENTATION OF A LUMINESCENCE EMISSION SPECTROMETER

A THESIS SUBMITTED TO
THE GRADUATE SCHOOL NATURAL AND APPLIED SCIENCES
OF
MIDDLE EAST TECHNICAL UNIVERSITY

BY

EVREN TOGAY

IN PARTIAL FULFILLMENT OF THE REQUIREMENTS
FOR
THE DEGREE OF MASTER OF SCIENCE
IN
PHYSICS

FEBRUARY 2012

Approval of the thesis:

DESIGN AND IMPLEMENTATION OF A LUMINESCENCE EMISSION SPECTROMETER

submitted by **EVREN TOGAY** in partial fulfillment of the requirements for the degree of **Master of Science in Physics Department, Middle East Technical University** by,

Prof. Dr. Canan Özgen
Dean, Graduate School of **Natural and Applied Sciences** _____

Prof. Dr. Mehmet T. Zeyrek
Head of Department, **Physics** _____

Assoc. Prof. Dr. Enver Bulur
Supervisor, **Physics Dept., METU** _____

Examining Committee Members:

Prof. Dr. Güneş Tanır
Physics Dept., Gazi University _____

Assoc. Prof. Dr. Enver Bulur
Physics Dept., METU _____

Prof. Dr. Hamit Yurtseven
Physics Dept., METU _____

Prof. Dr. Nizami Hasanli
Physics Dept., METU _____

Assoc. Prof. Dr. Akif Esendemir
Physics Dept., METU _____

Date: 09/02/2012

I hereby declare that all information in this document has been obtained and presented in accordance with academic rules and ethical conduct. I also declare that, as required by these rules and conduct, I have fully cited and referenced all material and results that are not original to this work.

Name, Last name: EVREN TOGAY

Signature :

ABSTRACT

DESIGN AND IMPLEMENTATION OF A LUMINESCENCE EMISSION SPECTROMETER

Togay, Evren

M.Sc., Department of Physics

Supervisor: Assoc. Prof. Dr. Enver Bulur

February 2012, 121 pages

Luminescence is the emission of light resulting from radiative transition of an atom from an excited state to a ground state. This radiative transition yields emission of photons and the luminescence is the general name which is used to classify "cold emission" other than the blackbody radiation. Spectroscopy involves the measurement of intensity of emitted, absorbed or scattered electromagnetic radiation as a function of wavelength. Thus, it is a valuable tool in the study of understanding the luminescence production mechanisms. Measurement of emission spectra gives information about the energy levels of transition and structure, geometry and composition of the sample. In this study, a versatile luminescence emission spectrometer was designed and developed with the main aim of measuring Photoluminescence (PL), Thermoluminescence (TL) and Optically Stimulated Luminescence (OSL) emission spectra of materials relevant for dosimetry. The spectrometer was constructed around a Littrow type monochromator by developing the necessary hardware, firmware and software. Wavelength calibration, measurement of spectral response and determination of resolution of the spectrometer were done using calibration lamps and a calibrated spectroradiometer. Finally the performance of the constructed spectrometer was tested by measuring the

emission spectra of materials such as BeO, Al_2O_3 and CaF_2 wherever possible the measured spectra were compared with the ones reported in the literature.

Keywords: Spectroscopy, Emission Spectrometer, Photoluminescence (PL), Optically Stimulated Luminescence (OSL), Thermoluminescence (TL).

ÖZ

LÜMİNESANS EMİSYON SPEKTROMETRESİ TASARIMI VE GERÇEKLEŞTİRİLMESİ

Togay, Evren

Yüksek Lisans, Fizik Bölümü

Tez Yöneticisi: Doç. Dr. Enver Bulur

Şubat 2012, 121 sayfa

Lüminesans atomun ışınımsal şekilde yüksek enerji seviyesinden düşük enerji seviyesine geçişi neticesinde ortaya çıkan ışık yayılımıdır. Atomun bu geçişi foton salımı ile gerçekleşir ve lüminesans bu geçişler neticesinde gözlenen 'soğuk emisyon'a (karacisim ışımasından farklı) verilen genel bir isimdir. Spektroskopi ise yayılan, soğurulan ya da saçılan elektromanyetik ışımanın şiddetinin ışımanın dalgaboyuna göre ölçülmesine dayanır. Bu nedenle lüminesans üretim mekanizmalarının anlaşılması için yapılan çalışmalarda kullanılan değerli bir araçtır. Emisyon spektrumlarının ölçülmesi geçiş enerji seviyeleri, örneğin yapısı, geometrisi ve bileşenleri hakkında bilgi verir. Bu çalışmada, radyasyon dozimetrisi için uygun malzemelerin Fotolüminesans (PL), Termolüminesans (TL) ve Optik Uyarmalı Lüminesans (OSL) emisyonlarının ölçülüp çözümlenebilmesi için çok yönlü bir lüminesans emisyon spektrometresi tasarlanmış ve geliştirilmiştir. Bu spektrometre, Littrow tipi bir monokromatör etrafında gerekli donanım ve yazılım geliştirilerek tasarlanıp gerçekleştilirmiştir. Kalibrasyon lambaları ve kalibre edilmiş bir spektroradyometre cihazı kullanılarak dalgaboyu kalibrasyonu, spektrometrenin tayfsal tepkisinin ölçülmesi ve çözünürlüğünün belirlenmesi işlemleri gerçekleştirilmiştir. Sistemin genel performansını test etmek amacıyla BeO, Al_2O_3 ve

CaF_2 gibi çeşitli malzemelerin emisyon spektrumları ölçülmüş ve sonuçları literatürde yayınlanmış ölçümler ile karşılaştırılmıştır.

Anahtar Kelimeler: Spektroskopi, Emisyon Spektrometresi, Fotolüminesans (PL), Optik Uyarmalı Lüminesans (OSL), Termolüminesans (TL).

To my family

ACKNOWLEDGEMENTS

First and foremost, I would like to express my endless thanks and gratitude to my mother Nermin Togay and my father Emre Togay for their love, patience, encouragement and limitless support throughout this thesis work. I could always overcome the most troublesome and tiring times by the help of them. Thus, without them, none of what I have achieved would have been possible.

Next, I would like to thank my advisor, Assoc. Prof. Dr. Enver Bulur, for his advice and guidance through my thesis work.

I wish to thank my dear friend Mahmut Emre Yağcı for being always ready to help, for sharing with me his valuable ideas and of course for his friendship. It is impossible to forget the times that we worked in the laboratory up to midnight.

I want to extend my sincere thanks to Özden Keskin for her understanding, help and support throughout my thesis work.

I wish to thank Assoc. Prof. Dr. Hakan Altan and Dr. Halil Berberoğlu for their help and support.

I wish to thank my dear friends Turgut Aydemir and Nazmi Sedefoğlu. They always like brother for me.

Finally, I wish to thank technicians Yücel Eke, Mustafa Yıldırım and Muharrem Kuzu from Physics Department for their help.

TABLE OF CONTENTS

LIST OF FIGURES

FIGURES

LIST OF TABLES

TABLES

CHAPTER 1

INTRODUCTION

Spectroscopy examines matter when it interacts with electromagnetic radiation via absorption, emission and scattering of electromagnetic radiation. It is used in analyzing these interactions through investigating the matter according to which wavelength of light is being absorbed, emitted or scattered.

Spectrum can be defined as to make a display out of something. It shows the functional relationship between two things generally as a graph. It was first proposed by Isaac Newton. Newton suggested an idea that white light is composed of various colored light (Ball, 2001). However, the nature of light, both theoretically and experimentally, could not be illuminated until eighteenth century. In 1801 English scientist Thomas Young performed double slit experiment and demonstrated the well-known phenomena of interference of light, proving that light must be a wave. In December 1900 German physicist Max Planck was first suggested quantum mechanical behavior of light. In 1905, Einstein postulated on particle behavior of light. He explained the photoelectric effect and concluded with the idea that light is acting like a particle of energy and the word “photon” was used to describe it. Moreover, Arthur Compton, in 1923, discovered that photons have momentum in addition to energy with the experiment on scattering of X-rays.

In 1925 Austrian physicist Erwin Schrödinger postulated the behavior of system of particles in an expression, called wavefunction which yields the energy of the system. According to the Schrödinger’s equation the energy of system of particles is quantized; that is, has a discrete value. Using the Schrödinger’s equation, spectra of many of the atoms and the molecules have been predicted.

Spectroscopy, which tries to examine the matter in terms of emitted, absorbed or scattered wavelength of light, is referred as a purely applied quantum mechanical phenomena (Ball, 2001). It is the term to express the measurement of intensity of emitted, absorbed or scattered electromagnetic radiation as a function of energy (or wavelength). In the field of measurement of electromagnetic radiation, spectrum can be regarded as a wavelength-intensity distribution of energy and is defined as a plot of intensity of detected electromagnetic radiation with respect to corresponding wavelength. In addition, spectrometer is the general name of the devices used in this type of measurements.

Interaction of matter with electromagnetic radiation can cause the excitation of atom or molecule, then which ends up with either radiative or nonradiative transition of electrons from excited state to ground state. Radiative transitions yield emission of photons, whereas nonradiative transitions yield emission of phonons which are quanta of lattice vibrations. Luminescence is a general name used for emission of photons and it can be defined in the following; when atom or molecule is excited from lower energy state to higher energy state, it tends to back its initial lower energy state by releasing energy in order to conserve equilibrium conditions. At this point, upon transforming the excitation energy into light by a radiative transition to lower energy state, emission of light is observed. This process is called luminescence.

There are many different types of luminescence which are categorized with respect to excitation source. The most common ones are; Radioluminescence (excitation with particles or photons emitted from radioactive materials), Cathodoluminescence (excitation with beam of energetic electrons), Röntgenoluminescence (excitation with X-rays), Photoluminescence (PL, excitation with visible or ultraviolet light), Optically Stimulated Luminescence (OSL, excitation of previously irradiated sample with visible light) and Thermally Stimulated Luminescence, Thermoluminescence (TL, excitation of a previously irradiated sample with heating). In order to apply OSL or TL technique, material should previously be irradiated with ionizing radiation which creates free electron-hole pairs and some of them are captured and

stored at crystal defects. With proper stimulation energy, electrons and holes could recombine in the recombination center which results in luminescence emission. If the material is heated, the observed luminescence is called TL. On the other hand, if the material is exposed to light, process is called OSL which is actually a kind of PL. However, there is an extra irradiation part in OSL mechanism and intensity of luminescence is dose dependent, whereas PL intensity depends on concentration of excited defects.

Luminescence spectroscopy examines the energy levels of the luminescence centers and gives their spectral distribution as an output. Energy level can be described as a characteristic state that is related to the physical nature of the center (i.e. relation between particle's energy and wavelength) and to the energetic and dynamic processes that the center exposes (Gaft et al., 2005). There are three subsections of luminescence spectroscopy; luminescence emission spectroscopy, luminescence excitation spectroscopy and time resolved emission spectroscopy. Luminescence emission spectroscopy investigates the energy levels of recombination centers. The spectrum of this type of measurement represents the intensity of emitted luminescence as a function of wavelength at a fixed excitation wavelength. Luminescence excitation spectroscopy deals with the selection of most appropriate wavelength of excitation source. The spectrum of this method is a plot of intensity of luminescence emission at a proper emission wavelength for a range of excitation wavelengths. Time resolved emission spectroscopy is used to measure the lifetime of luminescence emission. It is a plot of intensity of luminescence emission with respect to time. Measurement of emission spectra is an essential requirement for the understanding of the underlying physical processes involved in the luminescence (Bos et al., 2002). In this study, luminescence emission spectra of various dosimetry materials (Al_2O_3, BeO, CaF_2, $Gd(Mg,Zn)B_5O_{10}$:Ce-Mn, Zn_2SiO_4:Mn) have been measured using PL, OSL or TL methods.

The main purpose of the present thesis is to design and develop a spectrometer to reach an experimental setup which can be utilized for the measurement of emission spectra in UV and visible range. The main interest is to obtain PL, OSL or TL

emission spectra of materials relevant for dosimetry. Over the years a variety of spectrometers have been integrated with TL/OSL readers. The first generation spectrometers consisted of scanning monochromator or variable narrow-band filters which could detect only one wavelength at any given time; therefore, it was causing a loss of signal. The second generation ones consisted of Fourier transform spectrometers which could measure the whole spectrum at the same time. The present generation spectrometers are using high sensitive charge coupled device (CCD) detectors (Bos et al., 2002). Several instruments based on measurement of luminescence emission with different optical principles have been developed and described in the literature. Jackson and Harris (1970) described dispersive rapid scanning systems based on diffraction gratings. Methods using optical filters have also been employed: Bailiff et al. (1977) reported a rapid scanning TL spectrometer based on successive narrow band interference filters of 20 nm bandwidth fixed on a common turntable. Huntley et al. (1988) built a spectrometer based on a custom-made concave holographic grating in connection with a micro channel plate photomultiplier tube (PMT) and image converter to obtain wavelength-resolved spectra of a variety of mineral samples. Poolton et al. (1994b) developed a compact computer controlled scanning monochromator based on a moveable variable interference filter. Townsend and Luff (1994) reported a highly sensitive TL spectrometer for producing 3-D isometric plots of TL intensity against wavelength and temperature. Rieser et al. (1994) reported a high sensitivity TL/OSL spectrometer based on liquid nitrogen cooled CCD camera, with simultaneous detection in the range 200 to 800 nm. Rieser et al. (1999) improved the spectral response of the spectrometer based on CCD detector in the range 200 to 1100 nm with extremely low readout noise and added a new option for optimizing the detection efficiency and resolution with exchangeable gratings. By integrating a high sensitivity 2048-element CCD-linear array detector without cooling requirement into a compact sized spectrometer and including wide range of possibilities (automatized sample handling, beta irradiation, heating, optical stimulation with a selected source), Bos et al. (2002) could measure the OSL and TL emission spectra with more versatile instrument. However, the designed and developed emission spectrometer

within thesis project is consisted of scanning monochromator with diffraction grating and PMT which can detect only one wavelength at any given time.

Design and development of an electronic control unit, computer software, wavelength calibration, determination of spectral response and resolution of luminescence emission spectrometer form the basis of this thesis work. In addition, results of some test experiments which were applied in order to check the wavelength calibration and spectral response curves will be presented. Finally PL, TL and OSL emission spectra of some materials relevant for dosimetry will be shown and results will be compared with the ones which had been published.

In chapter 2, spectroscopy beginning with the basic concepts of light interaction with matter will be discussed and physical principles and optics of emission spectroscopy will be described in detail.

Chapter 3 of the thesis starts with an introduction to luminescence phenomena. Then the theoretical aspects of luminescence will be explained and fluorescence and phosphorescence processes will be represented and examined over configurational coordinate diagram. In addition, brief description and principles of OSL and TL will be discussed.

In chapter 4, the design and development of an emission spectrometer, which consist of computer software, electronic hardware and firmware parts, will be explained. In addition, optical properties and structure of the measurement setup will be mentioned in detail.

Chapter 5 is the results and discussion part which includes the wavelength calibration and determination of the spectral response (i.e. spectral correction curves) of spectrometer. In addition, test results of various light sources will be shown. Finally, PL emission spectra of Al_2O_3, BeO, CaF_2, $Gd(Mg,Zn)B_5O_{10}$:Ce-Mn, Zn_2SiO_4:Mn, TL emission spectra of Al_2O_3, BeO and OSL emission spectrum of Al_2O_3 will be represented and the results will be discussed.

Overall conclusions of the research will be presented in chapter 6. Additional figures associated with the luminescence measurement system are given in the Appendices.

CHAPTER 2

SPECTROSCOPY

2.1 Introduction

Spectroscopy is the technique that studies the interaction of matter with radiation to perform an analysis. Interaction of light with matter can cause redirection of radiation or transition of electrons between energy levels of atoms or molecules. Transition of electrons from a lower energy level to a higher energy level with transfer of energy of radiation to atom or molecule is called 'Absorption'. Radiative transition of electrons from a higher energy level to a lower energy level is called 'Emission'. Nonradiative transition of electrons from a higher level to a lower level is called 'nonradiative decay'. Redirection of radiation whether losing energy or not due to interaction with matter is called the 'Scattering of light.'

Spectrum is generally refers to a plot of the intensity of light versus wavelength or frequency. It can carry information about the atomic or molecular energy levels of transition and the structure and the geometry of the sample or compounds of the sample to perform a qualitative analysis. It can also be used to measure the concentration of elements in the matter to perform quantitative analysis. Spectrometers are the devices used in spectroscopy. They are generally composed of monochromator which enables the diffraction of light and detector to measure the light intensity. In addition, various widths of slits are integrated for adjustment of light intensity.

2.2 Basic Concepts in Spectroscopy

There are three basic concepts in spectroscopy that requires a good understanding of

(i) The wave nature of light
(ii) The particle properties of light
(iii) The emission and absorption of light

Light is described as the energy of particles which are called photons. According to the electromagnetic theory of radiation, developed by Scottish physicist James Clark Maxwell, light is transferred in the form of propagating electromagnetic radiation that consists of oscillating electric and magnetic fields. Therefore, it should have definite wavelength and frequency. The observations that light can give rise to interference patterns, diffraction etc. also prove that light must behave like a wave.

Starting with Planck's assumption in explaining the blackbody radiation, further investigations on light with Albert Einstein's explanation of photoelectric effect and Arthur Compton's discovery of scattering of light proved that it has momentum and specific energy which supported the theory of particle behavior of light.

In twentieth century, with the suggestion of quantum theory, many of unknown properties of light were explained. Niels Bohr denoted that the energy levels of the atom or molecule were quantized and transitions were possible only if the electrons have discrete energy.

Absorption is the transition of electrons from a lower energy level to a higher level by taking the energy of photon. It occurs when certain wavelength of light strikes the atom and gives its energy to an electron in lower level. *Emission* is called the transition of electrons from a higher level to a lower level by emitting a photon. Conservation of energy dictates that the frequency *v* of the photon should satisfy;

$$E_2 - E_1 = h\nu \tag{2.1}$$

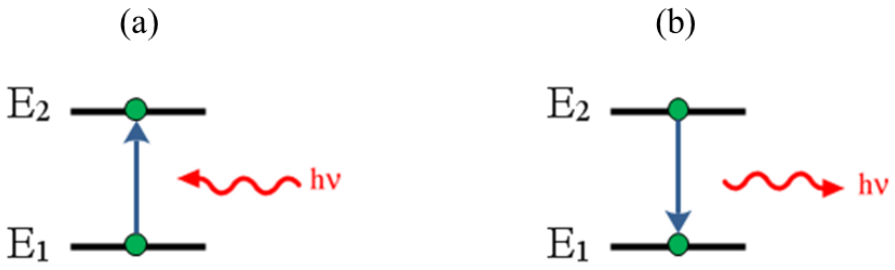

Figure 2.1: Optical transitions in a two level system. (a) Absorption, (b) Emission.

Where E_2 is the energy of higher level or excited state and E_1 is the energy of lower level. Absorption process is shown in Figure 2.1 (a). According to the statistical physics, atoms in excited state have a natural tendency to lose energy and de-excite. Thus, emission of a photon by an atom itself during transition from higher level to lower level is called 'spontaneous emission' (see e.g., Fox, 2001). This process is illustrated in Figure 2.1 (b). The frequency of the photon emitted during this process is directly proportional with the energy difference of two levels; therefore, every atom has a unique emission spectrum.

It is also possible to analyze the transitions using Einstein coefficients. Eq. (2.2) explains the rate of change of number of atoms in excited state with respect to time:

$$\frac{dN_2}{dt} = -A_{21}N_2 \tag{2.2}$$

N_2 (t) is the number of atoms in higher level. Therefore, the rate of photon emission is proportional with the number of atoms in higher level and Einstein's spontaneous emission coefficient A_{21} for the transition. Right hand side of the equation is minus since N_2 (t) decreases with time. Furthermore, the solution of the equation above yields the radiative lifetime τ of the emitted photon.

$$\begin{aligned} N_2(\mathrm{t}) &= N_2(0)\exp(-A_{21}\mathrm{t}) \\ &= N_2(0)\exp(-t/\tau) \end{aligned} \tag{2.3}$$

This yield:

$$\tau = \frac{1}{A_{21}} \tag{2.4}$$

Similar implementation can be made for the rate of absorption transitions per unit time as:

$$\frac{dN_1}{dt} = -B_{12}N_1\delta(\nu) \tag{2.5}$$

N_1(t) is the number of atoms in lower level at time t. B_{12} is the stimulated emission coefficient, $\delta(\nu)$ is the energy density of electromagnetic radiation at frequency 'ν'. This term should be added to the Eq. (2.5) as the transition is not spontaneous like the emission case. Absorption process is stimulated by the photon energy. Right hand side of the equation is minus as N_1 (t) decreases by time.

One may refer to book by Fox (2001) for additional information about transitions between energy levels.

The basic concepts for the study of spectroscopy, namely, the wave properties of light, the particle properties of light and the quantum theory of radiative absorption and emission processes are explained briefly. It is time to move on basic parameters used in spectroscopy.

Spectroscopy can be categorized according to the type of radiative energy (e.g., electromagnetic radiation, pressure waves), nature of the interaction of radiative energy with matter (e.g., emission, absorption, reflection) or any other specific applications (e.g., Fourier transform spectrometers, magnetic resonance spectrometers, mass spectrometers).

Within the scope of thesis project, an emission spectrometer was planned to be developed therefore only the basic principles and components of a luminescence emission spectrometer will be discussed.

2.3 Principles of an Emission Spectrometer

The energy of emitted photons from an atom is proportional to the energy difference of transition levels. Depending on a stimulating source and atomic structure, every atom emits different wavelengths of light. Specific wavelength of radiation yields a specific spectrum for every element. Therefore, analysis of the emission spectrum gives fundamental information about the atomic or molecular energy levels which can yield emission of photons.

By using an emission spectrometer, one can measure the emission spectrum of any kind of light source (e.g., Light Emitting Diode (LED), halogen lamp, deuterium arc lamp) depending on its spectral response. However, in PL or OSL experiments, light of interest is not the excitation light but the light emitted by the sample. In many applications, photons interact with the sample and re-emitted at a different wavelength than the excitation light. In TL experiments, light of interest is the light emitted by the sample which is excited with heat energy.

2.4 Structure of an Emission Spectrometer

Following components are necessary for emission spectrometer; a source of energy for excitation, a suitable narrow band filter to select the wavelength of excitation light, a sample that absorbs this energy and re-emits photons with different wavelength, optical components (i.e., lenses, mirrors) to collect the re-emitted light as much as possible, a device that could discriminate this energy in terms of

wavelength and a detector to detect the signal. Monochromator, prisms or the colored filters are the main devices used in discrimination of energy in spectrometers. Figure 2.2 below shows the basic components of an emission spectrometer.

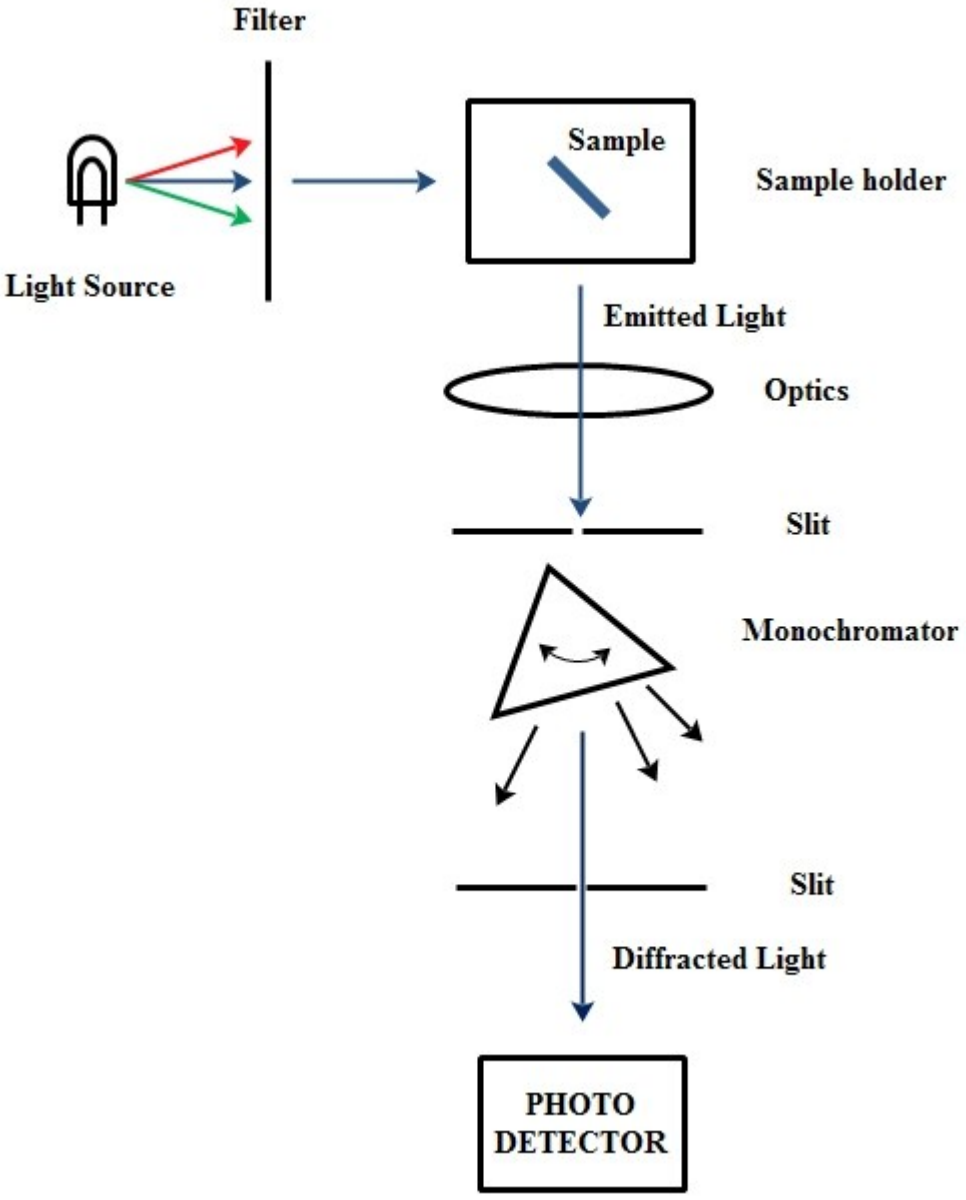

Figure 2.2: A simple schematic diagram of an emission spectrometer. In this case, light given off by a sample is passed through a monochromator that allows only certain wavelengths of light to pass onto a detector (Redrawn after, Ball, 2001).

2.5 Components of an Emission Spectrometer

In the following part, the basic optical components of an emission spectrometer which are the monochromator and the detector will be investigated in detail.

2.5.1 Monochromator

Monochromator is an optical device which is used to select the emitted light in terms of wavelength and to focus this selected light on a detector. Moreover, different widths of slits are integrated in front of the detector and optical entrance of the monochromator to adjust the intensity of light. It contains an entrance slit in which the emitted light passes through, an exit slit that is placed in front of the detector, a diffraction grating or prism that is used to select the incident light and some optical components; such as, mirror and lens to converge both the emitted and diffracted light.

There are many types of monochromator configurations when using diffraction gratings. The most popular ones are Fastie-Ebert, Czerny-Turner and Littrow configurations. Each of them have some advantages or disadvantages depending on the cost, number of optical components used, optical path differences of light or geometrical aberrations of the system. In this project, Littrow type of monochromator is used. Therefore only this configuration will be discussed. One may refer to book by Palmer and Loewen (2005) for further detail.

2.5.1.1 Littrow Configuration

In Littrow configuration, grating diffracts light back along the same direction with the incident light. Spectrum is recorded by rotating the grating and the wavelength of diffracted light depends on the angle of rotation; this changes the angle of incidence α and angle of diffraction β with respect to the normal of grating; however, the condition 'α=β' remains constant (i.e., constant deviation) for all constructively interfered wavelengths of light. Spherical mirror is used to collimate both the incident and diffracted light and direct the incident light to the grating and re-focused the diffracted light into exit slit (Palmer and Loewen, 2005). The advantages of this configuration are using less number of optical components, cost and constant deviation mount. However, the disadvantages are long focal length, relatively large size and spherical aberration.

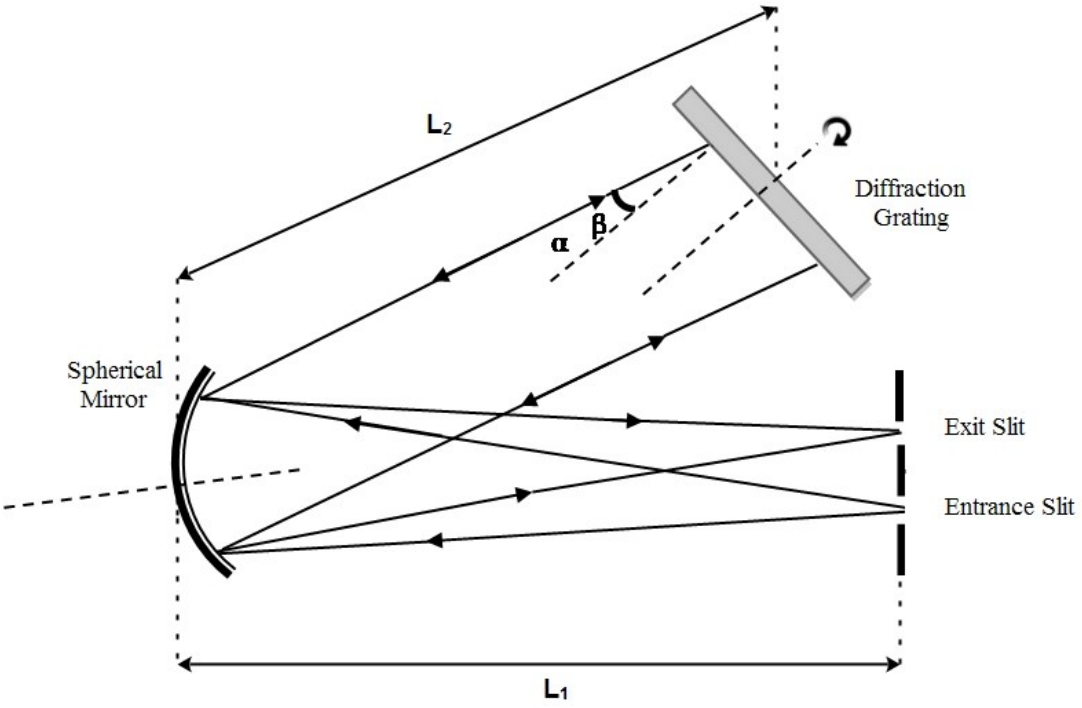

Figure 2.3: The Littrow mounted monochromator of spectrometer.

Table 2.1 below gives the definition of parameters related to Littrow configuration. Some of them are also shown in Figure 2.3. In addition, these parameters will be used in many of the formulas given in the following sections.

Table 2.1: Definitions of some of the optical parameters that will be used in the following sections (see Figure 2.3 for more detailed review).

Name	**Definition**
L_1	Distance between entrance slit and aspherical mirror
L_2	Distance between diffraction grating and aspherical mirror
L_{EX}	Distance between diffraction grating and slits ($L_1 + L_2$)
α	Angle of incidence
β	Angle of diffraction
w	Width of entrance and exit slits
Ω	Half angle, angle of the maximum cone of light that can enter or exit the lens.

2.5.1.2 Aperture Ratio (f/number), and Numerical Aperture (NA)

Numerical aperture (NA) of the system is described as the range of angles over which the system can accept or emit light. It is a dimensionless number (Lerner and Thevenon, 1988) and is defined as;

$$NA = nsin\Omega \tag{2.6}$$

Where n is the refractive index (n = 1 for air). Definition of f number ($f/\#$) is then given by the following equation;

$$f/\# = \frac{f}{D} \tag{2.7}$$

Where D is the diameter and f is the focal length. According to Fischer et al. (2008), $f/\#$ can be written in terms of NA by assuming that it is less than 0.5.

$$f/\# = \frac{1}{2NA} \tag{2.8}$$

The beam of light near to paraxial region can easily enter the system; however, for marginal rays which are propagating away from the paraxial region, there is a limit of acceptance to enter into system. Therefore, $f/\#$ is important in optical systems as it determines the range of angles over which the system accepts or emits light. That is to say, if $f/\#$ gets larger, Ω becomes smaller and this decreases the acceptance of optical system. However, if $f/\#$ gets smaller, Ω becomes larger and acceptance of optical system increases.

2.5.1.3 Bandpass and Resolution

The terms bandpass and resolution define the ability of how well a monochromator can separate adjacent spectral lines. Spectral bandpass means the distance at the full width at half maximum height (FWHM) of the trace. Figure 2.4 shows the point of interest.

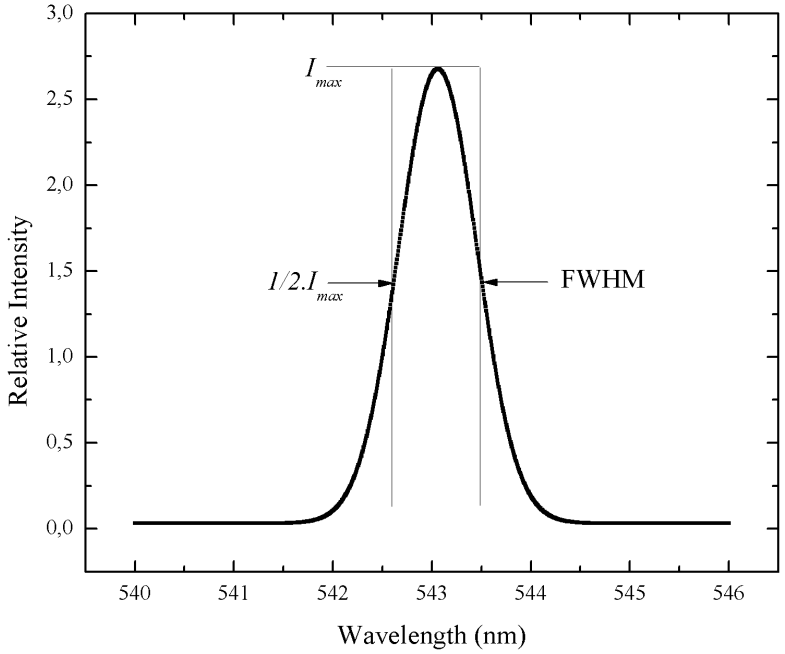

Figure 2.4: Emission spectrum of a line emitter measured with He-Ne green laser. FWHM is the width in wavelength of the region between the points on the curve where the intensity has dropped to half of its maximum.

Resolution is related to bandpass but it determines how well the separation of two peaks is observed.

Instrumental bandpass of a monochromator can be measured easily. If a source which emits monochromatic light at wavelength λ_o is considered; the theoretical emission spectrum of the light source should consist of a single sharp line at wavelength λ_o which is shown by Figure 2.5 (a). Suppose that the spectrum of the same source is measured by a perfect monochromator then the recorded experimental spectrum should look like in Figure 2.5 (b). However, nothing is perfect in real world as the spectrometer is. Therefore, actual recorded spectrum will have a spectral broadening which will cover λ_o. This is called instrumental line profile and shown by the Figure 2.5 (c). The instrumental bandpass is then defined as the FWHM of that curve (Lerner and Thevenon, 1988).

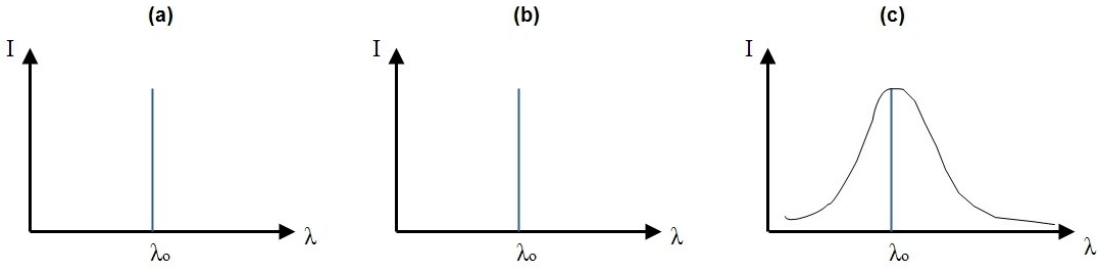

Figure 2.5: (a) – Real spectrum of a monochromatic light source. (b) – Recorded spectrum of a monochromatic light source with a perfect instrument. (c) – Recorded spectrum of monochromatic light source with a real instrument (Redrawn after, Lerner, 1988).

However, the spectrum covers all possible lines of different wavelengths of light. Thus, there is a general relationship between the instrumental line profile, actual spectrum and recorded spectrum. Let, $I(\lambda)$ be the instrumental line profile, $R(\lambda)$ be the recorded spectrum and $A(\lambda)$ be the actual spectrum. Then the relation is given by the following equation, namely:

$$R(\lambda) = I(\lambda)A(\lambda) \tag{2.9}$$

Instrumental line profile of spectrometer depends on some factors which are entrance and exit slit widths, system aberrations, grating width and the spatial resolution of the detector.

Mathematical description of FWHM of $I(\lambda)$ is given by the following equation:

$$FWHM = \sqrt{(\, d\lambda_{slits}^2 + \, d\lambda_{resolution}^2 + \, d\lambda_{line}^2 \,)} \tag{2.10}$$

$d\lambda_{slits}$ is the line broadening due to slits, $d\lambda_{resolution}$ is the limiting resolution of spectrometer which includes the system aberration and diffraction effects and detector response, $d\lambda_{line}$ is the natural spectral line width of used source.

FWHM of a spectrometer can be measured by a line emitter (laser) which has line width less than that of the instrument so that the observed spectrum can be referred as the instrumental line broadening.

In most of the spectrometers, line profile of emitted light mostly expands while passing through slits. Thus, slits are the dominant factors in line broadening and bandpass could also be calculated by slit width multiplied by linear dispersion (Lerner and Thevenon, 1988):

$$BP = WR_d \tag{2.11}$$

W is the width of exit slit. R_d is reciprocal linear dispersion. It represents the number of wavelength intervals contained in each interval of distance along the focal plane. It will be mentioned in diffraction grating part in detail:

$$R_d = \frac{d\lambda}{dx} = \frac{\cos\beta}{mnL_{EX}} \tag{2.12}$$

Where β is the angle of diffraction, L_{EX} is the exit arm length of the system, k is the groove density, m is the order and $\cos\beta \backsim 1$ for $(\beta \leq 20^0)$. Therefore, Eq. (2.11) can be expressed as:

$$BP = \frac{W}{mkL_{EX}} \tag{2.13}$$

The basic properties of monochromator have been discussed in detail. In the next section, the other important component of an emission spectrometer, the diffraction grating, will be examined.

2.5.2 Diffraction Grating

Diffraction grating is an optical device which is used to separate the incident light into its constituents. It has been used in every aspect of science and technology. In astrophysics, it is used to analyze the compositions of stars and planets. In mechanics, optical strain gauges which measure the strain of an object have a grating at their structure (Palmer and Loewen, 2005). However, in physics, diffraction grating is widely used in spectroscopy. It diffracts the incident light into many discrete directions. In the following parts, starting with the physics of diffraction grating, its characteristics and properties will be investigated in detail.

2.5.2.1 The Grating Equation

Figure 2.6 illustrates the behavior of grating when wavefronts (surfaces of constant phase) are incident on its surface. Two rays, *ray 1* and *ray 2*, are in phase with each other. When they hit the surface, they diffract into discrete directions by the grating grooves which have a certain length *d*. In accordance with the theory of diffraction of waves (or light), constructive or destructive patterns are generated. Only if the path difference of two rays is equal to integer multiple wavelength of λ then constructive interference occurs. In according with the theory of constructive interference, grating equation is explained by the following equation:

$$m\lambda = d(sin\alpha + sin\beta) \tag{2.14}$$

The left hand side of the equation, $m\lambda$, describes the wavelength and its orders of magnitude where *m* is the order of light and should be an integer. At all other angles, the wavelets originating from the groove facets will interfere destructively (Palmer and Loewen, 2005).

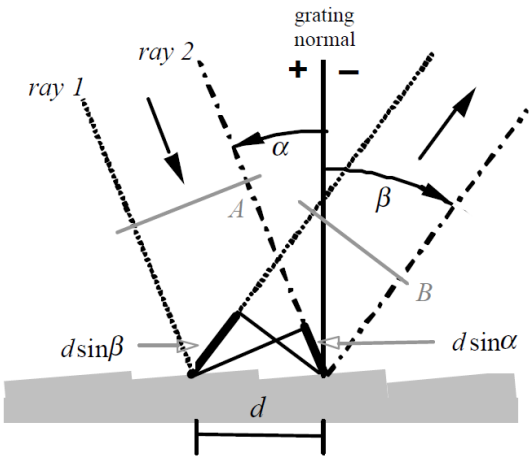

Figure 2.6: Geometry of diffraction for planar wavefronts. Two parallel rays, labeled 1 and 2, are incident on the grating one groove spacing d apart are in phase with each other at wavefront A (Palmer and Loewen, 2005).

Table 2.2 below explains the parameters used in the grating equation.

Table 2.2: The parameters used in the grating equation.

α	Angle of incidence (degree)
β	Angle of diffraction (degree)
m	Diffraction order (integer number)
λ	Wavelength (nm)
d	Groove spacing (mm)
k	Groove density (N# of grooves/mm)

However, in Littrow configuration, incident light which hit on the surface of the grating diffracts back with the same direction that is, the angle of incidence and the angle of diffraction remain equal to each other for all λ ($\alpha = \beta$) (see Figure 2.3). Thus, the grating equation for Littrow configuration can be expressed by:

$$m\lambda = 2dsin\alpha \tag{2.15}$$

2.5.2.2 Diffraction Orders

According to general grating equation, order number depends on the incident and diffracted angle. Therefore, there are finite numbers of orders of λ. This relation can be investigated as;

$m\lambda = d(sin\alpha + sin\beta)$ and maximum value for $sin\alpha + sin\beta = 2$. Thus;

$$\left|\frac{m\lambda}{d}\right| < 2 \tag{2.16}$$

$$-2d < m\lambda < 2d \tag{2.17}$$

Hence m is an integer value; it can also take negative values which means positive and negative orders of wavelength diffract at opposite sides of zeroth order. However, zero order occurs only if m=0 and it means that the incident light reflects back in the same direction and no diffraction is occurred. Figure 2.7 below shows some possible orders of given incident light.

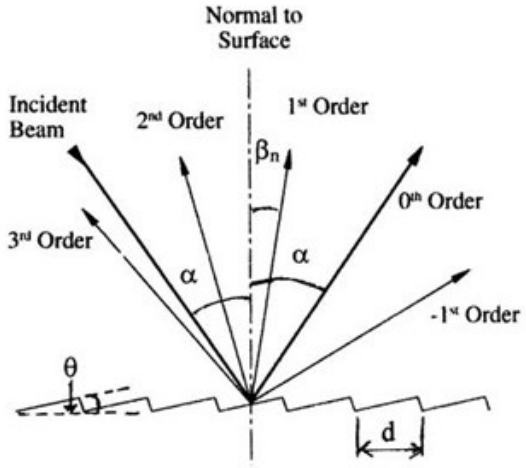

Figure 2.7: Diffracted orders of incident beam.

2.5.3 Light Detection Unit

Light detection unit is the place where the light signal is converted to electrical current signal and the intensity of light is measured as electrical charge. Furthermore, light detection unit consist of primarily a detector and peripheral electronic devices. Photomultiplier tube (PMT), photo-resistors, photodiode arrays and charge coupled devices (CCD) are the main detectors widely used in spectroscopy. Within the scope of thesis project, PMT was used to measure the light intensity. Thus, principles, characteristics, operating modes and the main advantages or disadvantages of PMT will be investigated in detail.

2.5.3.1 Principles of Photomultiplier Tube

A photomultiplier tube is a device that measures the intensity of light. It creates an electric charge in proportion to the amount of light energy that it receives. The charge is integrated through some period and is taken as a measure of the input light power. Light which enters the PMT follows these processes respectively;

- Light enters inside the window and reaches the photocathode.
- If the frequency of the incident photons is over the cut-off level, than photoelectrons are emitted from the surface of photocathode into an external electric field that is generated between first dynode stages.
- When the photoelectrons reach the first dynode, they are multiplied by means of secondary emission and directed to next dynode. The process of secondary emission continues until last dynode. The multiplied secondary electrons emitted from the last dynode are collected by the anode.
- Electrons in the anode flow over a resistor and finally the electrical signal is generated.

The theory of operation of PMTs relies on important physical phenomenon, the photoelectric effect. According to the theory of photoelectric effect, electrons are emitted from the metal if the frequency of light is proper to overcome the work function of the metal.

In Figure 2.8 below, dynode stages and electron multiplication are shown where voltage divider network is built to generate electric field between dynodes and electrons are collected by the anode and a potential is generated which is shown as U_{out}.

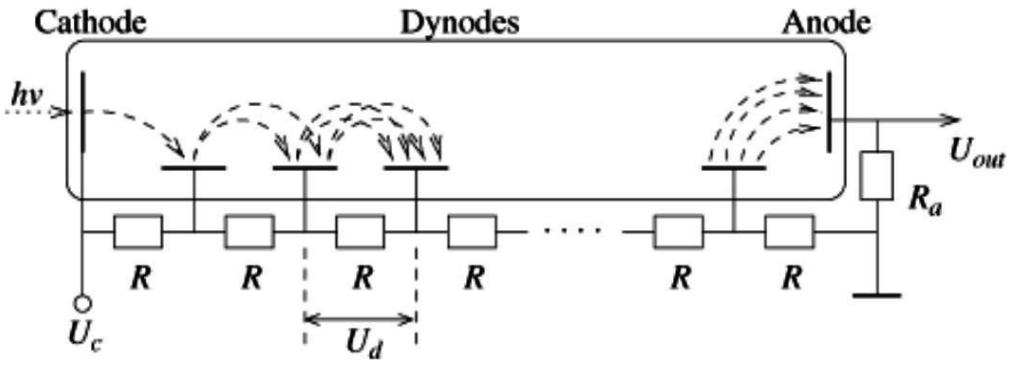

Figure 2.8: The schematic diagram of a PMT. U_c is cathode voltage, U_d denotes the potential difference between two dynodes, R is resistor and hv is the energy of incoming photon (Tkachenko, 2006).

2.5.3.2 Characteristics of Photomultiplier Tube

Radiant sensitivity, quantum efficiency, spectral range, gain, electron transit time and dark noise are the basic optical characteristics of PMT essential for spectroscopic measurements (Hamamatsu, 2007).

Radiant Sensitivity and *Quantum efficiency* are the two properties which express the spectral response of PMT. They determine the number of ejected photoelectrons when a photon is incident on photocathode.

Spectral range is another characteristic of PMT and is defined as the spectral region in which the PMT gives response to electromagnetic radiation.

Gain of PMT describes the total multiplication factor between the first dynode and the last dynode. In other words, it is the ratio of the number of electrons in last dynode divided by the number of photoelectrons that reach to first dynode.

Electrons transit time; in other words, the time needed for the photoelectrons to reach at the anode is one of the fundamental properties of PMT. Electron transit time determines the time response of PMT.

Dark noise can be expressed as noise signal at the output due to the thermal emission of electrons from the dynodes without light being incident on photocathode.

2.5.3.3 Basic Operating Modes of Photomultiplier Tube

The main operating modes of PMT are DC or AC modes and photon counting. AC and DC measurements are preferred in measurement of intensity of relatively high light levels. In DC mode, only DC portion of PMT output signal is detected by means of an amplifier and lowpass filter. However, in some experiments, the light intensity is too low to be measured with AC or DC mode. Thus, photon counting is used in such applications. It depends on measurement of intensity of light by counting individual photons incident on PMT. Amplifier, discriminator and counter are the external devices required for performing photon counting. Each photon incident on a photo-detector creates an electrical signal which is then amplified and if

the amplitude of pulse is higher than the preset discrimination pulse height, it is counted as a photon signal (Hamamatsu, 2007).

2.5.3.4 Advantages and Disadvantages of Photomultiplier Tube

Main advantages of PMTs can be expressed by high sensitivity or high multiplication factor (in the order of 10^6), good time resolution (up to 20 ps), photon counting option and relatively big photo-sensitive area. However, the main disadvantages of PMTs can be sorted as size, cost, construction, high voltage requirement, possible instabilities on output signal due to external magnetic field and wavelength dependent sensitivity.

CHAPTER 3

LUMINESCENCE

3.1 Introduction

Luminescence is the emission of light resulting from radiative transition of an atom from an excited state to a ground state as a result of a proper excitation. Figure 3.1 shows a general luminescence mechanism of a two level system.

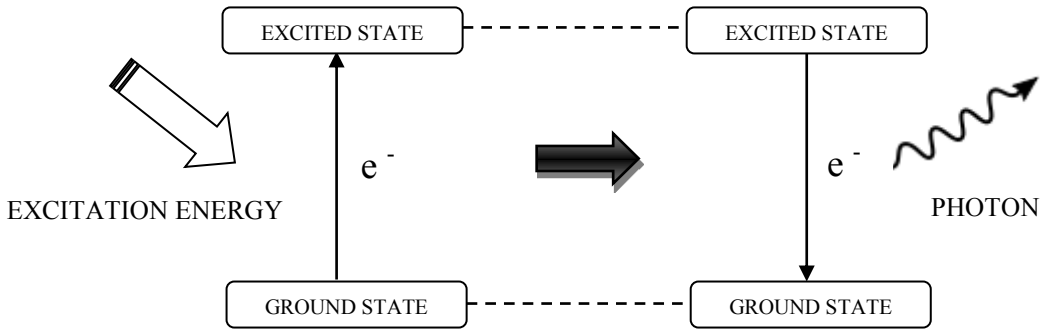

Figure 3.1: A simplified sketch describing the luminescence mechanism. Left hand side describes the absorption of energy in which electron is transferred from ground state to excited state. Right hand side describes the emission of luminescence as a result of relaxation of the electron back to its initial state.

In the case of many atoms and ions, transition of electrons occurs only by absorption and emission of photon where the energy of photon equals to the energy difference of those states. However, in nature, it is simply impossible to find single isolated

atom or ion. Most of solid luminescent materials have crystalline structure in which there are many atoms or molecules having interactions with each other. Under the influence of those interactions, energy levels merge into bands of energy levels which are defined as valence band and conduction band. In addition, there is a transition forbidden region between these bands which is called the forbidden gap.

Luminescent materials have some defects in their structures which are generated due to environmental effects, nuclear and chemical reactions. The most important ones are vacancies, interstitials and impurity ions whose energy positions are located in the forbidden gap. According to energy position, the ones which are near the conduction band are called *trap*, however, the ones which are near the valence band are called *luminescence center* (Krbetschek et al., 1998). Luminescence is produced by these centers as a result of radiative transition and recombination of electrons with holes.

When an atom or ion is placed in lattice structure, non-radiative transitions are also possible by absorption or emission of phonons (quanta of lattice vibrations). Moreover, the possible electron interactions which are electron-electron, spin-orbit interactions and crystal field make it difficult to observe the relevant energy levels and luminescence centers easily (Krbetschek et al., 1998).

Luminescent materials convert the excitation energy into electromagnetic radiation. The wavelength of emitted photons give information about defect of the material and it could be in the range of ultraviolet (UV) to infra-red depending on excitation energy. There are techniques used in measurement of luminescence which do differ in excitation. The most common ones are Radioluminescence that is excitation with particles emitted from radioactive materials, Cathodoluminescence that is excitation with beam of energetic electrons, Röntgenoluminescence that is excitation with X-rays, Photoluminescence (PL) that is excitation with UV or visible light, Optically Stimulated Luminescence (OSL) that is excitation of previously irradiated material with visible light and Thermally Stimulated Luminescence, Thermoluminescence (TL) which is the excitation of previously irradiated material with heating. Those

given methods are preferred depending on analyzes of defects with different energies.

The luminescent material consists of a host lattice and a luminescent center, called an activator (Gaft et al., 2005). Luminescence is generally characterized by its *quantum yield* and *life time*. Quantum yield actually means the efficiency of transition in terms of electromagnetic radiation. In other words, it is the ratio of number of emitted photons to number of absorbed photons. Luminescence centers which have high quantum yield display the brightest emission (Gaft et al., 2005). Life time is the time that an activator spends in excited state prior to its return to the ground state and can be defined as the time to be required for the intensity of luminescence drops its 1/e.

3.2 Process of Luminescence Production

Luminescence is produced by the process of electron-hole recombination. There are three possible ways for radiative recombination transitions which are band to band, band to center and center to center transitions (McKeever, 1985). In order for luminescence to occur, the recombination should result in emission of photons and so the transition should be radiative. Band to band transition is subject to *direct recombination* in which the electron directly transfers from excited state to ground state by emission of photon, therefore it is radiative. However, band to center and center to center transitions are subject to *indirect recombination* process which involves phonon interaction and momentum transfer during transition, thus indirect recombination results in either radiative or non-radiative transition (McKeever, 1985). Following sections explain radiative and non radiative transitions in detail.

3.2.1 Radiative Transition and Luminescence Emission

A configurational coordinate diagram denotes the potential energy curves of ground state and excited state and so the absorbing center between these states as a function of the relative distance *R* of nucleus to the equilibrium position (Krbetschek et al., 1998).

The excitation and emission of a luminescence center is shown by configurational coordinate diagram in Figure 3.2.

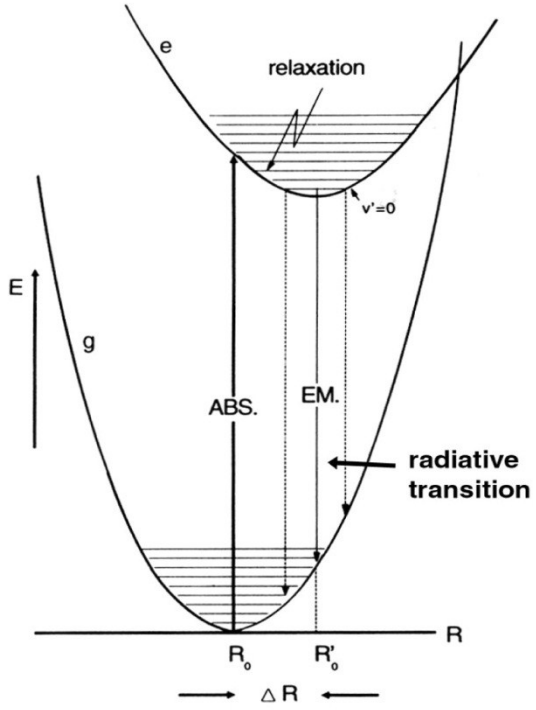

Figure 3.2: The excitation and emission of a luminescence center where *g* and *e* stand for ground and excited states respectively (Blasse and Grabmaier, 1994).

Each electronic state is represented as a harmonic oscillator system, with interatomic distance *R* on the horizontal axis, and energy *E* on the vertical axis. Vibrational states

are represented by horizontal lines. Ground state is represented by *g* and *e* stands for excited state.

Figure 3.2 illustrates the absorption of an electron from lowest vibrational level of ground state to higher vibrational level of excited state. The luminescence center returns to lowest vibrational level of excited state, $v'=0$, by giving excess energy in the form of phonon emission. This process is called *relaxation* and configurational diagram shifts by ΔR. During relaxation, nuclei adjust their position to reach equilibrium condition for the excited situation. Then, electron transfers to higher vibrational level of ground state under emission of radiation. Finally, circle completes with relaxation to the lowest vibrational level of ground state (Blasse and Grabmaier, 1994).

As seen in Figure 3.2, absorption and emission processes are shown vertically compared to lattice vibrations during relaxation. This situation can be explained by Franck-Condon principle. The principle states that during transition of an electron between states, position of nucleus does not change since electron transitions occur much faster than the nuclear motion because of huge difference between masses of an electron and a nucleon (Gaft et al., 2005).

In addition, due to relaxation process ΔR, absorption occurs at a higher energy than emission. This energy difference is called Stokes shift. Thus, it explains the energy difference between maximum of excitation and emission spectra of any luminescent material. In addition, Stokes shift becomes larger when ΔR gets larger (Krbetschek et al., 1998).

3.2.2 Nonradiative Transition and Efficiency

Radiative return of electron from excited state to ground state is not the only way of transition. Nonradiative return is the other possibility in electronic transitions. Figure 3.3 below shows the configurational coordinate diagram for nonradiative transition.

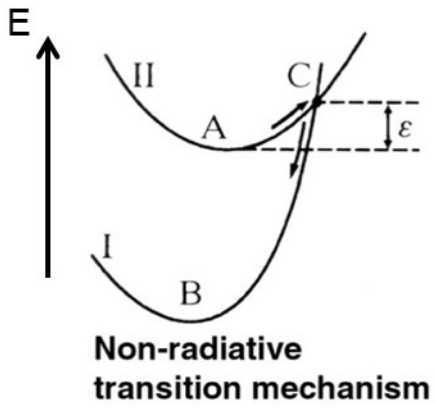

Figure 3.3: Nonradiative transition of electron from excited state II to ground state I (Yen et al., 2007).

The energy diagram given in Figure 3.3 shows a non-radiative transition. According to theory, if the electron in the lowest vibrational level of excited state absorbs an amount of thermal energy ε, then transition from vibrational level *A* to vibrational level *C* can take place which enables the transition of electron from *C* to ground state *I* without emission of radiation. However, reverse transition of the electron from *C* to *A* is still possible by dissipating heat energy (McKeever, 1985).

Nonradiative transitions directly affect the quantum yield of luminescence. Luminescence efficiency is related to probability of radiative transition and probability of non-radiative transition (see e.g. McKeever, 1985). In addition, radiative transition is unaffected by temperature but the probability of a non-radiative

transition is related to the temperature by a Boltzmann factor $e^{E/(k_b T)}$. Thus, the luminescence efficiency η is interpreted by the following equation:

$$\eta = \frac{1}{(1 + se^{E/k_b T})} \tag{3.1}$$

Where E represents the energy level of the trap, T is the temperature, k_b is the Boltzmann constant, s is a constant and it represents the frequency factor.

3.3 Photoluminescence

Photoluminescence (PL) is the production of luminescence upon excitation of a luminescent material with UV or visible light. In PL process, substance absorbs radiation energy and then re-emits radiation energy at different wavelength. PL can be seen in two different forms which are called fluorescence and phosphorescence. In order to discuss about the differences between fluorescence and phosphorescence, the electronic transitions between energy levels should be well understood.

3.3.1 Electronic States and Selection Rules

Each orbital have characteristic quantum numbers, n, l, m_l and m_s where n is the principle quantum number, it determines the size and energy of orbital, l is the orbital quantum number and it determines the shape of orbital, m_l is magnetic quantum number which describes the possible orientations of orbital around nucleus and m_s is spin quantum number.

According to selection rules, which are explained in detail by Corney (1977), not all of transitions between all pairs of energy levels are allowed. Some of them are

allowed and others are forbidden transitions. Electrons are transferred with respect to principles of selection rules which are given by the following expressions;

$$\Delta l = \pm 1 \ (not\ zero) \tag{3.2}$$

$$\Delta m_l = \pm 1, 0 \tag{3.3}$$

$$\Delta S = 0 \tag{3.4}$$

According to Pauli Exclusion Principle, an orbital can hold 0, 1, or 2 electrons only and if two electrons occupy the same orbital, they should have opposite spins. Any transition out of scope of these rules are not allowed and called forbidden transition.
There are mainly two electronic states in molecules important for fluorescence and phosphorescence; *singlet state* and *triplet state*. When all electrons are in pairs, related molecule is said to be in singlet state and there is no net spin angular momentum for this state. However, when molecule is excited, spin of the electron in excited state may be reversed and the electron no more remains in paired and molecule is said to exist in a triplet state (Skoog et al., 1998). The molecule in triplet state has distinguishable spin angular momentum.

3.3.2 Fluorescence and Phosphorescence

Electron in ground state can jump to any vibrational level of excited singlet state when the molecule absorbs energy. After excitation, electron relaxes back to lowest vibrational level of first excited singlet state due to inter-atomic collisions. Then, it can return to any vibrational level of ground state, emitting its energy in the form of electromagnetic radiation. Such emission is called *fluorescence* and the lifetime of excited singlet state is approximately 10^{-8} s.

When an electron is promoted to an excited state, it preserves its spin direction and resumes its pair in ground state without disturbing the parity. However, sometimes, the direction of spin can change due to spin orbit coupling and this time molecule has

two independent electrons with the same spin in different orbital. This situation of the molecule is called a "triplet state". When the molecule exists in triplet state, transfer of an electron from the lowest vibrational level of singlet state to upper vibrational level of triplet state becomes possible to occur as they have nearly the same energy level. This is called *inter-system crossing*. Then the transition of electron from triplet state to ground state is occurred by emitting its energy in the form of electromagnetic radiation. Such an emission is called *phosphorescence*. The life time of excited triplet state is at least 10^{-4} s.

In accordance with the selection rule $\Delta S = 0$, transfer of electron from ground state to excited triplet state is forbidden which makes the reverse transition from excited triplet state to ground state difficult to happen. This explains the life time difference between fluorescence and phosphorescence.

Figure 3.4 below shows the processes of fluorescence and phosphorescence respectively. S_1 and S_2 are excited singlet states, T_1 and T_2 are excited triplet states, S_0 is the ground state. Horizontal lines represent the vibrational energy levels. Zigzagging arrows express the emission of phonons during relaxation period.

Arrow boxes next to the singlet and triplet states represent the occupation of electrons into quantum state in terms of their spin direction.

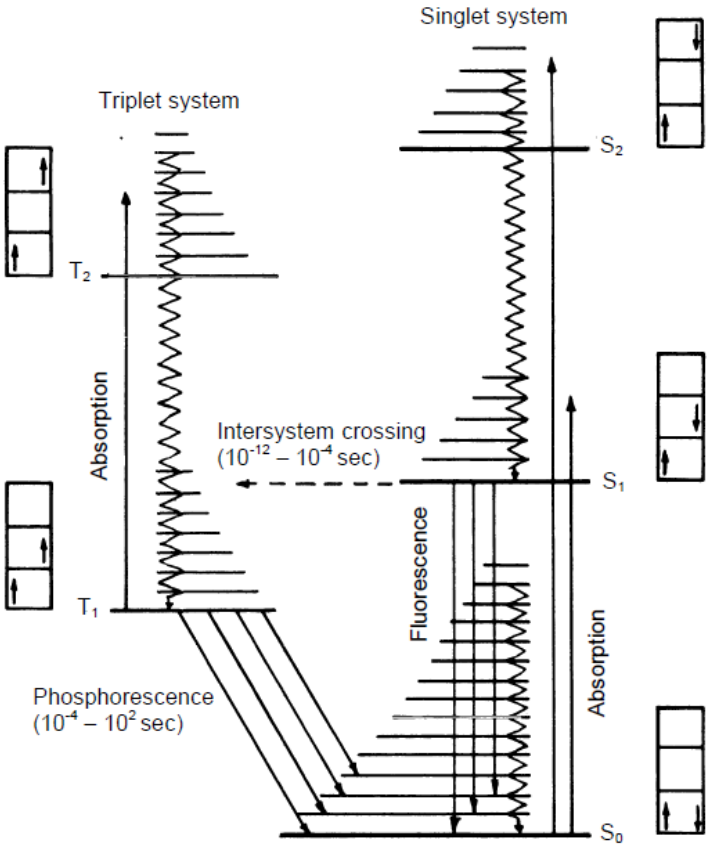

Figure 3.4: Partial energy diagram for a photoluminescent system (PerkinElmer Inc, 2000).

3.3.3 Optically Stimulated Luminescence

Optically stimulated luminescence (OSL) is a subclass of PL in terms of excitation and emission of radiation; however, it includes one more process. OSL is based on irradiation of a wide band gap semiconductor or insulator with ionizing radiation where PL generally does not depend on. Irradiation causes the ionization of valence electrons and creation of electron/hole pairs. The freed electron/hole pairs can be captured by defects whose energy levels lie in the forbidden region (Bøtter-Jensen et al., 2003). Then, excitation with a proper light, energy can lead trapped electrons to be transferred into conduction band. Finally, recombination of freed electrons with

optically active trapped holes during radiative transition produces luminescence and it is called OSL. Figure 3.5 shows basic principles of OSL mechanism.

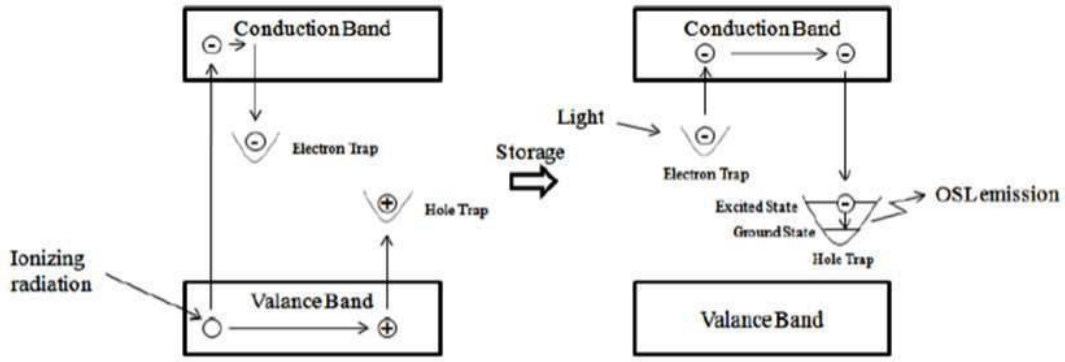

Figure 3.5: The OSL process (Kuşoğlu-Sarıkaya, 2011).

OSL measured in such a process is not constant but decay monotonically. The intensity of the luminescence decay is dependent on radiation dose and this dependence constitutes a basis for passive integrating dosimetry method (Bøtter-Jensen et al., 2003).

3.3.4 Thermally Stimulated Luminescence

Thermally Stimulated Luminescence or Thermoluminescence (TL) is based on excitation of previously irradiated luminescent material with heating. TL emission occurs as a result of the same process as that of OSL except that electrons are stimulated with heating in TL. As a result of absorption of proper heat energy, trapped electrons are freed and then captured by the trapped holes during transition from conduction band to valence band. Recombination of freed electrons with the trapped holes results in emission of luminescence. The observed luminescence is

called TL. Similar to OSL case the intensity is dose dependent which makes this method suitable for the passive integrating dosimetry (McKeever, 1985).

3.4 Luminescence Spectra and Its Interpretation

Study of interaction of electromagnetic radiation with matter is the general definition of spectroscopy. Luminescence spectroscopy measures the energy levels of the luminescence centers. The energy level of a luminescence center is defined as its characteristic state (Gaft et al., 2005).

Luminescence excitation, spontaneous emission and scattered light are three possible measurements in luminescence spectroscopy.

Luminescence excitation and emission spectra yield very important information about luminescence centers of samples having complex lattice structures. *Luminescence excitation spectrum* is a plot of intensity of emitted light from the material with respect to excitation wavelength. In the light of excitation spectrum, the most suitable wavelength of electromagnetic radiation to be used as an excitation source is determined. *Luminescence emission spectrum* is a plot of intensity measured over a range of emitted wavelengths at a fixed excitation wavelength. It contains information about the energy levels of luminescence centers and, in the case of time dependent measurements, the lifetime of excited states (Krbetschek et al., 1998). The information gathered from an emission spectrum is limited. That is to say, luminescence emission of nearby luminescence centers could be overlapped since the intensity of emitted light is measured in much longer periods compared the life time of excited states. This method is referred as steady state technique and only the most intensive centers are detected (Gaft et al., 2005). However, *time-resolved luminescence spectroscopy* is the most effective method to overcome this problem. The process is to measure the intensity at fixed wavelength with respect to time thus intensity decay curves of each recombination sites would be measured and materials

which contain large amount of emission centers at intimate energy levels could be measured. Unlike the steady state one, this method requires pulsed form of excitation. Vital point of this technique is to arrange the most suitable gate width and delay time for the excitation source. Time resolved luminescence spectrum enhances the knowledge about luminescence centers or activators. Moreover, this technique is useful to distinguish the fluorescence and phosphorescence emissions.

The following chapter introduces the design and implementation of the luminescence emission spectrometer used in this project.

CHAPTER 4

DESIGN AND DEVELOPMENT OF A LUMINESCENCE EMISSION SPECTROMETER LE-282

Within the framework of this study, a versatile luminescence emission spectrometer was designed and developed with the main purpose of measuring photoluminescence, thermoluminescence and optically stimulated luminescence emission spectra of materials relevant for dosimetry. The monochromator and the detector used in the study are actually retrieved from an old Atomic Absorption and Flame Emission Spectrophotometer (Shimadzu AA-680). In this study this monochromator and detector combination was converted into a luminescence emission spectrometer by developing necessary hardware and software to control it. The spectrometer was named as LE-282 where LE stands for "Luminescence Emission" and 282 stands for the focal length of the monochromator used in millimeters. In the rest of the text LE-282 will be used for the developed luminescence emission spectrometer.

In this chapter, structure, properties and components of luminescence measurement system built around LE-282 will be explained. Moreover, hardware and software of electronic control unit, computer software of user interface, light collection unit, optical components and measurement modes of LE-282 will be explained in detail.

4.1 Structure and Properties of Luminescence Measurement System

This part includes the explanation of structure, properties and optical components of luminescence measurement system. Figure 4.1 shows the simplified block diagram of the luminescence measurement system built on LE-282.

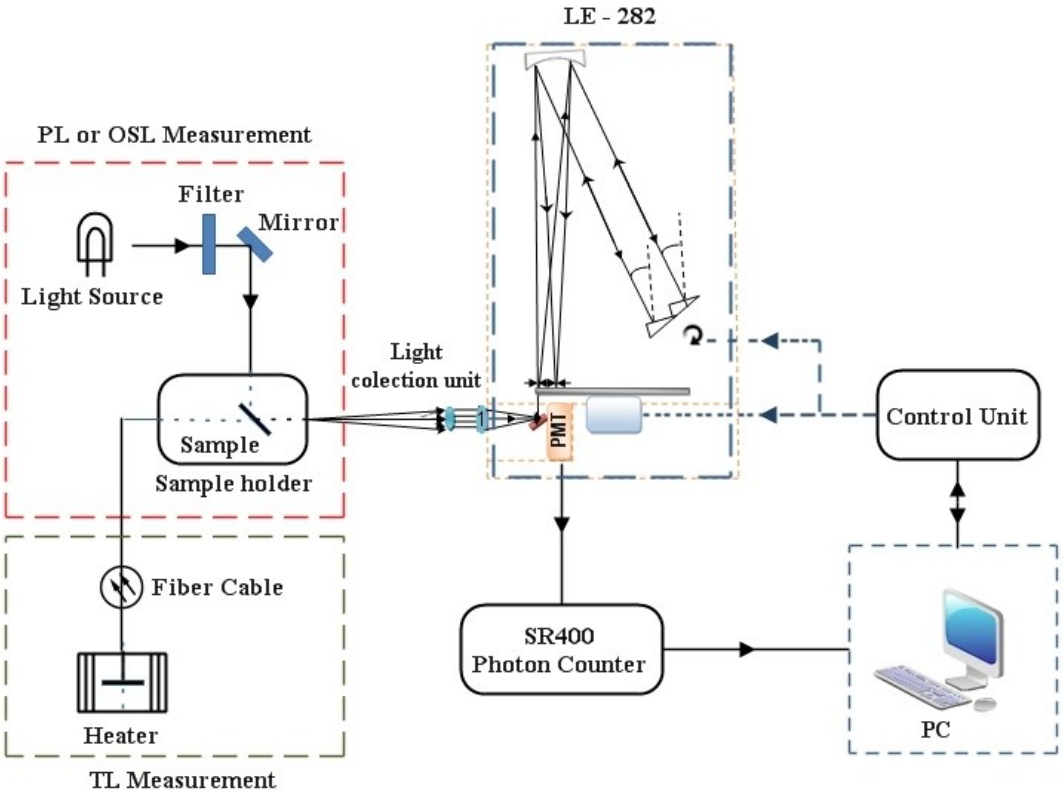

Figure 4.1: Simplified block diagram of the luminescence measurement system built on LE-282.

LE-282 is consisted of scanning monochromator (Littrow configuration) with reflective type of diffraction grating, photomultiplier tube (PMT, Hamamatsu R787-04) and six slits of different size.

As seen in Figure 4.1, there are two different measurement configurations related to PL-OSL and TL experiments. In order to use LE-282 as a TL emission spectrometer, the necessary components are heater and fiber cable. A sample is heated and the emitted light is transferred from heater to light collection unit of LE-282 by a fiber cable which is mounted in place of the sample. However, LE-282 can be configured as a PL-OSL emission spectrometer with proper light sources, filters and a mirror. Filter is placed in front of a light source in order to obtain a proper wavelength of excitation radiation for PL or stimulation radiation for OSL. Mirror is used to focus the incoming light onto a sample. Light collection unit is consisted of two quartz lenses. It is used to collect the light that spreads out from sample into an entrance slit of monochromator as much as possible.

Gated photon counter (SR-400 model, Stanford Research Systems) is used to count the number of photons incident on the PMT. The details will be mentioned in the section where photon counting mode is explained.

A personal computer is used to communicate with control unit and to save and monitor the graph of emission spectrum of any sample by taking wavelength information from control unit and intensity information from SR-400 respectively.

Control unit is an electronic device built in the laboratory which can communicate with computer via RS-232 and handle both data handling and data sending processes together. Control unit will also be mentioned briefly in the following parts.

With this type of instrumental configuration, signal reshapes or modifies at each step of luminescence measurement. Figure 4.2 shows the signal conversion chart.

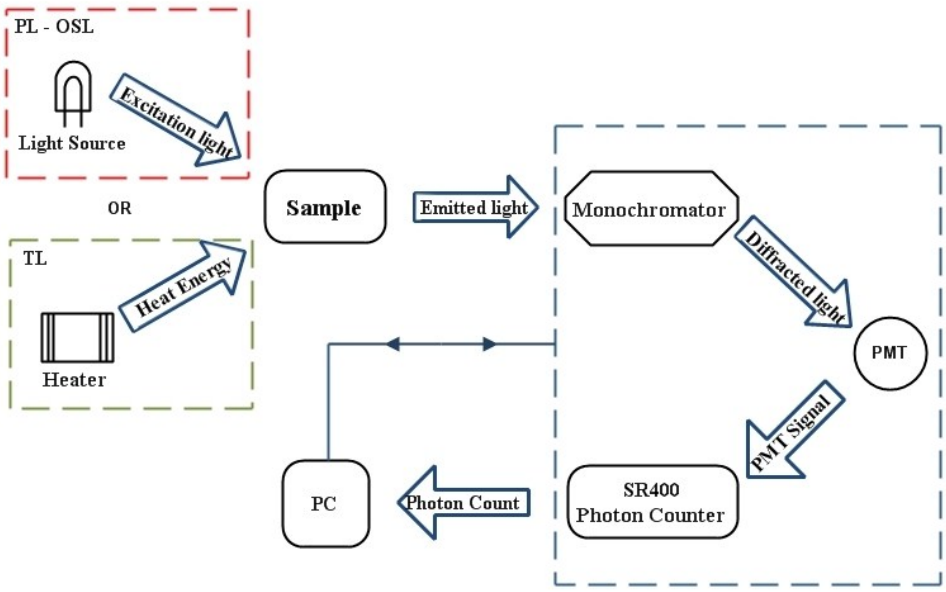

Figure 4.2: Signal conversion chart in luminescence measurement.

Proper wavelength of excitation radiation is absorbed by the sample and then emitted at different wavelength in PL measurements. In addition, previously irradiated sample is stimulated either with proper wavelength of light or heat energy in order to observe OSL or TL emission. The emitted light is diffracted into discrete directions by the monochromator and the intensity of diffracted light is converted into an electrical signal by the PMT. Then, the generated PMT signal is read by SR-400 in terms of number of photons. Finally, the information related to photon count is periodically sent to PC and monitored. The PC is always in communication with LE-282 and SR-400 during the measurement. Hence, user can control everything and be informed about the progress of the experiment.

Table 4.1: Properties of measurement system (see the manual of Shimadzu AA-680).

Measuring Mode			Emission Analysis
Measurement Modes			DC and Photon Counting
LE-282	**Monochromator**	Model	Littrow Type
		Focal Length	282 mm
		Diffraction Grating	Blazed Holographic Grating
		Groove density	1800 lines/mm
		Blazing Wavelength	250 nm
		Number of Slits	6
		Aperture Ratio	F9
		Resolution	0.17 nm (maximum)
	Detector	Type	Photomultiplier tube (PMT)
		Model	Hamamatsu R787-04
		Spectral Range	200 – 750 nm
		Operating Voltage	1150 V
Light Collection Unit	**Lens 2**	Model	Spherical biconvex, quartz lens
		Focal Length	50 mm
		Diameter	25 mm
		Thickness	5 mm
	Lens 1	Model	Spherical biconvex, quartz lens
		Focal Length	30 mm
		Diameter	18 mm
		Thickness	5 mm
Control Unit	Main Power Source		220V AC
	Motor Power Source		24V DC
	Microcontroller		PIC 18F4550 (8 bit, Microchip)
	Communication Standard		RS-232
	Baud Rate		115200 bps
Computer Interface			LabVIEW 8.6 (National Instruments)

4.2 Components of Luminescence Measurement System

4.2.1 Optics of LE-282 and Light Collection Unit

The luminescence measurement system around which LE-282 is constructed basically consists of a monochromator and a detector. The monochromator is used to select the desired wavelength in the range 190-900 nm (see the manual of Shimadzu

AA-680). The detector is a PMT which is used to measure the intensity of incident light. The structure of optical system of measurement setup is given in Figure 4.3.

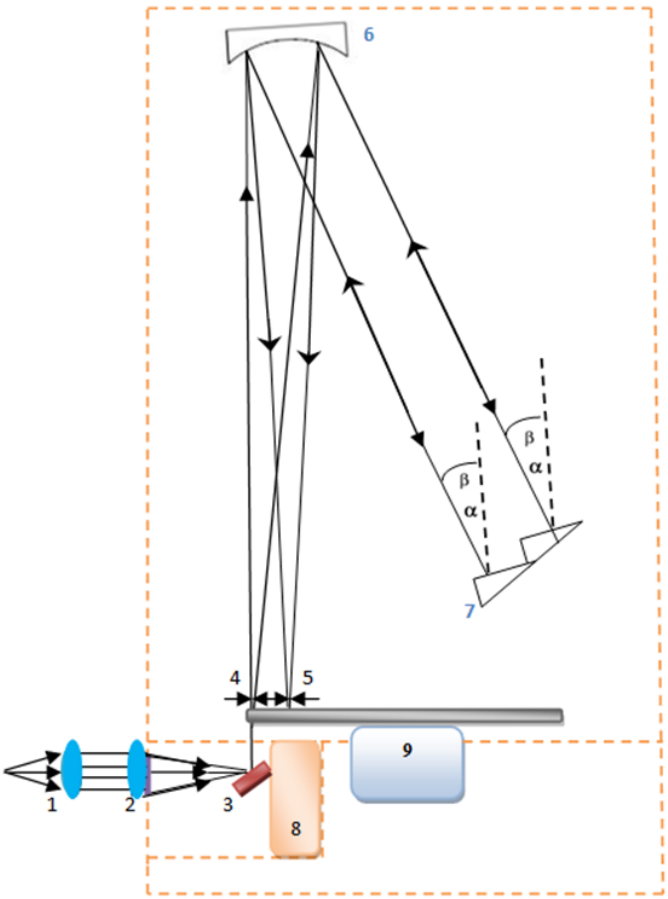

Figure 4.3: The geometric structure of optical system of LE-282. The part list is composed of 1 and 2 (spherical biconvex quartz lenses), 3 (flat mirror), 4 and 5 (entrance and exit slits), 6 (aspherical mirror), 7 (diffraction grating), 8 (PMT) and 9 (slit motor).

As seen in Figure 4.3, LE-282 has a Littrow mounted grating monochromator (see Chapter 2). The monochromator of LE-282 is consisted of a reflection type diffraction grating and a single aspherical mirror which directs the incident light onto diffraction grating and focuses the diffracted light through exit slit. The diffraction grating used in this monochromator is a blazed holographic grating with blazing

wavelength at 250 nm. In addition, groove density of the grating is 1800 lines/mm (see the manual of Shimadzu AA-680). The grating is rotated using a stepper motor with the help of a fine mechanical drive.

Spherical biconvex quartz lenses, which were shown in light collection unit (see Figure 4.1) are used to collect the light that spreads out from sample into an entrance slit of monochromator as much as possible and the flat mirror directs the beam through entrance slit.

Moreover, there are six entrance slits and exit slits with different widths mounted on a circular disk. They can be selected by rotation of slit motor at discrete steps.

The PMT used in LE-282 is sensitive in UV-VIS region. It is a "Side-on-Type" photomultiplier tube and has 9 dynodes where each one is connected with 100 KΩ resistors. The optimum operating voltage of PMT was determined to be 1150 V.

4.2.2 Electronic Control Unit of LE-282

In this part hardware components and software of electronic control unit of LE-282 will be explained in detail.

4.2.2.1 Hardware

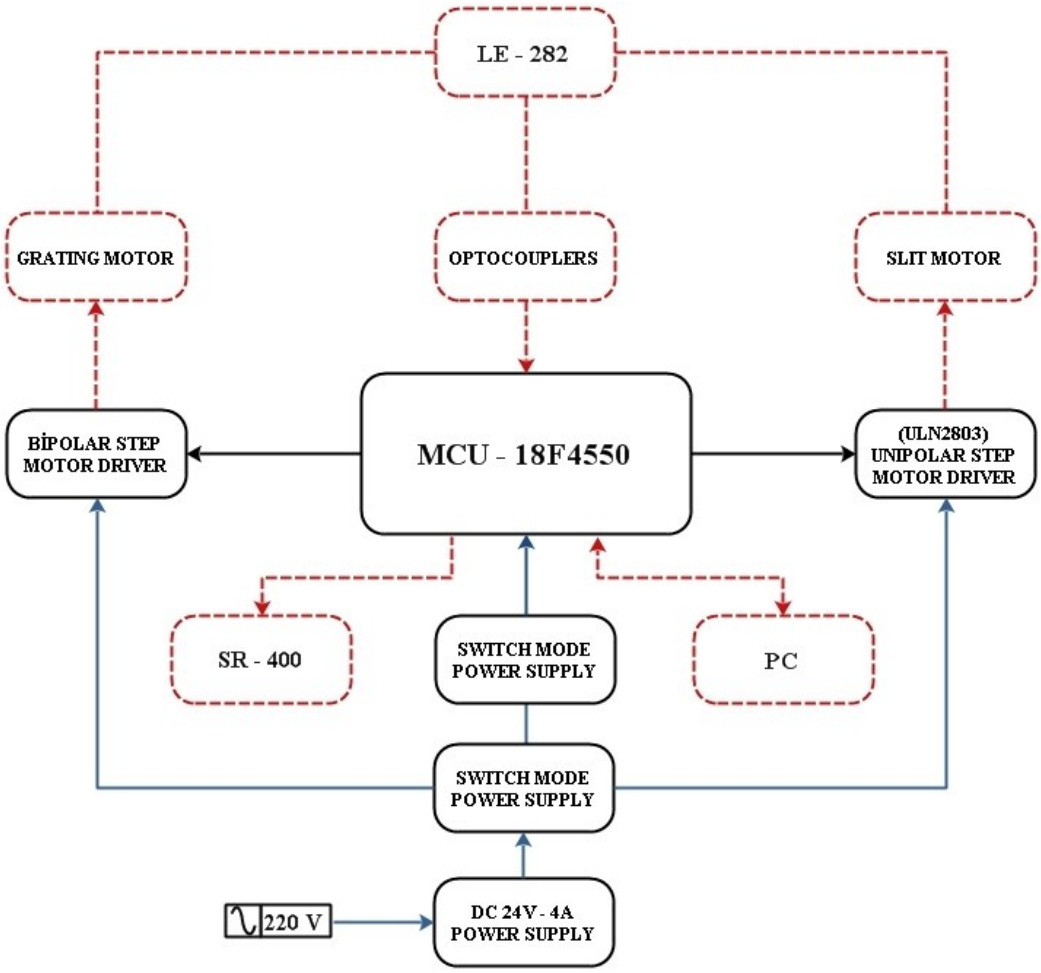

Figure 4.4: Block diagram of hardware of electronic control unit (Dashed lines correspond to connection of electronic control unit to other components of luminescence measurement setup).

Figure 4.4 shows the block diagram of hardware of electronic control unit which is consisted of step motor drivers, switch mode power supplies, 24V DC power supply, RS 232 module and PIC 18F4550 microcontroller (Microchip). 18F4550 is actually a small computer on a single integrated circuit containing a processor core, memory, and programmable input/output peripherals. It is the central unit of control system which provides a required trigger signal for SR-400 and driver cards of the

diffraction grating and slit motors to operate. The number of trigger signals determines the angle of rotation and thus the position of diffraction grating and slit disk. Moreover, 18F4550 has an ability to communicate with external devices via RS 232. Thus, all the required information and data are sent and received in this way.

There are three optocouplers (2xOmron EE-SH3 and Optek OPB840L) placed in the body of LE-282. Two of them enable diffraction grating to reach its default home position. The other one which is placed above slit disk provides a reference point for the slit selection. They give a feedback by using peripheral interrupt feature of 18F4550. Next part explains the software of electronic control unit of LE-282.

Moreover, wiring diagrams of control unit are shown in Appendix A.

4.2.2.2 Software

C programming language based software was compiled with MikroC (MikroElektronika) and the generated firmware was embedded into flash memory of 18F4550. The software can be examined in two parts. The first part deals with the wavelength scanning routine which was programmed to rotate the diffraction grating by user defined speed, interval and region. However, the second part of software deals with the control mechanism of slit disk.

Figure 4.5 below shows the flow chart of wavelength scanning part of the software.

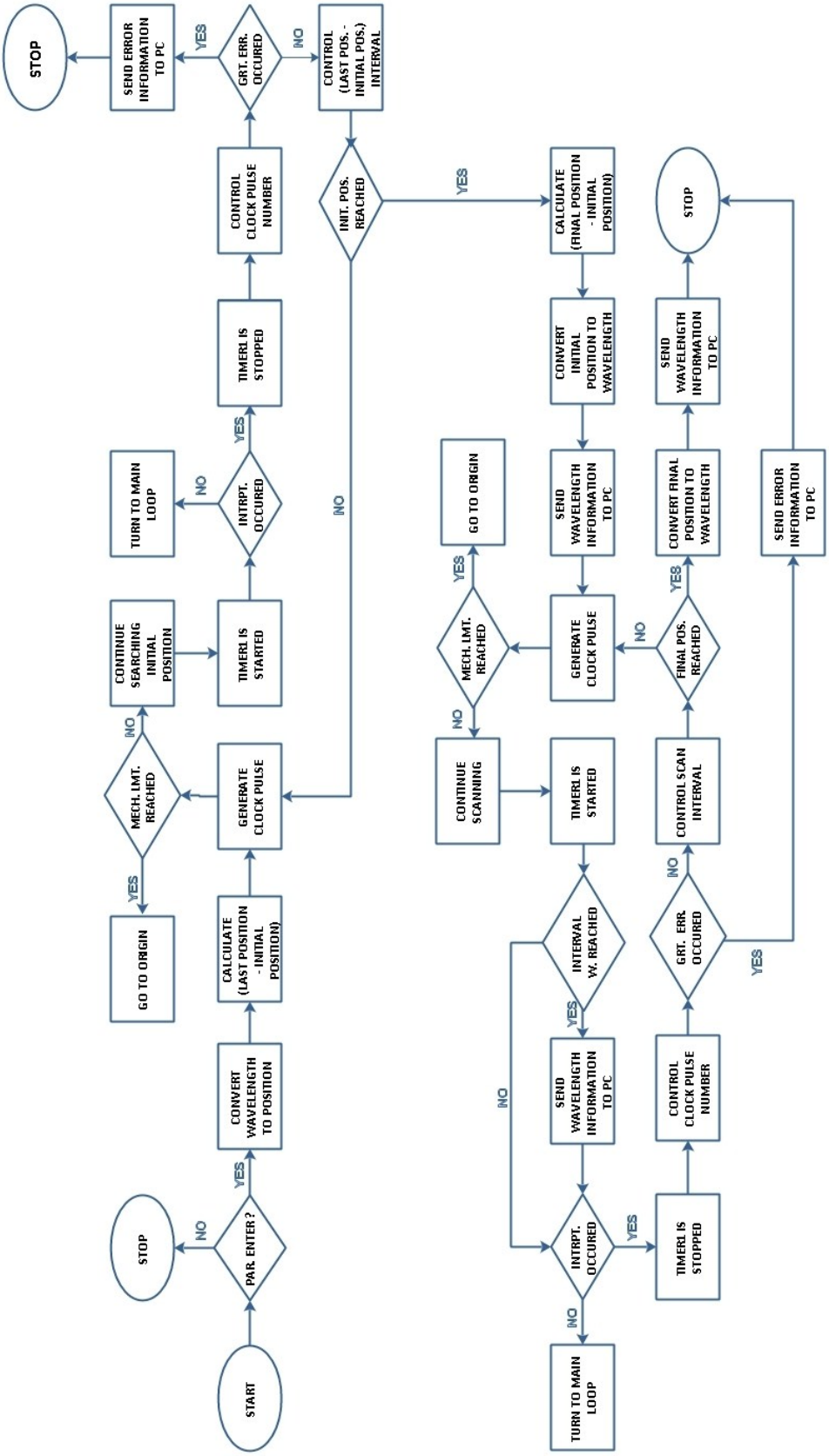

Figure 4.5: Flow chart of wavelength scanning part of the software.

The step motor which is used to rotate the diffraction grating is driven by a bipolar step motor driver and it requires clock pulses to operate (see Figure 4.4). Frequency of them, which is controlled by the counter (timer) of 18F4550, determines the speed of the motor. Thus, the speed information should be sent to 18F4550 by user before starting to scan.

Scanning region is determined by initial and final wavelength parameters. Thus, user should also send these parameters before starting to scan. In addition, interval wavelength parameter should be sent in order to determine the required data transfer interval.

The first thing that software makes is to check whether parameters were entered or not. If entered correctly, they are converted into initial and final position parameters by using the polynomial function (Eq. 5.1) which will be explained in wavelength calibration part of chapter 5. The related position parameters are then saved in the memory of 18F4550. The next thing that software makes is to subtract the recent position from the initial position and thus determine the number of steps to be taken in order to reach initial position. Direction of rotation is determined by considering the sign of the subtraction of the initial position value from the recent position value.

When the initial position is reached, similar with initial position search process, both the direction of rotation and the difference between final position and initial position are calculated and the scanning is started in the given region. During the scan, at each user defined wavelength interval, recent position value is converted to related wavelength value by using the inverse polynomial function (Eq. 5.2) and sent to computer via RS-232.

While turning the grating, software always checks whether mechanical limit error or grating error are occurred. Mechanical limit error occurs when one of the micro switches placed at the end of mechanical limits are closed. Grating error occurs when the number of steps the grating motor took in one complete tour is more than one

step above or below than 1000. If any of these errors is occurred, everything is stopped and grating motor is automatically directed to the origin.

Moreover, if the scanning is stopped or finished, recent position is recorded as recent position. Thus, software always remembers the final location of grating.

Figure 4.6 below shows the flow chart of slit disk rotation part of the software.

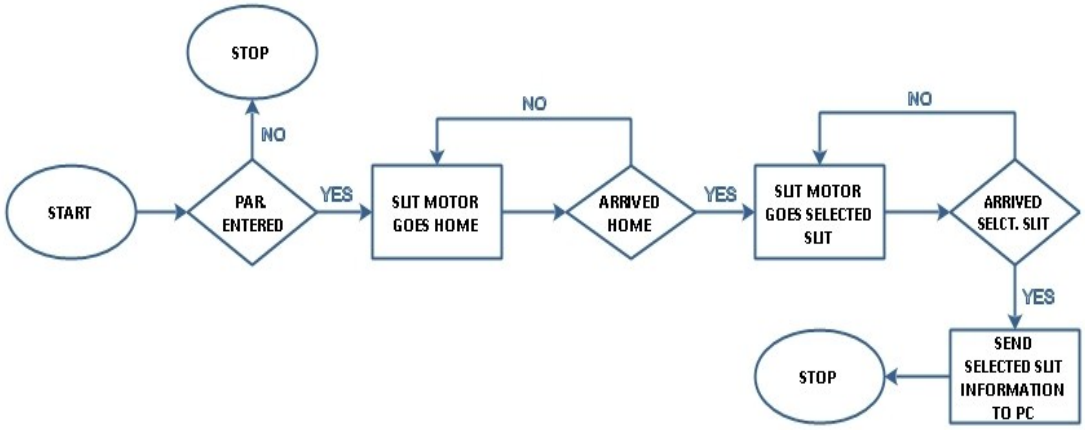

Figure 4.6: Flow chart of slit disk rotation part of the software.

The slit motor is driven by a unipolar step motor driver that requires clock pulses to operate (see Figure 4.4). Frequency of them, which is controlled by the counter (timer) of 18F4550, determines the speed of the motor. However, unlike the scanning case, this part of software does not require a user defined speed information and it always runs at constant speed.

There are six entrance and exit slits which are equidistantly placed from each other on slit disk. The position of each slit is calculated with respect to a home position and thus either initial position or final position parameters are not required. In this part of software, the only parameter that user should send to 18F4550 is the name of selected slit.

As seen in Figure 4.6, the first thing that software makes is to check whether slit name parameter was entered or not. If entered, slit motor starts to rotate and initially searches its home position. When it reaches the home position, the optocoupler sends related feedback to 18F4550. Next, slit motor rotates until selected slit position is reached. When it is arrived, related report is sent to the computer and it is stopped.

4.2.3 Computer Software

In order to control the whole system easily, a computer controlled, LabVIEW (National Instruments) based user interface was developed. Figure 4.7 shows the front panel screen of software. It is well designed and comprehensive software so that user can control and monitor everything by using this panel.

As seen in Figure 4.7, the left side of program is the main control unit and the scan parameters are entered according to chosen measurement method. If the experiment is to measure the *Intensity vs. Wavelength* than the four parameters which are *starting wavelength*, *final wavelength*, *interval wavelength* and *scan speed* should be entered by the user. However, if the experiment is to measure the *Intensity vs. Time* then, *scan period* and *selected wavelength* are the two required parameters that user should enter. In addition, there is a *select slit* part. It is used when recent slit is going to be changed. When the parameters are entered correctly and the *start button* is pressed, scanning starts and the graph of selected measurement mode is plotted.

At the end of each scan, data of related measurement can be saved into a file using *save data* function.

Go origin function is used to select home position. *Stop* function is used whenever stopping the measurement is required.

Status LEDs are very important functions of the software. They indicate the actual status of measurement setup. User can follow the active processes through them. Moreover, whenever an error is occurred, it is shown by these LEDs. As seen in Figure 4.7, each process or error statement has a discrete status led.

Moreover, Figure 4.8 shows only the little portion of the block diagram panel of computer software.

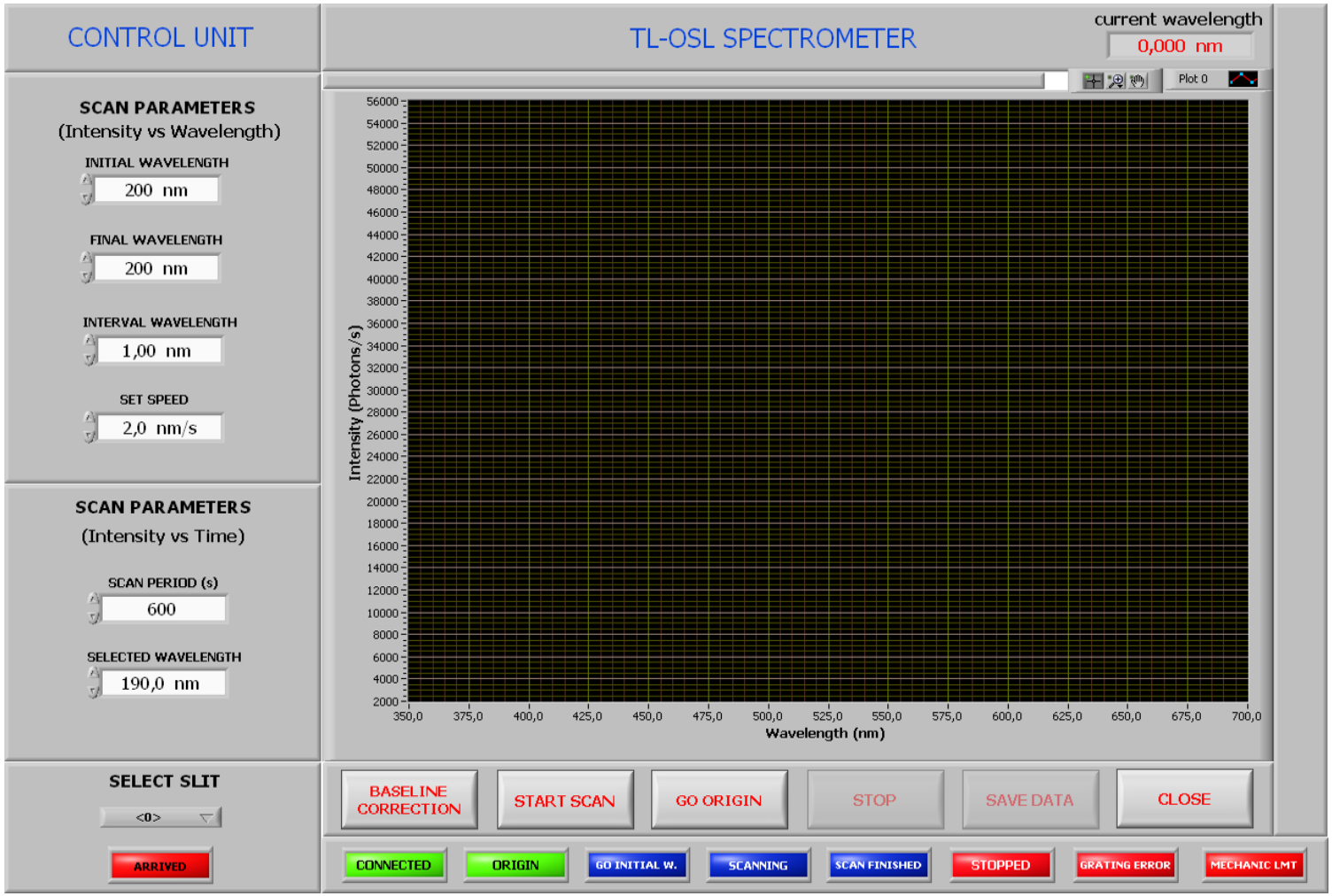

Figure 4.7: LabVIEW front panel screen of computer software.

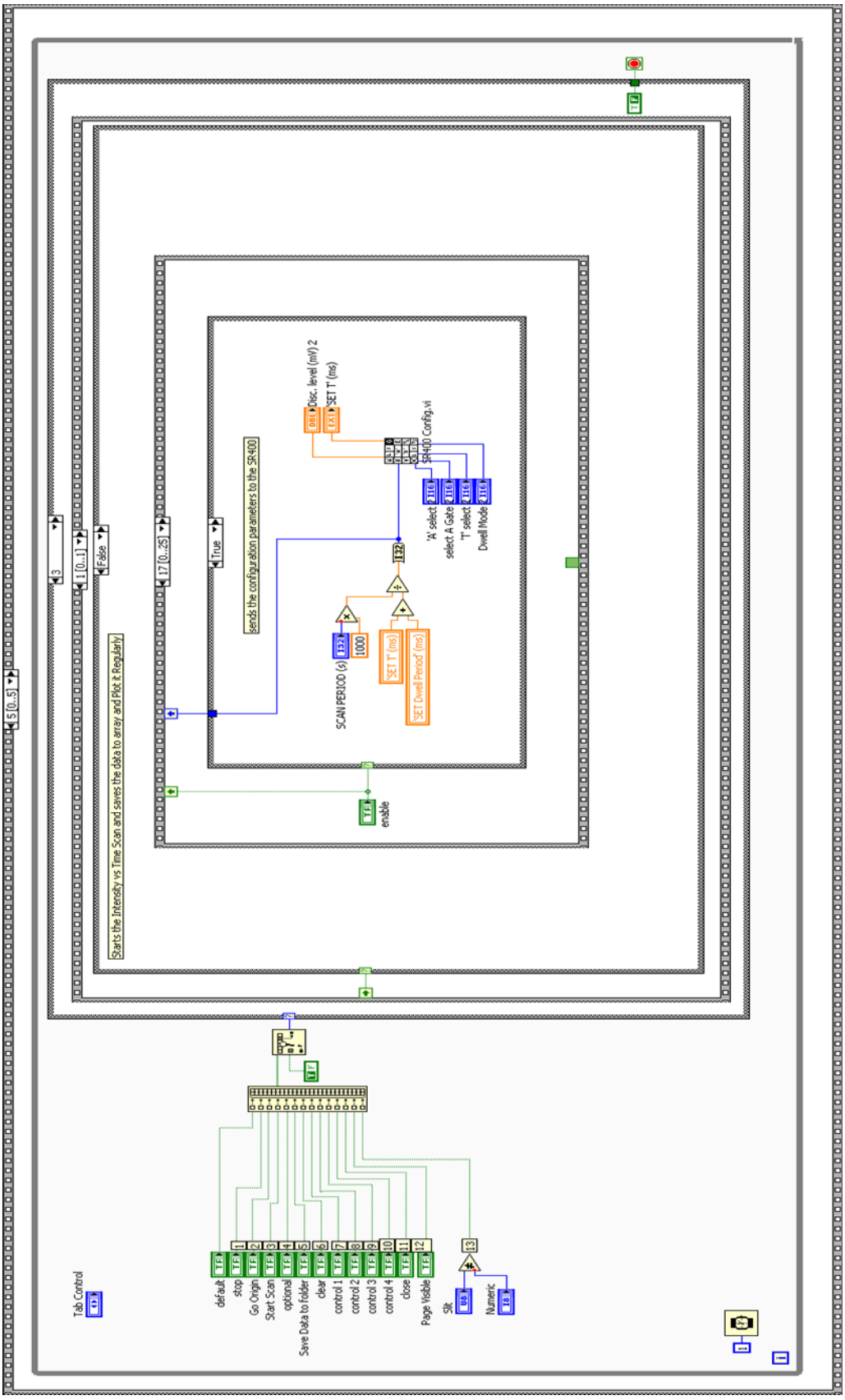

Figure 4.8: LabVIEW block diagram screen of computer software.

4.3 Principles of Measurement Modes

The main measurement mode of measurement system is photon counting. In determining the spectral response and wavelength calibration of the system and in test experiments, whose results are given in chapter 5, DC measurement mode was preferred since the light sources were very bright. In this part, these measurement modes will be explained in detail.

4.3.1 Photon Counting

Photon counting is one of the modes used in measurement of light intensity. It is generally preferred at very low light levels and depends on measurement of intensity of light by counting individual photons incident on PMT.

In this study, photon counting method was used for measurements of PL, TL and OSL emission spectra of various dosimetry materials. In the current setup there are two options of photon counting mode are available. They are named as Intensity vs. Wavelength and Intensity vs. Time. Figure 4.9 shows the simplified experimental procedures in both options during the measurement based on photon counting.

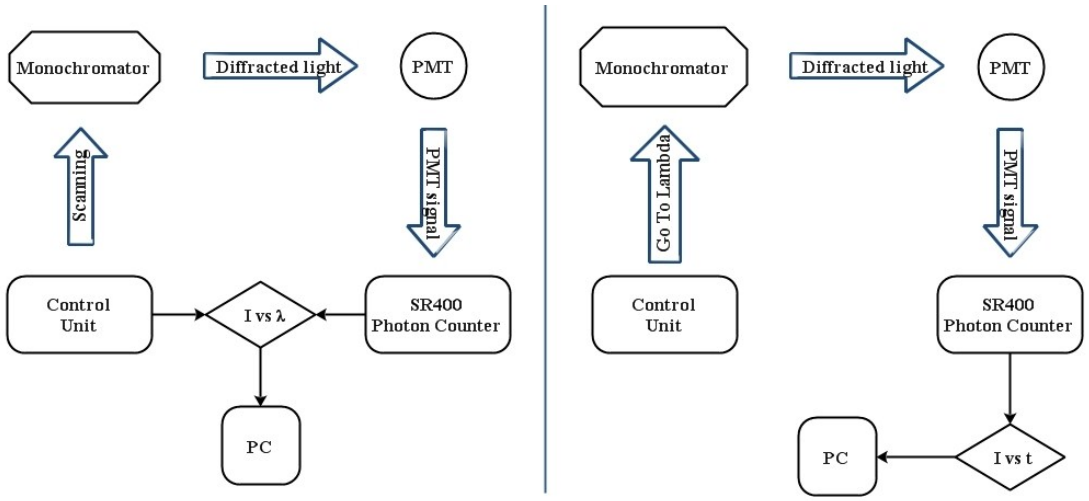

Figure 4.9: Simplified experimental procedures of two different photon counting modes. The left side describes the Intensity vs. Wavelength and the right side describes the Intensity vs. Time mode of photon counting.

The SR-400 contains discriminators, gate generators and counters together in a single device and makes it easy to determine the number of pulses coming from the PMT at a selected counting interval.

The SR-400 has two independent channels which can count at rates up to 200 MHz Thus; each of the channels has 5 ns pulse pair resolution. In addition, both analog signal inputs are internally terminated by 50Ω resistor and followed by 300 MHz DC amplifier which allows the discrimination and detection of pulses as small as 10 mV.

Photon counting process is handled in periodic time intervals defined by the user. The number of intervals determines the length of the measurement. In addition, SR-400 can easily communicate with a computer via RS 232. Thus, at the end of each count period, it sends the total number of counted photons.

If the Intensity vs. Wavelength option is selected, the monochromator is used to scan the area determined by the control unit with user defined parameters. At each defined wavelength interval, SR-400 is gated by 18F4550 (see Figure 4.4) and the counting is started. At the end of each measurement cycle, information related to recent

wavelength and intensity (i.e. number of photons) is obtained respectively from the control unit and SR-400 and is sent to PC.

Intensity vs. Time option is generally used in measurement of time dependence of a luminescence signal at a preselected wavelength. In this mode, the monochromator is set to a desired wavelength of observed light and the time evolution of the luminescence was observed as a function of time. Such a measurement mode can be useful in the study of dynamic behavior (kinetics) of the luminescence signals.

4.3.2 DC Measurement Mode

This measurement mode is suited for the detection of relatively high light levels. In this mode, only DC portion of PMT output signal is detected by means of an amplifier and lowpass filter. In this study, DC mode was used in determining the spectral response and wavelength calibration of the system. Moreover, luminescence intensities of light sources used in the test experiments were also measured in DC mode.

Figure 4.10 shows the simplified experimental procedure of measurement of light intensity in DC mode. The diffracted light incident on the PMT creates a DC current at the output. The current to voltage conversion and the gain of amplification of signal are adjusted by the amplifier circuitry whose wire diagram is given in Appendix A. Low-pass filter eliminates the fluctuations at the output signal and the undesired high frequency signal which is generated by the amplification of noise. The cleaned signal is converted to digital form by the analog to digital converter (ADC) of 18F4550 and the related information about intensity is sent to PC.

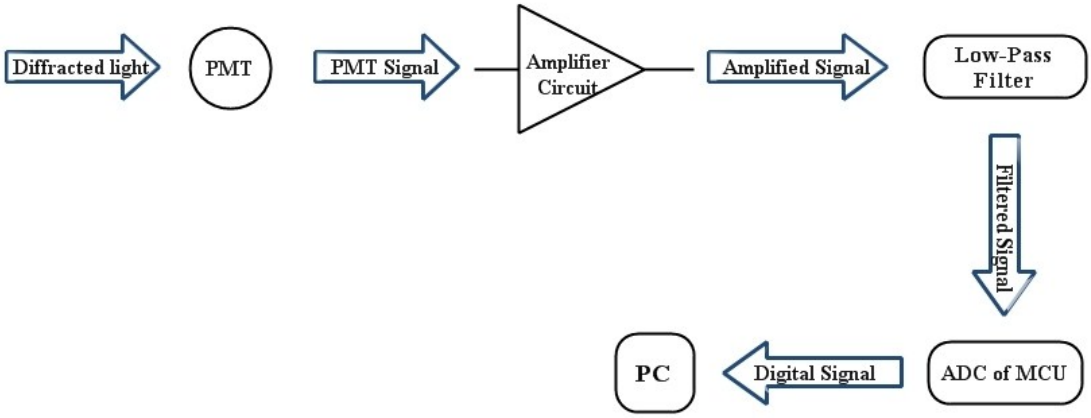

Figure 4.10: Simplified experimental procedure of measurement of light intensity in DC mode.

In this chapter, structure, properties, electronic hardware, software and computer interface of luminescence measurement system built on LE-282 which was designed and developed as an emission spectrometer in order to measure the luminescence emission signal of various dosimetry materials were explained. Some of the pictures of luminescence measurement system with components are given in Appendix B. Next chapter, results and discussion part, explains the results of calibrations, test experiments and performance tests of the system.

CHAPTER 5

RESULTS AND DISCUSSIONS

With the completion of the hardware and the firmware of electronic control unit and the computer software, development process of LE-282 continued with wavelength calibration, determination of spectral response and measurement of resolution of the system. Related results are given in the first four sections of this chapter. Next, with the aim of checking the performance of LE-282, some tests were carried out by using various light sources. In addition, PL, OSL and TL emission spectra of various samples were measured. In the following sections, experiments carried out to reach this aim and their results are discussed.

5.1 Wavelength Calibration of Monochromator

LE-282 luminescence emission spectrometer consists of a monochromator and a photomultiplier tube. Diffraction grating inside the monochromator is mounted on a drive shaft so that it can be rotated along its axis.

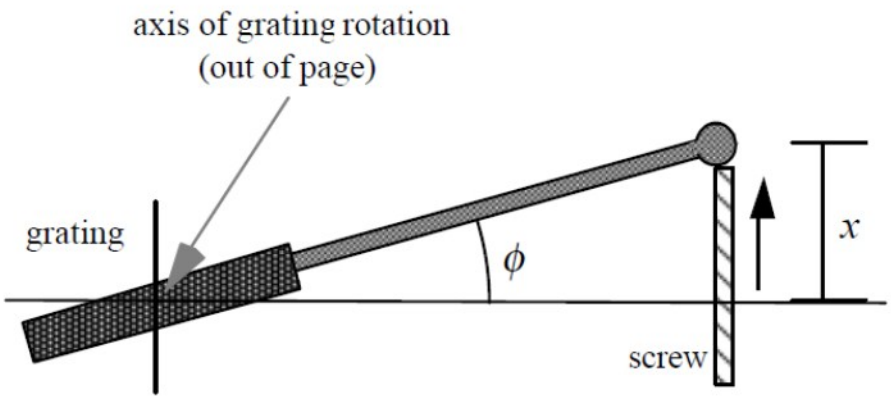

Figure 5.1: Sine bar mechanism for wavelength scanning (Palmer and Loewen, 2005).

In this monochromator a constant-deviation mount is used in which the wavelength λ is changed by rotating the grating about the axis coincident with its central ruling; with the directions of incident and diffracted light remain unchanged. In addition, as it is seen from figure 5.1, diffraction grating rotates through an angle ϕ in such a way that $\sin\phi$ is proportional to x. Constructive interference pattern is obtained by rotating the diffraction grating with proper angle. Mechanical design of the monochromator allows the position of screw along x direction to be changed in 70 mm of distance with the help of a stepper motor.

A relation between the wavelength of diffracted light and the screw position was obtained with the help of a mercury-argon calibration lamp of Ocean Optics (HG-1) by scanning the monochromator from an initial position to final one.

Figure 5.2 shows the spectral output of HG-1 given by Ocean Optics. Mercury emission lines lie in the region between 200 and 600 nm. However, argon emission lines lie in the region between 600 and 950 nm. Figure 5.3 shows the measured intensity of HG-1 with respect to the screw position. Ten of the sharp lines shown in Figure 5.3 were randomly chosen and scanning was made in approximately 1000

step interval for 4 times for each line in order to have an idea about the scatter of the results.

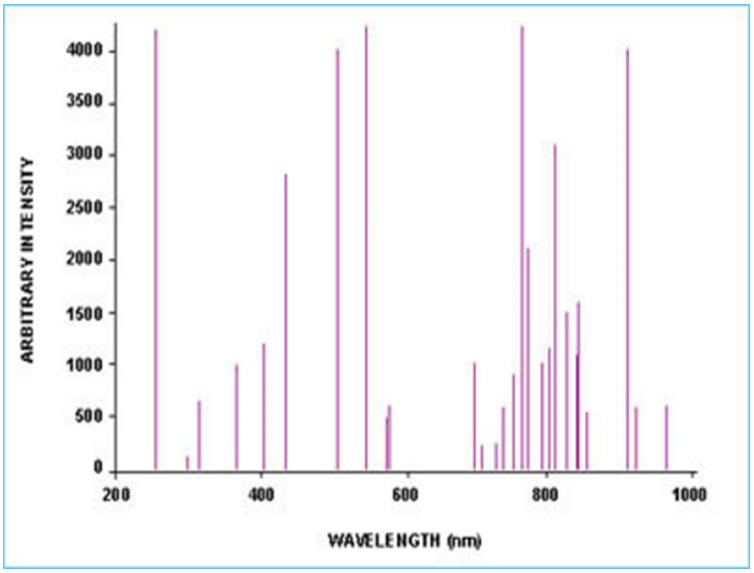

Figure 5.2: Emission spectrum of Hg-Ar calibration source. (Ocean Optics, 2011).

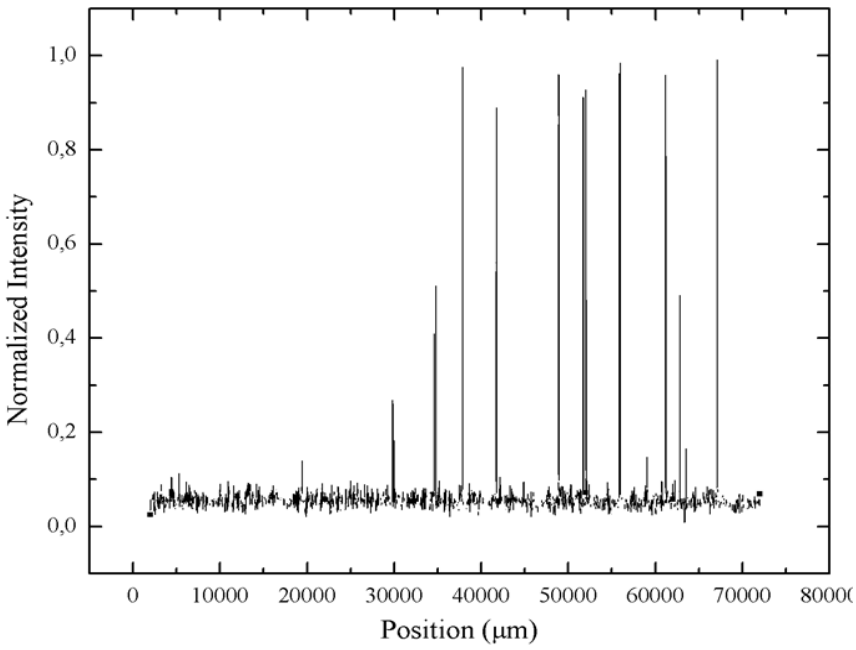

Figure 5.3: Measured Intensity of HG-1 with respect to the position of screw.

Selected set of experimental data points were fitted to a third order polynomial function in order to determine the relation between screw position and wavelength of light accurately. Figure 5.4 shows both the experimental data points and polynomial function.

Both the normal and inverse relations of wavelength (λ) and screw position (x) are given by the following equations;

$$x = (1{,}20 * 10^{-5})(\lambda)^3 - 0{,}017(\lambda)^2 - 92{,}81(\lambda) + 91525{,}52 \quad (5.1)$$

$$\lambda = (1{,}22 * 10^{-13})(x)^3 + (1{,}70 * 10^{-8})(x)^2 - 0{,}01(x) + 935{,}22 \quad (5.2)$$

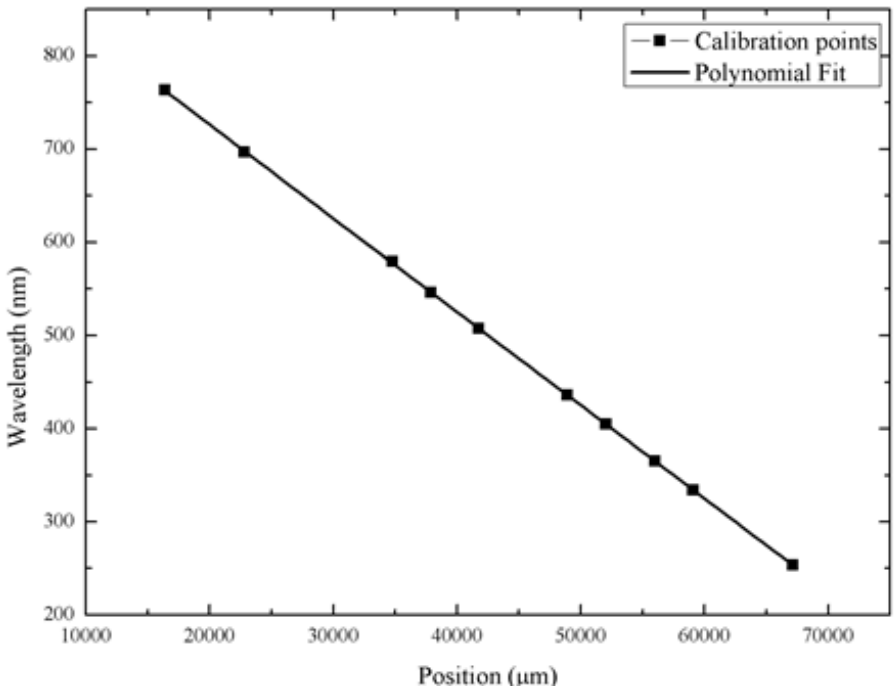

Figure 5.4: Wavelength as a function of screw position (Solid line represents the polynomial fit).

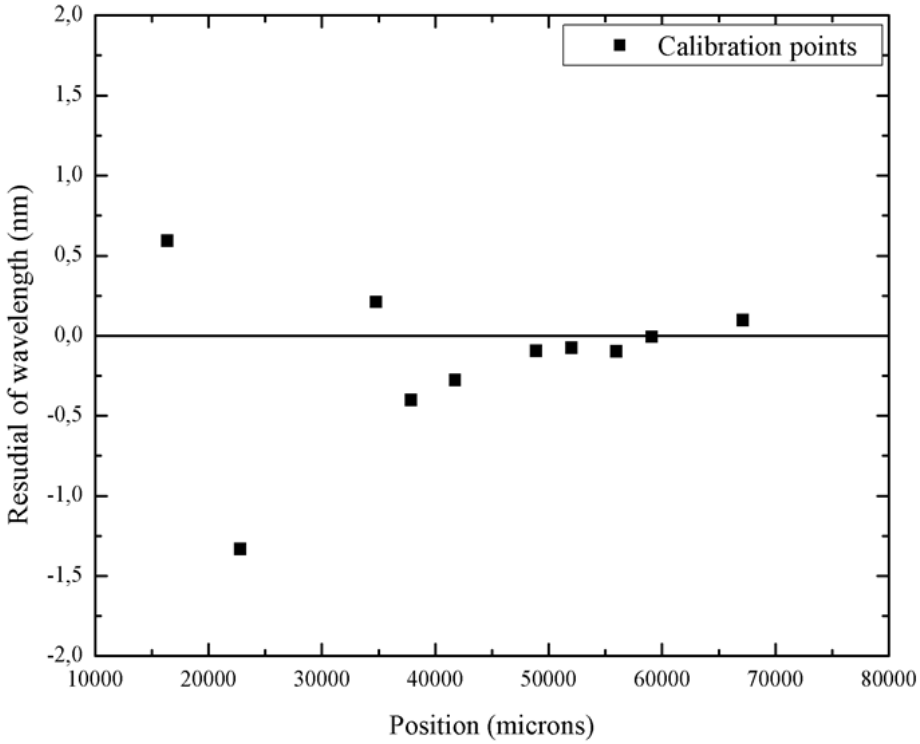

Figure 5.5: Residual plot of measurement points used for wavelength calibration.

As seen in Figure 5.5 above, except for the first two points, remaining points nearly fit the polynomial function with less than 0.5 nm difference. The problem with the first two points arises from the fact that spectral response of PMT is very low after 700 nm which corresponds to the screw position in the range of 10000 to 30000 μm.

By using equations Eq. (5.1) and Eq. (5.2), diffracted light from grating for a given screw position (and vice versa) can be determined. Moreover, by using these equations, one can explain that 0.1 mm displacement in position of the screw corresponds to 1 nm change in wavelength. However, mechanical resolution was obtained to be 0.01 nm in accord with this result since 0.1 mm displacement of the screw corresponds to 100 steps of grating motor which means that 1 step of grating motor should yield 0.01 nm change in wavelength.

5.2 Determination of Spectral Response of Measurement Setup

Overall spectral response of LE-282 was determined by using a halogen lamp (in the region 350 to 900 nm) and a deuterium lamp (in the region 200 to 400 nm) combination. Using the overlap region (350 to 400 nm) spectral response obtained for each lamp was matched to reach a single spectral response curve.

The spectrometer has six slits of different size, thus the experiment mentioned above was repeated for each slit.

5.2.1 Measurement of Spectral Response Using Halogen Lamp

The experimental setup that was built to determine the spectral response of LE-282 in the region 350 to 900 nm consists of a 55W Halogen Lamp (operated with 3.1A, 8V), reflective neutral density filters (Thorlabs ND Filters, 350-1100 nm of transmittance), fiber spectroradiometer (IntLightSpect RPS900) and LE-282.

Neutral density filters were used to prevent PMT from being saturated. Moreover, they have almost stable transmittance along the given spectral region.

The corrected spectrum was measured by the fiber spectroradiometer and the normalized result is shown in Figure 5.6.

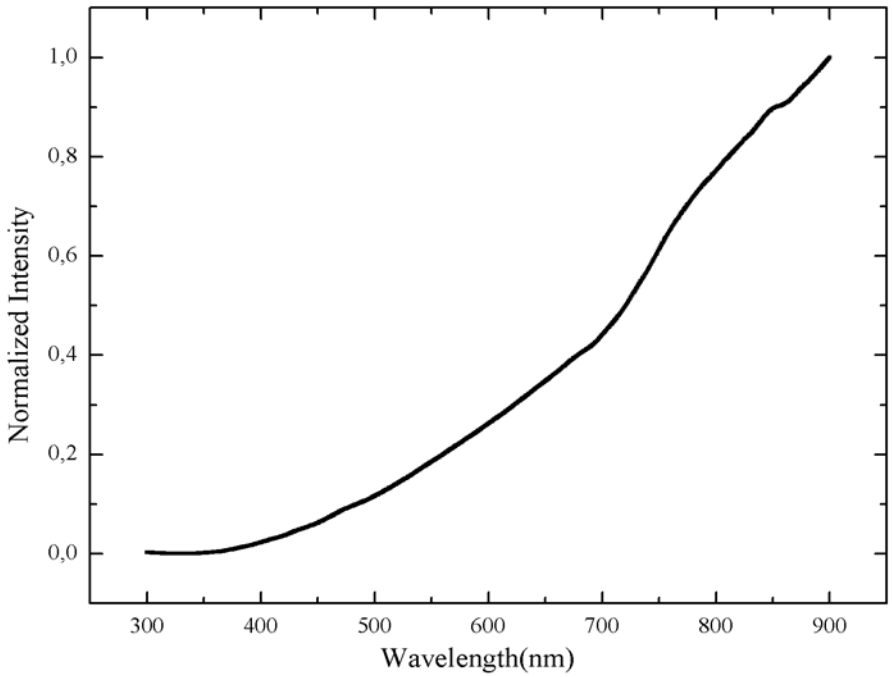

Figure 5.6: Corrected spectrum of halogen lamp, measured by fiber spectroradiometer.

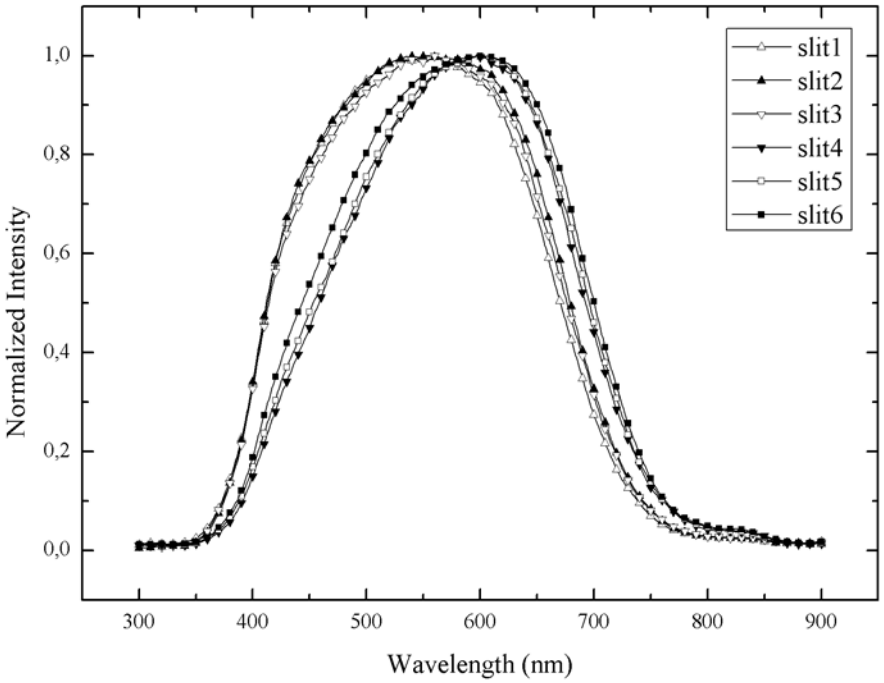

Figure 5.7: Spectra of halogen lamp for each slit, measured by LE-282.

For each slit, spectra of halogen lamp were measured for 4 times from 350 nm to 900 nm. Then the average of measurements was calculated and normalized (see Figure 5.7). As seen in Figure 5.7, there is an unexpected spectral shift between spectra of first three and last three slits. Such a discrepancy is supposed to be observed due to a skew on the surface of slit disk which makes the scattered light directly reach up to PMT and it shifts the spectrum to right as the intensity of halogen lamp increases toward infra-red region (see Figure 5.6). This kind of wavelength shift might be observed if high power light sources having broad continuous spectrum, like halogen lamp, are used. Fortunately, this is not a big problem in measurement of line emissions.

Finally, using the relation Eq. (5.3) given below, spectral response of system in region 350 to 900 nm was calculated for each slit. The results are shown in Figure 5.8.

Measured Intensity = Corrected Intensity x Spectral Response of System (5.3)

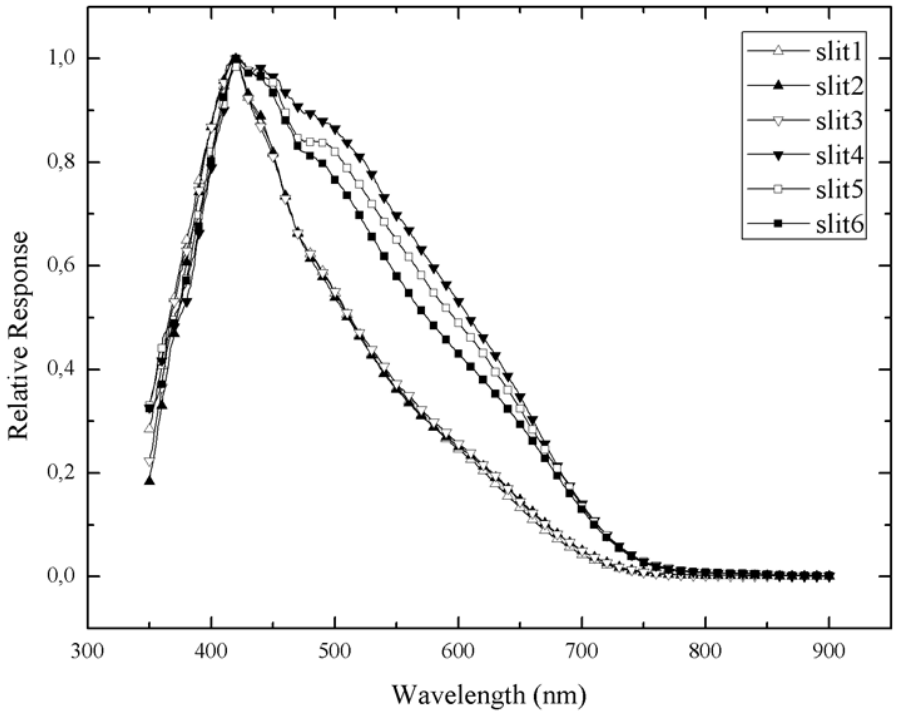

Figure 5.8: Spectral response of LE-282 in the range of 350 to 900 nm for each slit.

5.2.2 Measurement of Spectral Response Using Deuterium Lamp

In this part, spectral response of LE-282 in the range of 200 to 400 nm is determined by using a deuterium lamp which has a continuous spectrum in that region.

The experimental setup that was built to determine the spectral response of system in the range of 200 to 400 nm consisted of a deuterium Lamp (Hamamatsu DS 350U), fiber spectroradiometer and LE-282.

The corrected spectrum of deuterium lamp was measured by fiber spectroradiometer and the normalized result is shown in Figure 5.9.

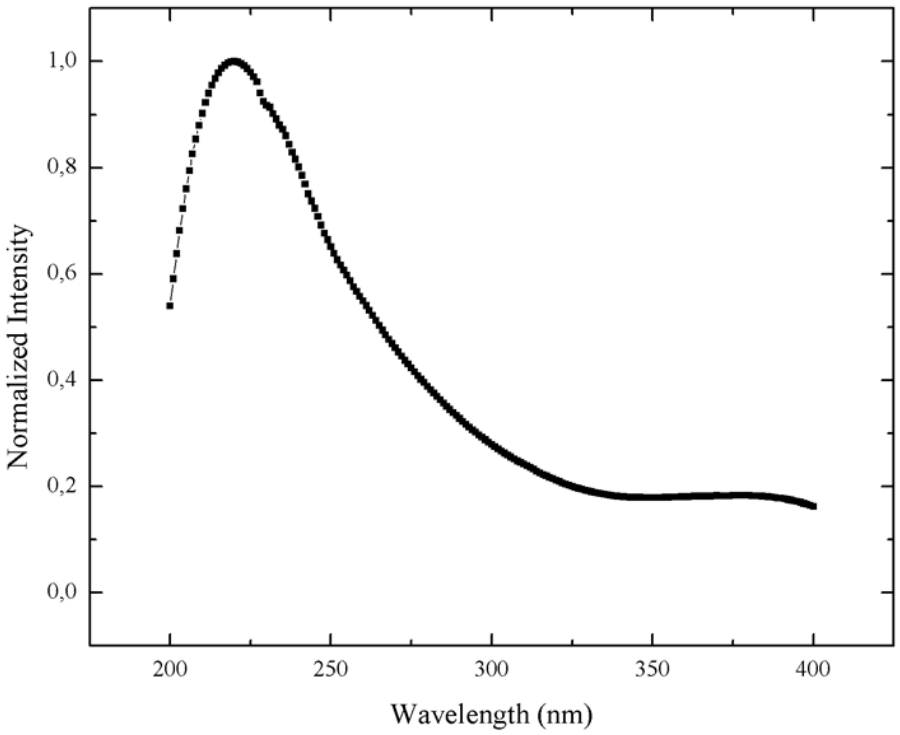

Figure 5.9: Corrected spectrum of deuterium lamp, measured by fiber spectroradiometer.

For each slit, spectra of deuterium lamp were measured for 4 times from 200 nm to 400 nm. Then the average of measurements was calculated and normalized. Results are shown in Figure 5.10.

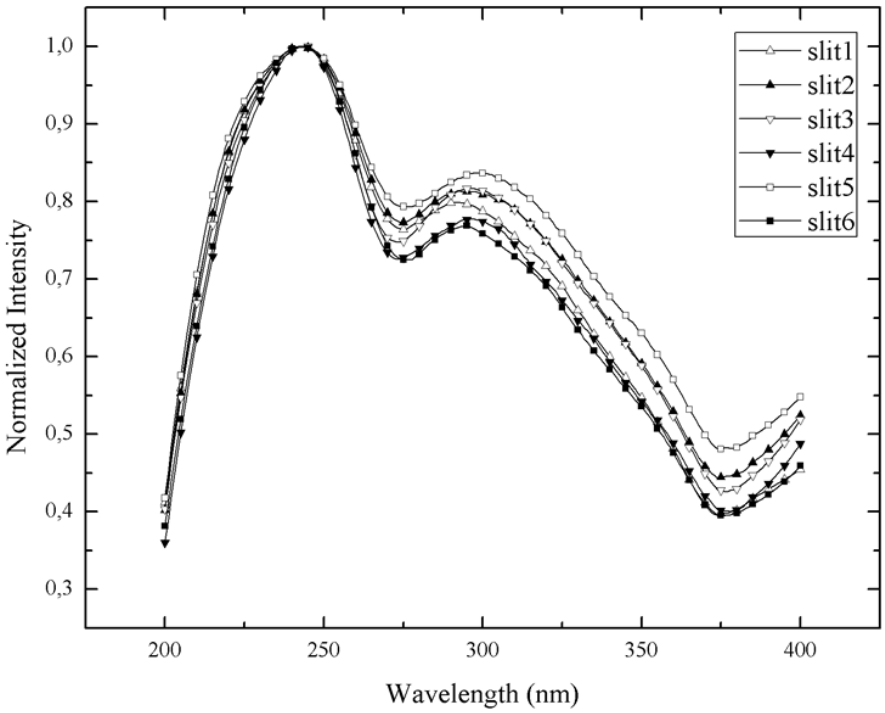

Figure 5.10: Spectra of deuterium lamp for each slit, measured by LE-282.

As seen in Figure 5.10, in contrast with the spectra of halogen lamp which are shown in Figure 5.7, no spectral shift was observed between measurements made with different slits since optical sensitivity of diffraction grating, which is blazed at 250 nm (see Figure 5.10, there is a peak nearly at 250 nm), is much more dominant than both the scattered light in that region and PMT sensitivity which is supposed to be highest around 450 nm.

The spectral response of LE-282 in region between 200 and 400 nm was calculated for each slit by using the same formula given by Eq. (5.3). The results are shown in Figure 5.11.

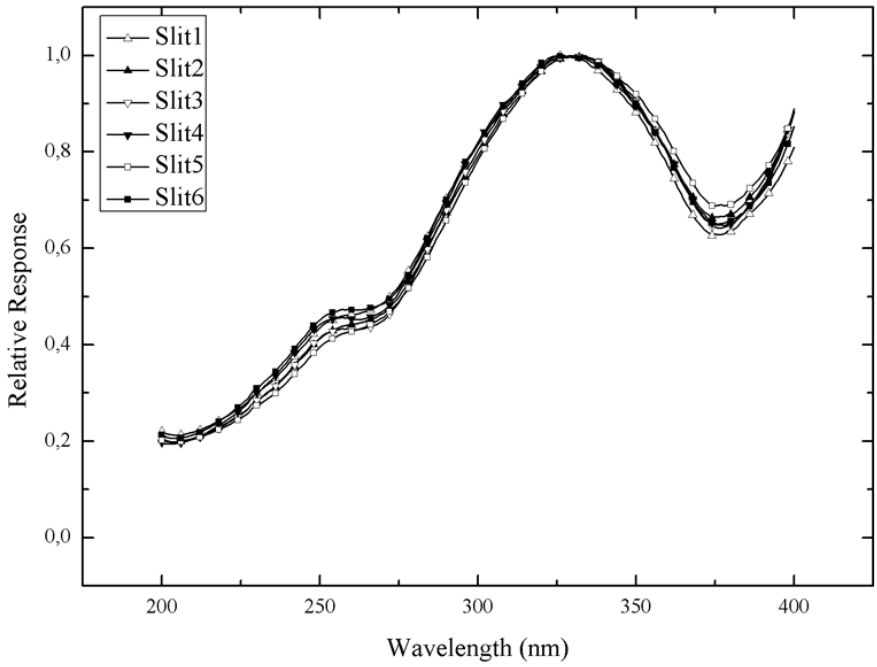

Figure 5.11: Spectral response of LE-282 in the range of 200 to 400 nm for each slit.

Finally, spectral response curves which are obtained by halogen and deuterium lamp measurements were matched in the overlapped region which contains the spectrum in the range of 350 to 400 nm. After the matching operation, the general spectral response curves for each slit were obtained as plotted in Figure 5.12.

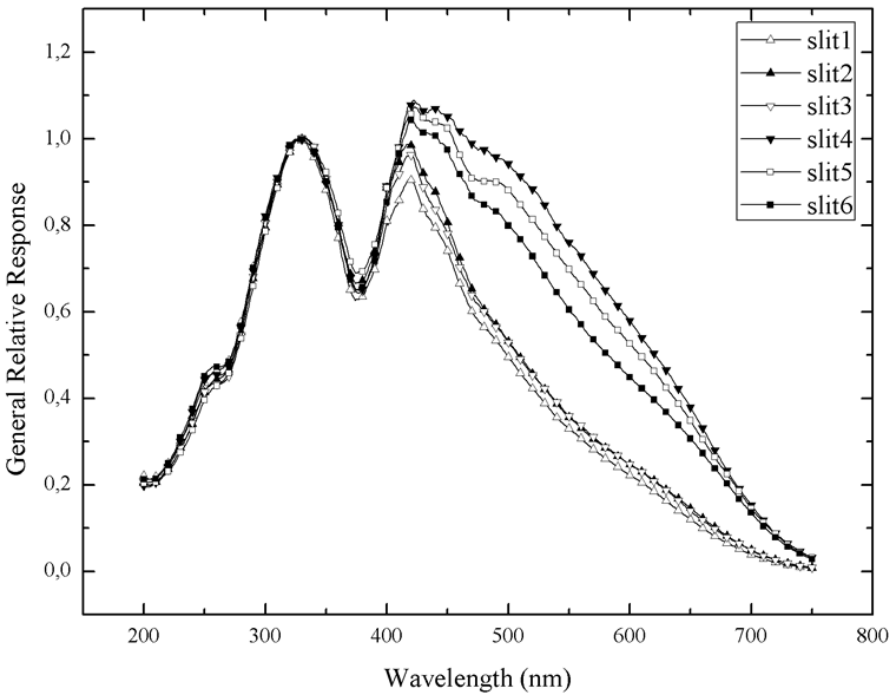

Figure 5.12: Overall spectral response of LE-282 for each slit.

5.3 Determination of Optical Resolution

The optical resolution of LE-282 was determined using line emitters (Melles Griot HeNe green and red lasers emitting at 543.5 nm and 632.8 nm respectively). For the six slits, laser emissions were recorded and full width at half maximum (FWHM) values were determined.

Experiment setup that was built for measurement of resolution consisted of line emitters, ND filters, concave lens and LE-282. ND filters were used with different combinations for different slits in order to prevent the photomultiplier tube from being saturated. Concave lens is used to expand the beam spot and so the intensity is decreased.

According to information obtained from Melles Griot, HeNe green laser is centered at 543.0 nm and has a very small full width at half maximum (FWHM) of approximately 1.4 GHz (0.001 nm). However, when measured by LE-282, the line broadening of laser beams related to various slits were obtained as plotted in Figure 5.13. According to measured spectra, FWHM of laser beam is recorded minimum at slit 1 as 0.17 nm and maximum at slit 6 as 2.28 nm. Thus, recorded spectra can be regarded as instrumental line profiles of monochromator at different slits. The whole results were listed in Table 5.1. In addition, since the broadening due to slits is the decisive factor in bandpass, FWHM increases with wider slits. However, resolution, which is explained individually separation of two close peaks in a given spectrum decreases with wider slits due to line broadening.

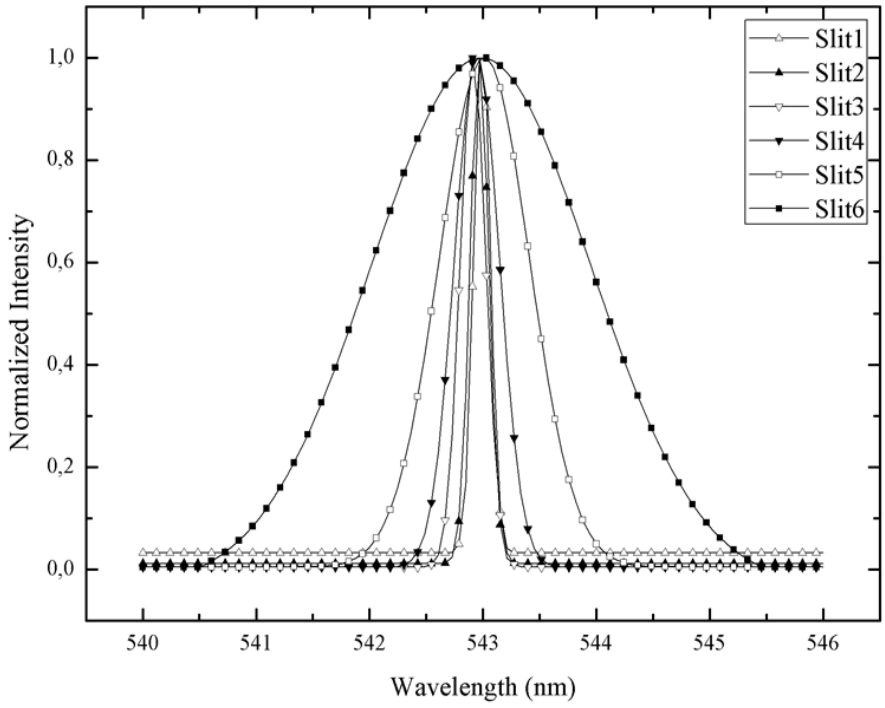

Figure 5.13: Instrumental bandpass of LE-282 for each slit, recorded with HeNe green laser, emitting at 543 nm.

The bandpass and resolution of LE-282 was also determined by using HeNe red laser whose emitting wavelength is given by Melles Griot as 632.8 nm. It has approximately the same FWHM (0.001 nm) with green laser. The similar line broadening was observed in this measurement. The instrumental line broadening of LE-282 related to different slits were shown in Figure 5.14. In addition, whole results were also listed in Table 5.1.

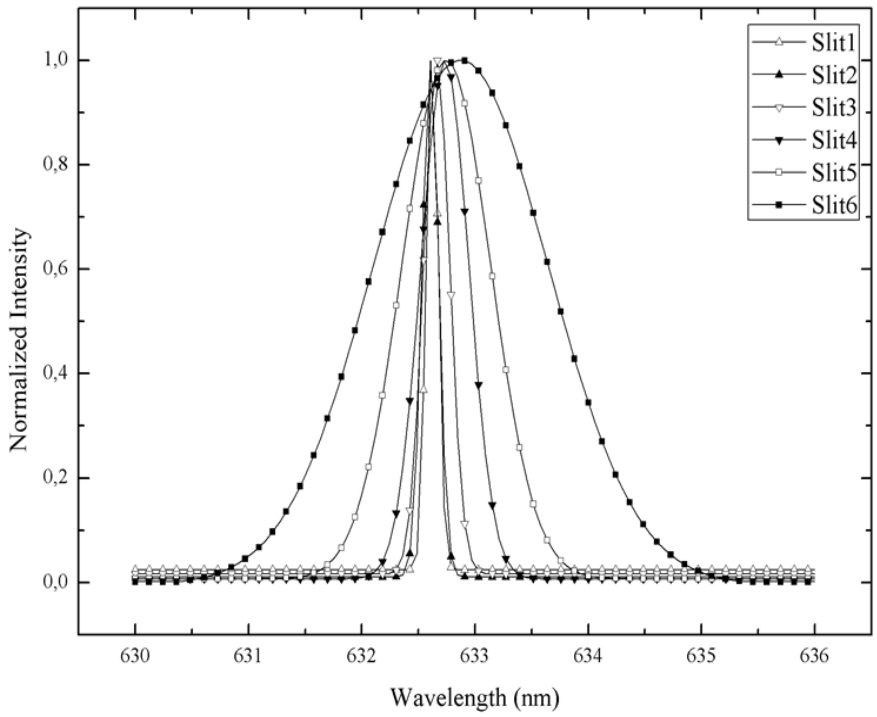

Figure 5.14: Instrumental bandpass of LE-282 for each slit, recorded with HeNe red laser, emitting at 632.8 nm.

Table 5.1 lists the FWHM values which are related to given measurements for each slit.

Table 5.1: FWHM values vs. slit number relation of LE-282.

Slit number	543 nm	633 nm
	FWHM (nm)	FWHM (nm)
1	0,17	0,12
2	0,19	0,17
3	0,26	0,27
4	0,46	0,50
5	0,93	0,92
6	2,28	2,15

Next, the instrumental line broadening of LE-282 depending on a slit number was analyzed. The minimum FWHM value is selected as a reference point (i.e., FWHM at slit1 is set to 1) and the remaining expansion factors in line broadening of monochromator due to different slits were calculated by using the FWHM values given in Table 5.1. Figure 5.15 shows the related results both for green and red lasers.

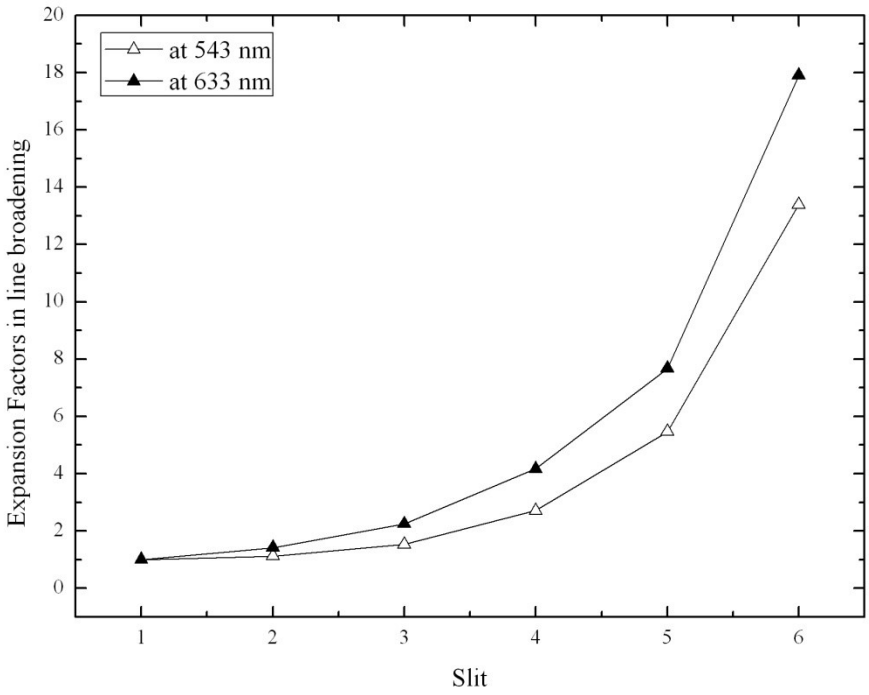

Figure 5.15: Relation between expansion factor in line broadening and selected slit. It is determined by HeNe green and red lasers separately.

As seen in Figure 5.15, instrumental line profile broadens approximately 15 times at slit 6 when compared to slit 1, on the contrary, resolution is decreased by the same ratio.

5.4 Determination of Intensity Scaling Factors

The intensity scaling factor is defined as the ratio of intensities measured by two different slits at a given wavelength of light. These factors give information about how much the intensity varies when the slit is changed.

The Intensity scaling factors of LE-282 were determined using line emitters (Melles Griot HeNe green and red lasers emitting at 543.5 nm and 632.8 nm respectively).

For the six slits, laser emissions were recorded by twos and so the intensity scaling factors were determined. Finally, the results obtained from each line emitter were compared with each other. Experiment setup that was built consisted of line emitters, ND filters, concave lens, pinholes and LE-282. ND filters and pinholes were used with different combinations for different slits in order to prevent the photomultiplier tube from being saturated. Concave lens is used to expand the beam spot and to decrease the laser beam intensity.

First, test setup is configured to measure the intensity of red laser with slit6 and slit5. Next, setup was configured and intensity was measured with slit5 and slit4. Then, setup was updated again and the intensity was measured with slit4 and slit3 and the tests continued so on. Measurements were finished when all scaling factors had been obtained. Finally, intensity and the slit relation was determined by setting slit 1 as a reference point (i.e. its value was assigned to 1) then all remaining scaling factors were calculated according to it.

Table 5.2 lists the intensity factors between slits obtained from measurement of intensity of green and red lasers.

Table 5.2: Intensity scaling factors vs. slit number relation of LE-282.

543 nm (green laser) Intensity Ratio		633 nm (red laser) Intensity Ratio	
S6/S5	1,69	S6/S5	2,16
S5/S4	2,06	S5/S4	1,85
S4/S3	2,25	S4/S3	1,92
S3/S2	4,01	S3/S2	3,98
S2/S1	2,85	S2/S1	2,32

Moreover, in order to clearly understand the relation between intensity scaling factors of slits, the value of S1 was taken as a reference and its value was assigned to be 1. Then by using the intensity scaling factors listed in Table 5.2, intensity multiplication factors between all slits were determined. Results are shown in Figure 5.16.

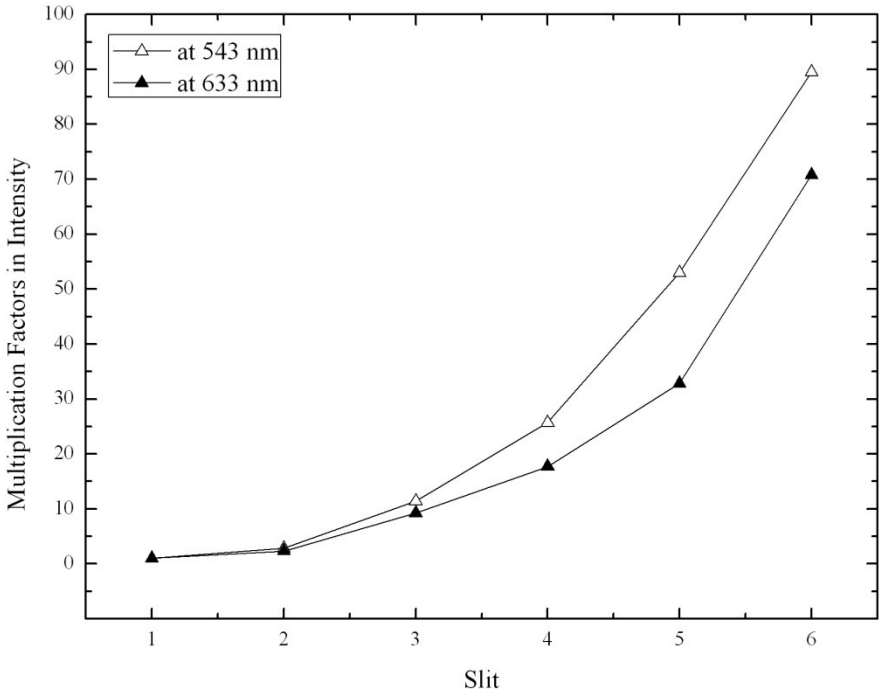

Figure 5.16: Relation between intensity multiplication factors and selected slits. It is determined by HeNe green and red lasers separately.

5.5 Test Experiments

According to the relation given by Eq. (5.4), the fraction of measured intensity by spectral response of system yields the corrected intensity. Thus, if the whole spectrum of measured intensity of light is corrected by using this relation and then normalized, the same corrected spectrum should be obtained for each slit. This will provide a mean (or a way) to check whether spectral response of system was properly determined or not. In order to confirm this relation and spectral response parameters, various tests were applied.

Corrected Intensity = Measured Intensity / Spectral Response of System (5.4)

Moreover, these tests involve various samples which have different emission spectra and thus they also helped to check the accuracy of wavelength calibration.

5.5.1 255 nm Excitation Filter

255 nm narrow band filters was used to confirm the spectral response curves in the range of 240 to 270 nm. Both measured and corrected spectra are shown in Figure 5.17. In addition, as seen in Figure 5.17, all corrected spectra are almost overlapped with each other in accordance with Eq. (5.4).

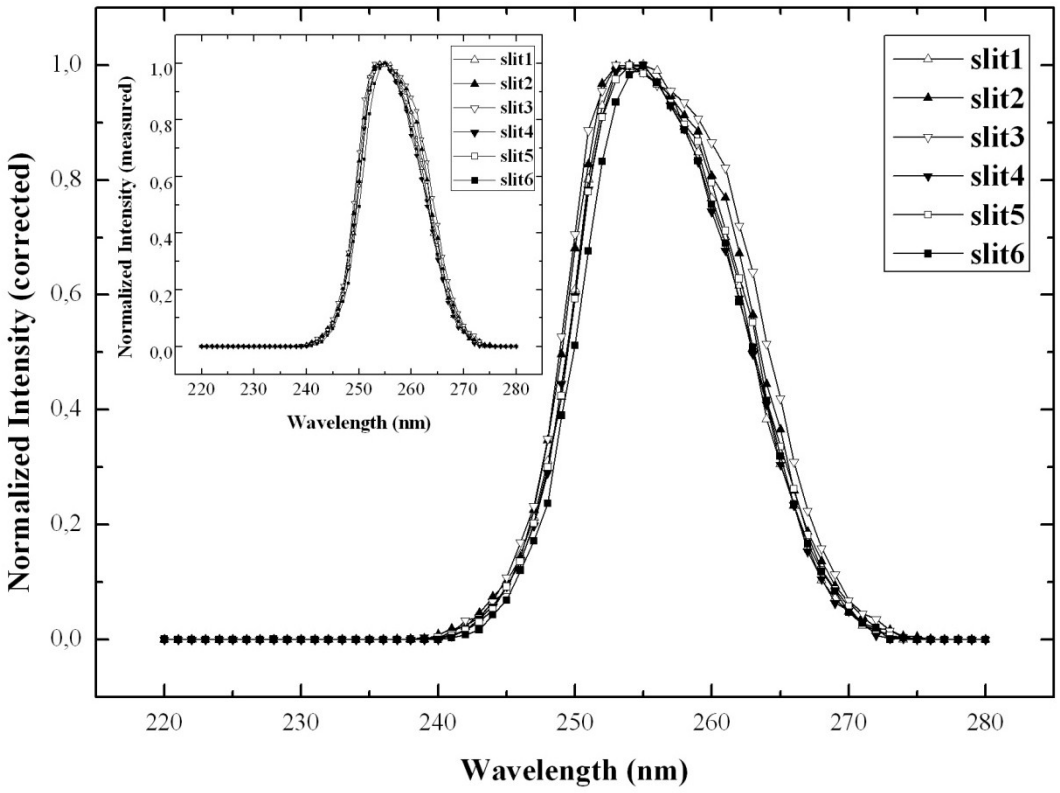

Figure 5.17: Corrected and Measured spectra of 255 nm filter for each slit.

5.5.2 Black Light Source

Second test was performed using a black light source which emits ultraviolet light whose emission is around 370 nm. This source has a broad continuous spectrum; hence it was used to confirm the spectral response in the range of 320 to 450 nm. Both corrected and measured spectra are shown in Figure 5.18.

The power of lamp used in the experiment was 8 Watt. It was a phosphor coated mercury vapor type of black light source. As seen in Figure 5.18, there are three sharp lines over a broad emission band. These sharp lines, which are recorded as 365, 404 and 435 nm, belong to mercury emissions (Ocean Optics, 2011). However, broad emission band should belong to europium doped strontium borate (SrB_4O_7: Eu^{2+}) phosphor since Eichmeier and Thumm (2008) reported that it was widely used material in blacklight sources with having a peak wavelength at 370 nm. For more details about this phosphor, studies of Iwamoto and Fujihara (2009) and Prakash et al. (2011) may be referred.

Since blacklight source has broad emission, the shape of corrected and measured spectra have a noticeable difference and the effect of spectral response curves can be observed better. However, sharp lines which were related to mercury emission also confirmed the wavelength calibration. Moreover, corrected spectrum of light source was also measured by fiber spectroradiometer and the result was compared with others to check the spectral response of LE-282 for the related region.

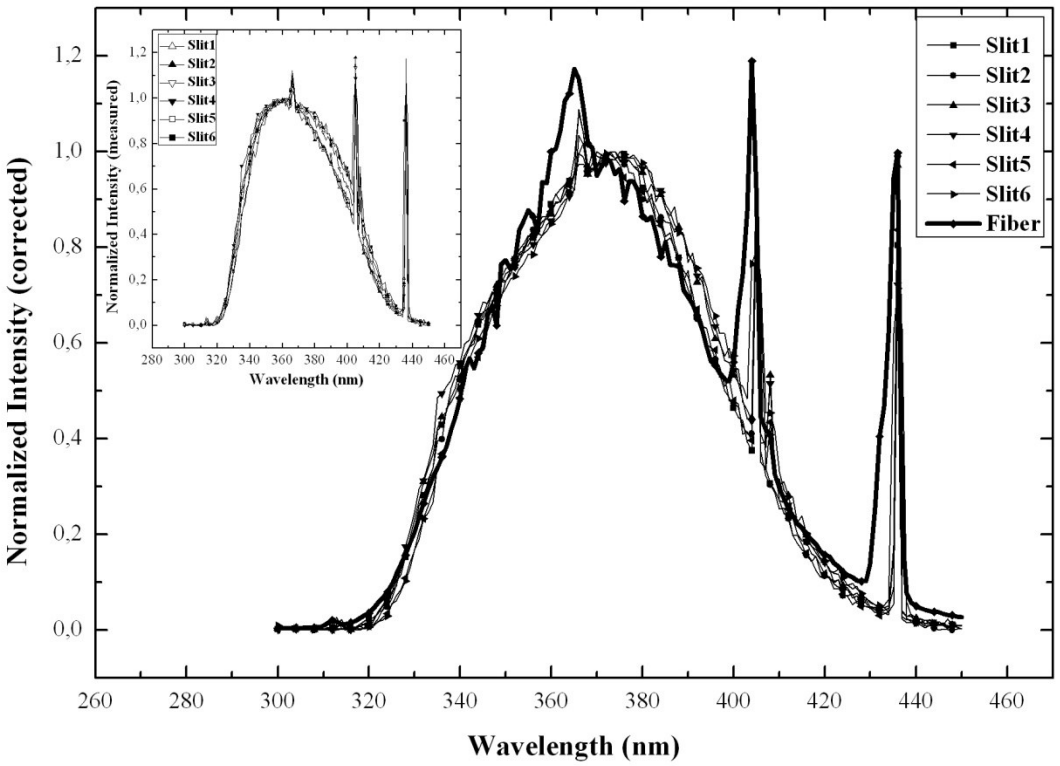

Figure 5.18: Corrected and Measured spectra of blacklight source for each slit.

Third test was performed using a flashlight whose UV emission is at 381 nm. This source does not have a broad emission band, yet it was used to confirm spectral response curves in the region between 360 and 420 nm. Corrected spectrum of light source was also measured by fiber spectroradiometer and the result was compared with others to check the spectral response of LE-282 for the related region.

Both corrected and measured spectra are shown in Figure 5.19. Apart from that, in order to get further information related to near UV (370 nm < λ < 400 nm) light emission LEDS, the studies of Nakamura (2000) and Mierry et al. (2007) may be referred.

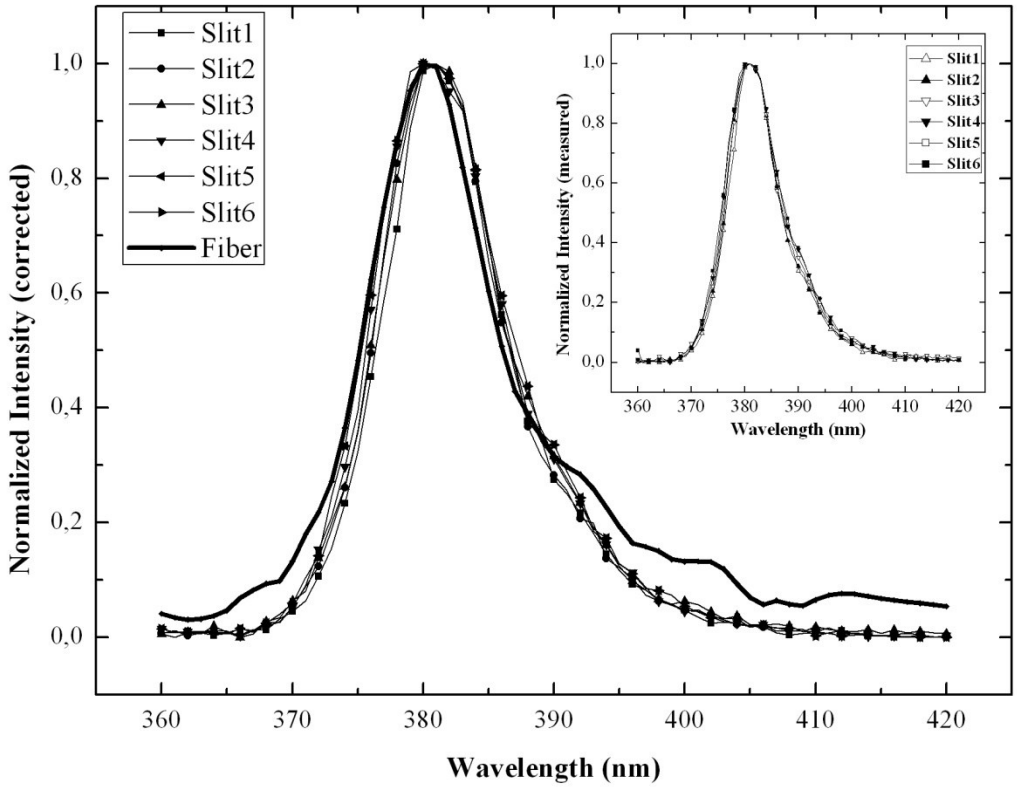

Figure 5.19: Corrected and Measured spectra of UV LED flashlight for each slit.

5.5.3 RGB High Power LED (blue)

Forth test was performed using a RGB high power LED triplet. However, to perform a spectral analysis in the range of 440 to 510 nm, only blue LED was activated. According to results shown in Figure 5.20, light emission was observed at 465 nm. The study of Zach (2004) was also reported the emitting wavelength of RGB blue LED around 465 nm.

This source was used to confirm the spectral response curves in region between 440 nm and 510 nm. In addition, corrected spectrum of light source was also measured by fiber spectroradiometer and the result was compared with others to check the spectral response of LE-282 for the related region.

Both corrected and measured spectra are shown in Figure 5.20.

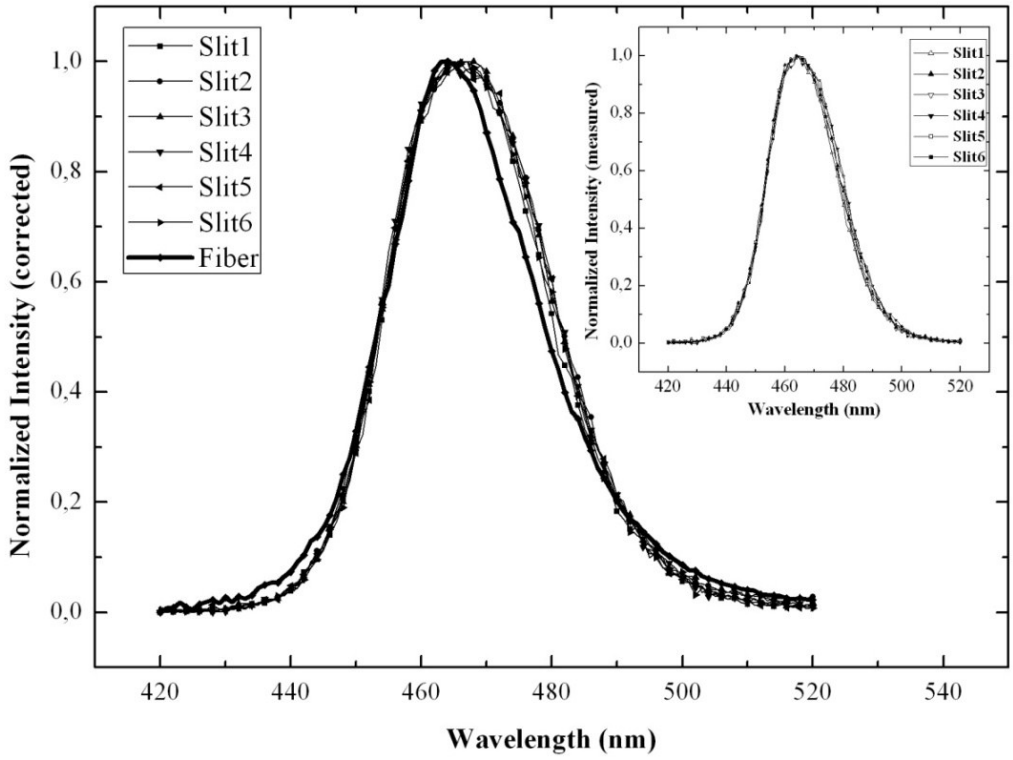

Figure 5.20: Corrected and Measured spectra of RGB high power LED for each slit.

5.5.4 Red and Green LEDs

The experiment setup consisted of red LED (635 nm) and green LED (562 nm), ND filters and LE-282. Firstly, the corrected spectra of both green and red LEDs were measured by fiber spectroradiometer. Afterwards, for each slit, emission spectra were measured four times in the range of 580 to 680 nm and 520 to 620 nm separately. Finally, results were compared with others to check the spectral response of LE-282 for the related region. Both corrected and measured spectra of red and green LEDs are shown in Figure 5.21 and Figure 5.22.

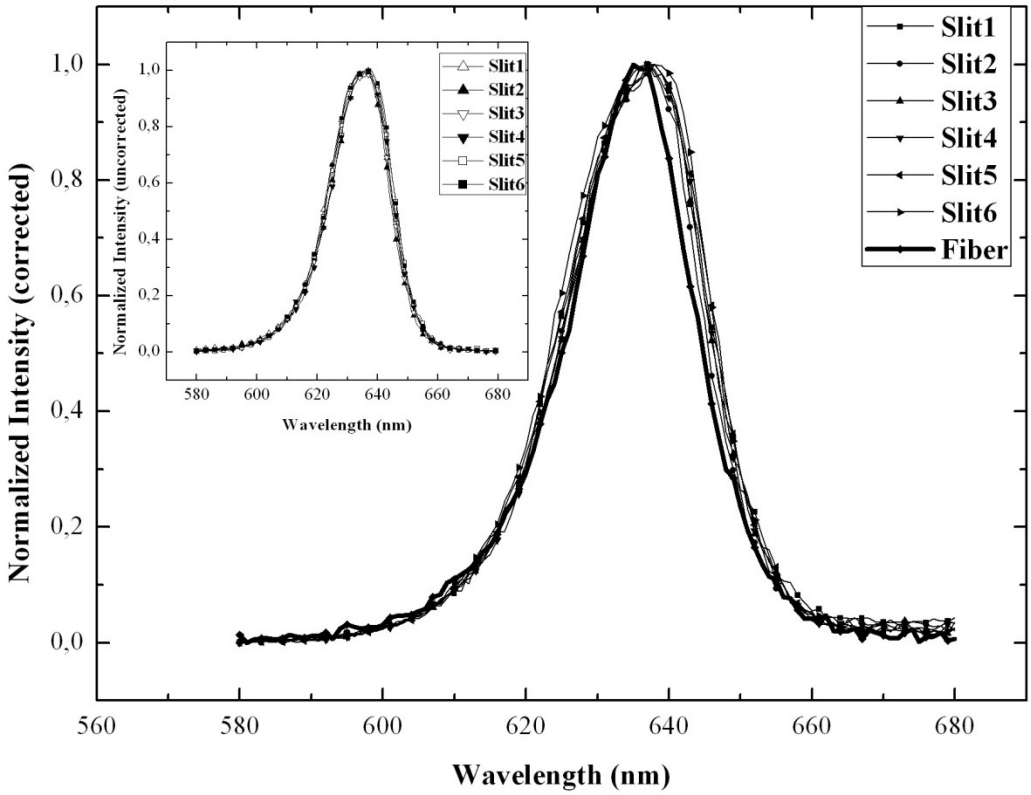

Figure 5.21: Corrected and Measured spectra of red LED for each slit.

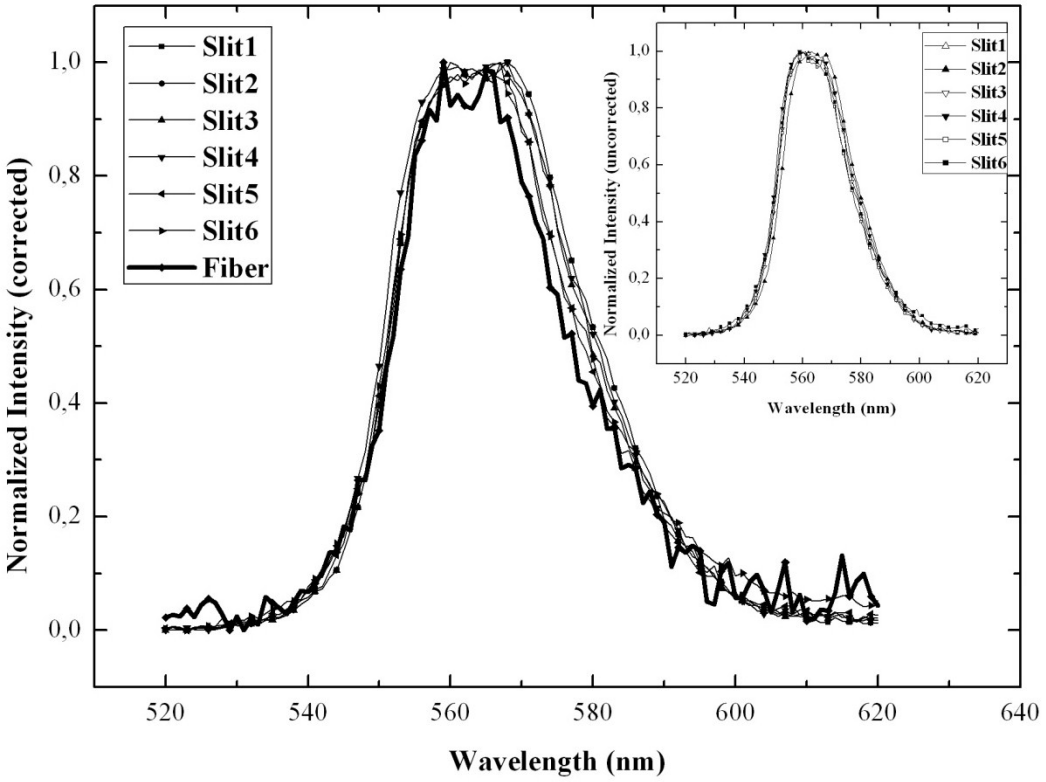

Figure 5.22: Corrected and Measured spectra of green LED for each slit.

5.6 Photoluminescence Measurements

After obtaining results from wavelength calibration and spectral response verification tests, photoluminescence (PL) emission spectra of beryllium oxide (BeO), carbon doped aluminum oxide (Al_2O_3:C), calcium fluoride (CaF_2), gadolinium magnesium zinc pentaborate (Gd(Mg,Zn)B_5O_{10}:Ce,Mn), and zinc silicate:Mn (Zn_2SiO_4:Mn) will be investigated in this part. The common feature of these samples is that they have very low intensities when compared light sources discussed above. Thus, measurement of PL spectra formed one of the challenging tasks of this project.

During measurements of PL spectra, samples were excited at 255 nm (see Figure 5.17). In addition, deuterium lamp was used as a main source and 255 nm narrow band filter was mounted in front of it. Moreover, to prevent PMT from being directly

exposed to radiation of 255 nm light due to reflection from surface of the sample or the sample holder, microscope objective lamella window was mounted between sample and monochromator. The transmission of lamella window starts around 300 nm and thus it blocks 255 nm.

All experiments were made using slit6 (i.e., the widest slit) as the PL intensities were too low to be measured with other slits. All the PL spectra given below are corrected.

BeO is a material used for TL and OSL dosimetry. Figure 5.23 below shows the PL emission spectrum of BeO at 25 ^{o}C.

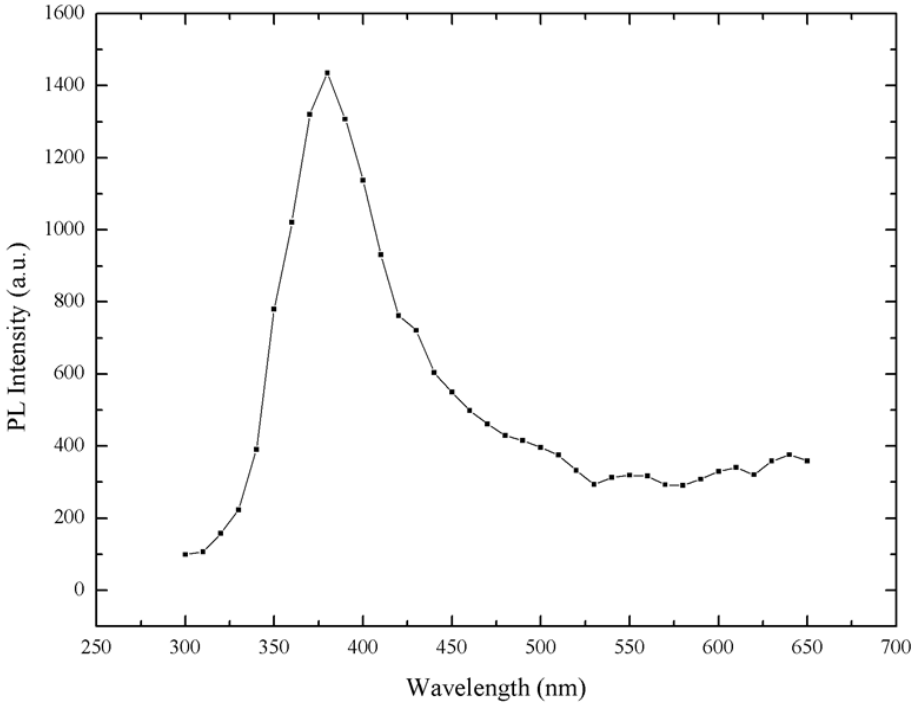

Figure 5.23: PL emission spectrum of BeO at 25 ^{o}C (λ_{ex} = 255 nm, λ_{em} = 380 nm).

PL intensity of BeO was measured with 0.5 nm/s speed and 10 nm intervals between data points. As seen in Figure 5.23, the peak was observed at 380 nm and the FWHM

was 75 nm. This result virtually acts in accordance with those obtained by Pustovarov et al. (2001) in which the BeO sample was excited at 188 nm.

Next graph, Figure 5.24 shows the PL emission spectrum of Al_2O_3:C. It was easy to excite and noise free when it is compared with BeO as the emission of Al_2O_3:C was much brighter. Peak wavelength was obtained at 330 nm. The spectrum was measured by 2 nm/s speed and 2 nm intervals.

However, in a study reported by Muthe et al. (2008), peak wavelength of PL emission spectrum of Al_2O_3:C was also reported at 330 nm which was obtained by using excitation wavelength in the range 220 to 270 nm.

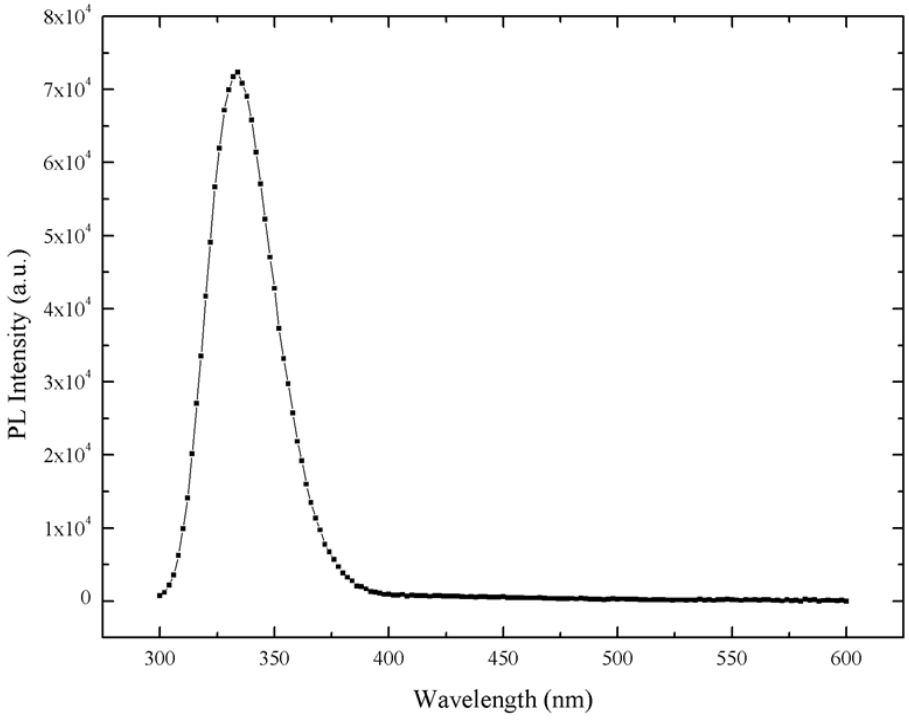

Figure 5.24: PL emission spectrum of Al_2O_3:C at 25 ^{o}C (λ_{ex} = 255 nm, λ_{em} = 330 nm).

Figure 5.25 shows the PL emission spectrum of a pure CaF_2. Peak wavelength of PL emission of CaF_2 was observed around 340 nm. In addition, spectrum was measured by 0.5 nm/s speed and 2 nm intervals.

According to Pandurangappa and Lakshminarasappa (2011), PL emission spectrum of a γ-rayed pure nano-crystalline CaF_2 was measured at 396 nm when the sample was excited at 265 nm. In addition, when the sample was excited at 360 nm a strong emission was observed at 415 nm. The given study of Pandurangappa and Lakshminarasappa (2011) does not clearly support the related spectrum of CaF_2 which is shown in Figure 5.25 since the excitation wavelengths were different; however, both luminescence emissions at 396 nm and 415 nm were almost observed by LE-282 as seen in Figure 5.25.

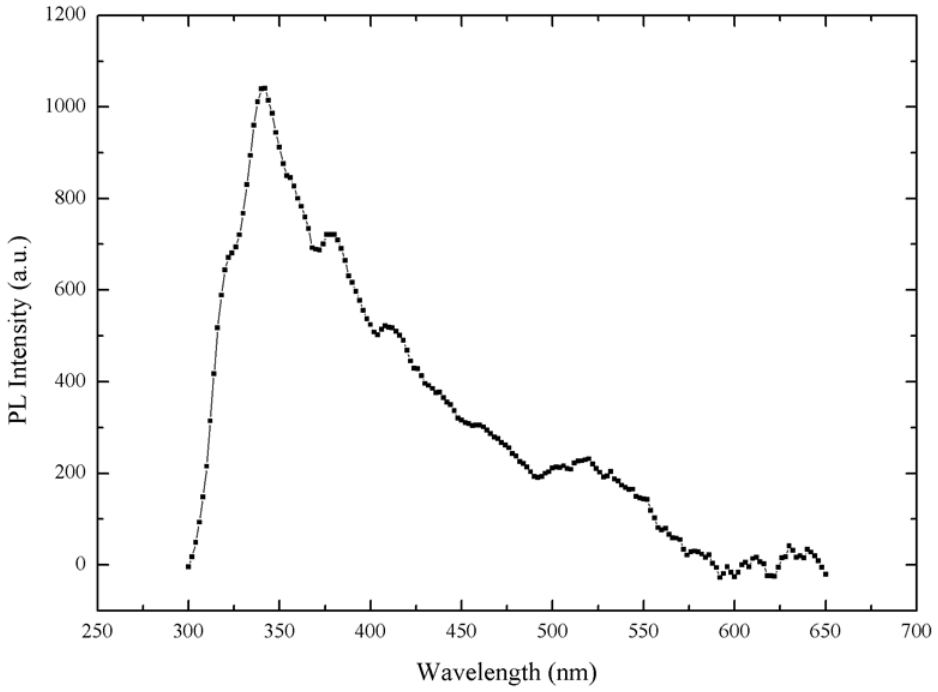

Figure 5.25: PL emission spectrum of a pure CaF_2 at 25 ^oC (λ_{ex} = 255 nm, λ_{em} = 340 nm).

Figure 5.26 shows the PL emission spectrum of Zn_2SiO_4:Mn. Peak wavelength was observed at 525 nm and the spectrum was measured by 2 nm/s speed and 1 nm intervals.

Zhenguo et al. (2003) reported the peak of PL emission as 525 nm where it was excited with 325 nm. In addition, FWHM of broad emission band was obtained as 50 nm. This result completely acts in accordance with the results measured by LE-282 as seen in Figure 5.26. Moreover, Sohn et al. (1999), Parmar et al. (2009) and Inoue et al. (2008) were all investigated the similar results of PL emission spectra of Zn_2SiO_4:Mn by using different measurement setups.

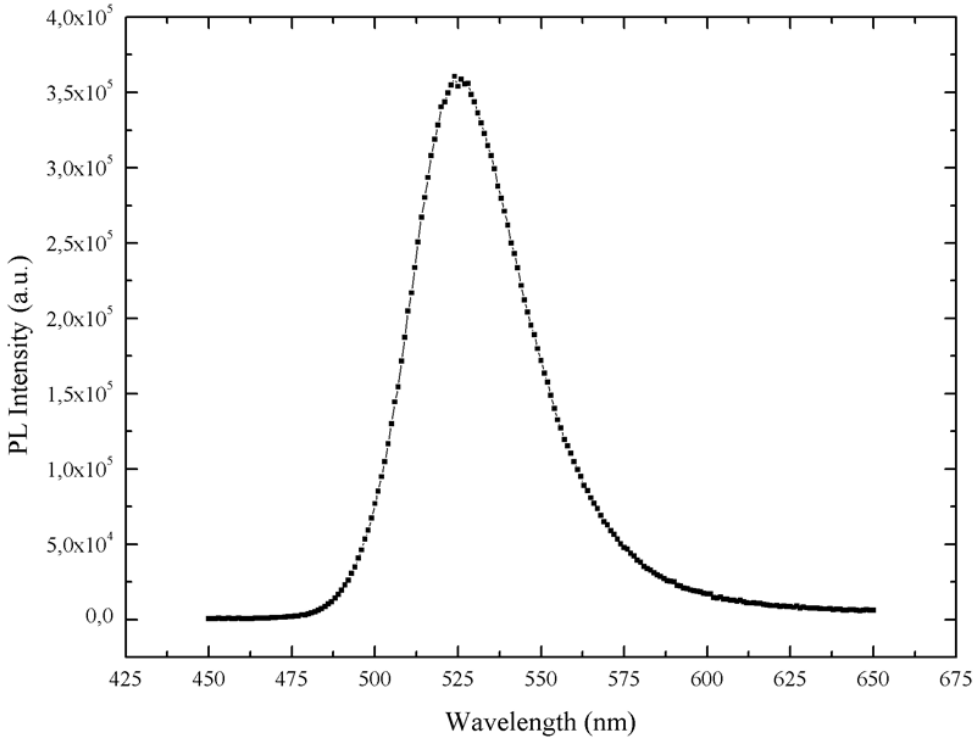

Figure 5.26: PL emission spectrum of Zn_2SiO_4:Mn at 25 ^oC (λ_{ex}= 255 nm, λ_{em} = 525 nm).

Final example of PL measurements is Gd(Mg, Zn)B_5O_{10}:Ce,Mn. Figure 5.27 shows the related spectrum. Peak wavelength of PL emission of Gd(Mg,Zn)B_5O_{10}:Ce,Mn

was observed at 628 nm and the spectrum was measured by 2 nm/s speed and 1 nm intervals.

The result which is shown in Figure 5.27 acts in accordance with the one obtained by Marking and Snyder (2008) who invented red emitting manganese (Mn) and Cerium (Ce) co-activated $Gd(Mg,Zn)B_5O_{10}$:Ce,Mn. According to their invention, luminescence emission of phosphor was observed in the range of 550 to 800 nm peaking at 630 nm.

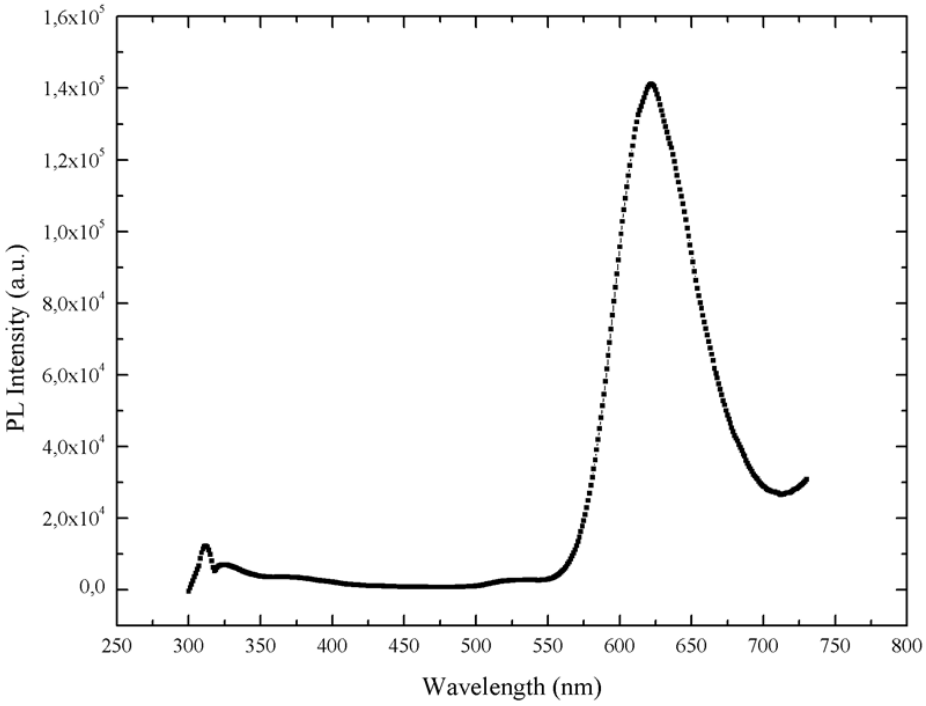

Figure 5.27: PL emission spectrum of $Gd(Mg,Zn)B_5O_{10}$:Ce,Mn at 25 ^oC (λ_{ex} = 255 nm, λ_{em} = 628 nm).

5.7 TL Emission Spectra

These experiments were performed to investigate the spectra of thermally active peaks of both Al_2O_3:C and BeO. Experiments were restricted only by those two samples since TL emission spectra of them had hardly been measured with fiber even though they had been the brightest ones.

5.7.1 TL Emission Spectrum of Al_2O_3:C

Al_2O_3:C was irradiated with 30 mGy and the isothermal decay was measured at 140 ^oC by an external TL measurement setup. The given amount of dose was enough to measure the isothermal decay as the PMT of this setup stands very close to sample; meanwhile, no optical components are placed in between them. According to calculations, only 8 percent of TL intensity decreased in 100 seconds.

Under those circumstances, when measured by LE-282, nothing was observed. Then, Al_2O_3:C was irradiated with 150 Gy and TL emission spectrum was measured again. This time it could be recorded; however, it was shifted and the peak wavelength was obtained at 400 nm, whereas Rodriguez et al. (2011) reported the TL peak of Al_2O_3:C at 200 ^oC as 415 nm following beta irradiation with 100 Gy. It was supposed that intensity should have decreased much more than expected; for this reason high portion of signal had been lost until scanning was completed and so the spectrum was obtained as shifted.

In order to understand the reason for this, Al_2O_3:C was irradiated with 120 Gy and 200 Gy separately and heated to 140 ^oC each time. The recording of isothermal decay was started at 140 ^oC and it was observed that 65 percent of intensity had decreased in 100 seconds. As a result, when irradiated with high amount of dose, TL signal of

Al_2O_3 decreases much faster. Figure 5.28 shows the nonlinear isothermal decays of Al_2O_3:C.

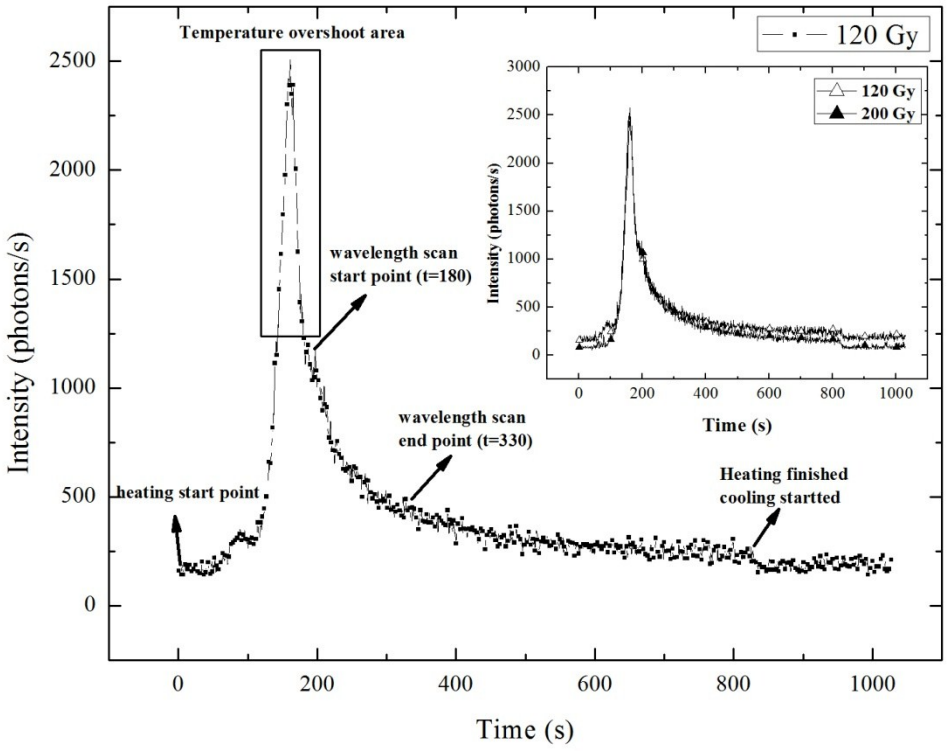

Figure 5.28: Isothermal decay of Al_2O_3:C, heating started at room temperature and 140 ^oC was reached when t = 150 s. Temperature overshoot period is shown in the range of t = 150 s to t = 180 s. Time interval (t = 180 s and t = 330 s) demonstrates the wavelength scanning period where the intensity decreased by 65 percent at that time interval.

After this nonlinearity was understood, Al_2O_3:C had been irradiated with 120 Gy and this time TL emission spectrum had been measured from both forward and reverse directions (i.e., 500 to 350 nm and 350 to 500 nm separately). In order to avoid losing a large portion of the TL signal of Al_2O_3:C, whose emission has peaking at 200 ^oC as shown in the study of Muthe et al. (2008), related spectra were recorded at

140 ^{o}C. Then, those measured spectra were averaged to acquire the correct TL emission spectrum of Al_2O_3:C. The related result is shown in Figure 5.29.

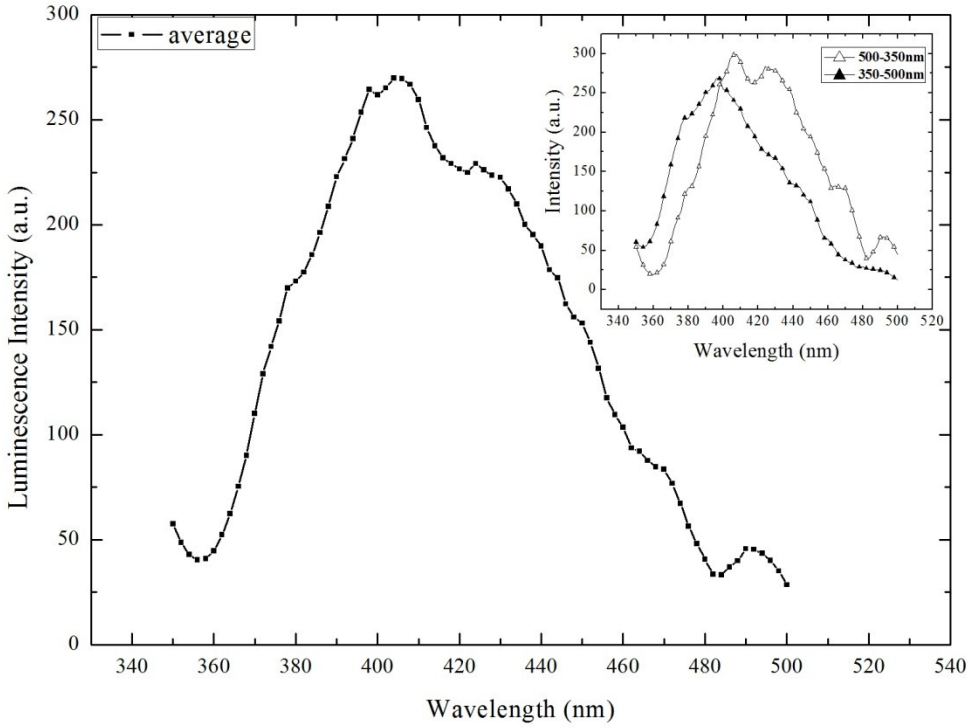

Figure 5.29: TL emission spectrum of Al_2O_3:C (Average of two spectra obtained from forward and reverse scan). It was irradiated with 120 Gy each time and the spectra were recorded at 140 ^{o}C.

However, in order to investigate much more reliable TL emission spectrum, Al_2O_3:C was irradiated with 3 Gy and heated to 140 ^{o}C each time and intensity was recorded point by point with 5 nm intervals in the range of 350 to 500 nm. Then all points were combined to each other. Figure 5.30 shows the related TL emission spectrum of Al_2O_3:C.

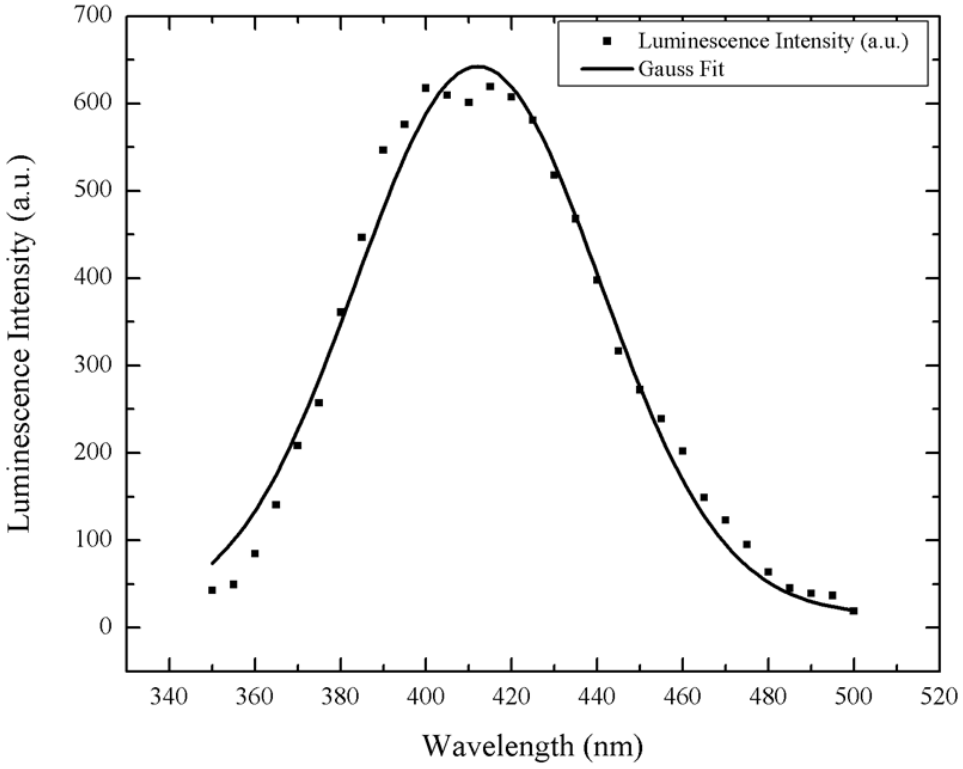

Figure 5.30: TL emission spectrum of Al_2O_3:C. At each point, it was irradiated with 3 Gy and heated to 140 ^oC then the intensity was recorded within short time periods (20 s).

As seen in Figure 5.30, and in accordance with the study of Rodriguez et al. (2011), Al_2O_3:C has a peak at 415 nm.

5.7.2 TL Emission Spectrum of BeO

BeO was irradiated with 180 Gy and heated to 150 ^oC. The recording of isothermal decay was started at 150 ^oC and it was observed that 58 percent of intensity had decreased in 250 seconds. Figure 5.31 shows the isothermal decay of BeO.

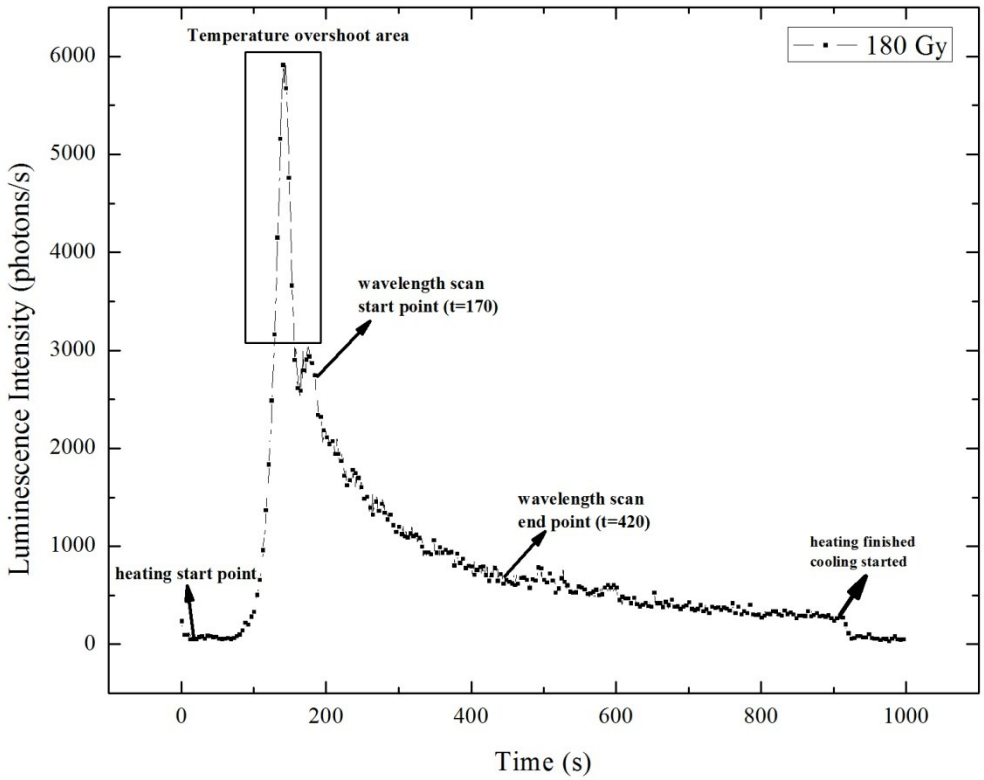

Figure 5.31: Isothermal decay of BeO, heating started at room temperature and 150 ^{o}C was reached when t = 150 s. Overshoot period is shown in the range of t = 150 s to t = 170 s. Time interval (t = 170 s and t = 420 s) demonstrates the wavelength scanning period where the intensity decreased by 58 percent at that time interval.

In measurement of TL emission spectrum of BeO by LE-282, it was irradiated with 10 Gy and heated to 200 °C each time and intensity was recorded point by point with 10 nm intervals in the range 250 to 450 nm. Then all points were combined to each other and Gaussian fit was applied. As a result, the peak wavelength of TL emission of BeO was recorded to be 335 nm. Figure 5.32 shows the corrected TL emission spectrum of BeO and its Gaussian fit applied form. In addition, the studies of McKeever et al. (1995) and Vij and Singh (1997) which report TL emission from the blue region of the visible spectrum to the ultraviolet up to the lower limit of 200 nm whose peak wavelength was observed around 335 nm when irradiated with 10 Gy also showed the same result.

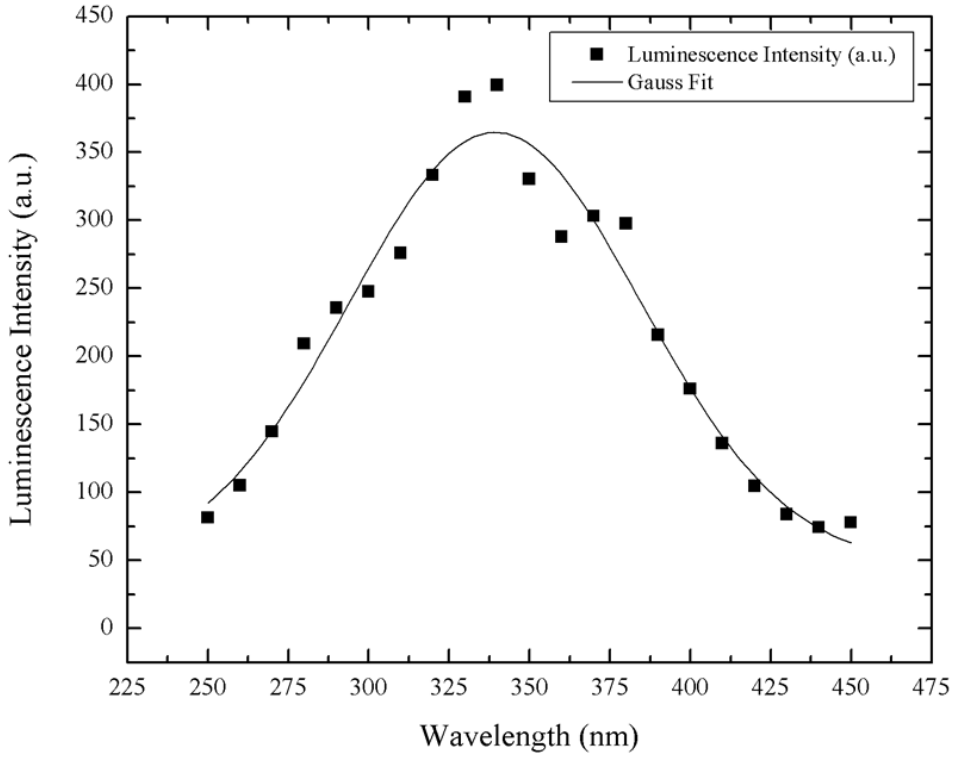

Figure 5.32: TL emission spectrum of BeO. At each point, it was irradiated with 10 Gy and heated to 200 ^{o}C then the intensity was recorded within short time periods (20 s).

5.8 OSL Emission Spectrum of Al_2O_3 :C

The studies of Markey et al. (1995) and Yukihara and McKeever (2006) showed that the OSL emission spectrum of Al_2O_3:C has two peaks at 330 nm and 420 nm when irradiated with 200 Gy-γ and stimulated with 532 nm.

However, as a result of measurement of OSL emission spectrum of Al_2O_3:C by LE-282, only the peak at 420 nm could be observed. The experiment was performed by irradiating the sample with 160 Gy and stimulating at 536 nm. Figure 5.33 shows the

related spectrum. In addition, OSL emission after 430 nm could not be measured as it started to overlap with the stimulation source.

Further information about OSL emission spectrum of Al_2O_3:C can be achieved from Bøtter-Jensen et al. (2003). Moreover, OSL emission spectrum of BeO was also tried to be measured, yet nothing could be detected.

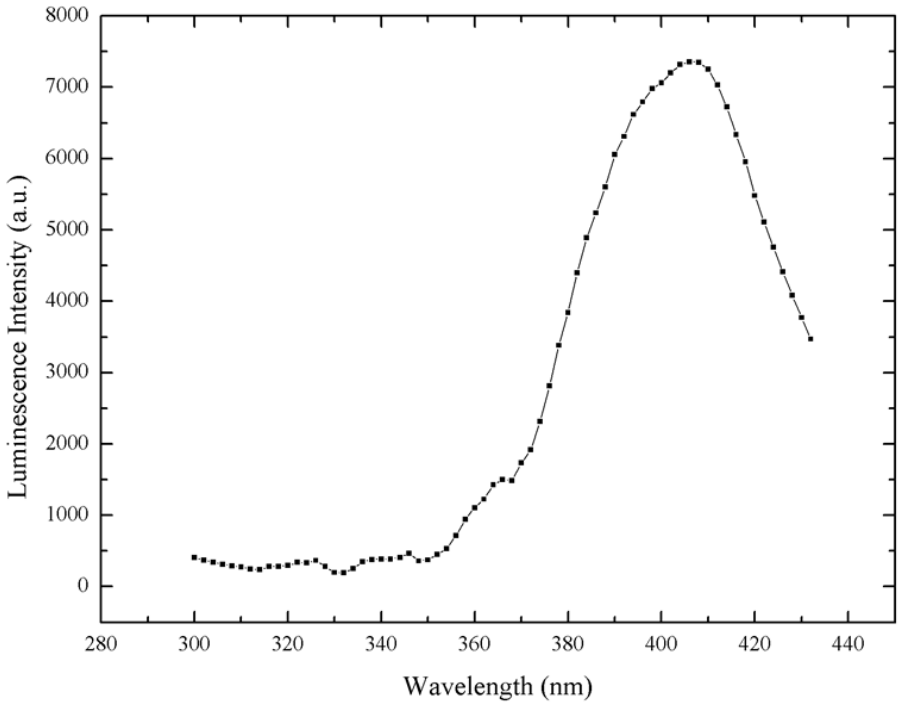

Figure 5.33: OSL emission spectrum of Al_2O_3. It was irradiated with 160 Gy. Then, at 25 ^{o}C, it was stimulated with 536 nm and the spectrum was recorded.

In this chapter, results of calibration tests and PL, OSL and TL emission spectra of various samples which are supported by the reported results were presented. Next chapter is a conclusion chapter and according to the findings, the usability of this spectrometer in measurement of luminescence emission applications will be discussed here.

CHAPTER 6

SUMMARY AND CONCLUSIONS

In this work, a versatile luminescence emission spectrometer (named as LE-282) was designed and developed with the main purpose of measuring PL, TL and OSL emission spectra of materials relevant for dosimetry. The spectrometer consists of a Littrow type monochromator, a PMT and six pairs of slits of different size together with the necessary hardware and software to control it.

Starting with the construction of an electronic control unit, the wavelength calibration was performed, wavelength resolution of the system was determined and spectral response of the whole measurement system for each slit was identified. Moreover, in order to focus the emitted light onto entrance slit as much as possible, light collection unit using fused silica lenses was designed. The spectrometer was finalized with a user interface developed by using LabVIEW (National Instruments) graphical design environment.

Electronic control unit of LE-282 is composed of a microcontroller (Microchip 18F4550), RS-232 interface, two stepper motor driver cards and power supplies for the motors and the circuitry. Firmware for the microcontroller was developed in *C* programming language using MikroC (MikroElektronika) and the generated machine code was embedded into 18F4550. Communication with computer and control of LE-282 were performed in this way.

Wavelength calibration of the spectrometer was performed by using a mercury-argon calibration lamp (Ocean Optics HG-1). Ten of line emissions of HG-1 were selected and the plot of actual wavelength as a function of driving screw position was fitted to

third order polynomial function. Then, by using line emitters (Melles Griot HeNe green and red lasers emitting at 543.5 nm and 632.8 nm respectively) wavelength resolution of the system was determined. According to results, the resolution at slit6 was obtained to be 2.2 nm. By the way, resolution at slit1 was obtained to be 0.17 nm. Resolution of LE-282 at the other slit dimensions lie in between that of slit1 and slit6.

In order to determine the overall spectral response of measurement system, halogen and deuterium lamps were used. They have both continuous emission band in the range 200-400 nm and 350-900 nm respectively. A calibrated fiber spectroradiometer (IntLightSpect RPS900) was used to measure the corrected spectra of lamp sources. Then, measured spectra of both halogen and deuterium lamp by LE-282 were corrected with respect to the spectra obtained from the spectroradiometer and so the spectral response of the system was determined. In addition, both spectral response curves were coupled in the overlapped region between 350 to 400 nm and the overall spectral response of system in the range 200-750 nm was determined.

After completing the design and development of electronic control unit, calibrations and achieving the computer control of the spectrometer, the performance of LE-282 was tested by the measurement of emission spectra of various light sources. Starting with a blacklight source, emission spectra of RGB high power LED (blue) and green and red LEDs were measured respectively. As it was reported in the study of Eichmeier and Thumm (2008), emission of blacklight source was measured 370 nm. Emission of UV LED flashlight was observed at 381 nm and the same result was obtained from both fiber spectroradiometer and the reported study of Mierry et al. (2007). In addition, RGB high power LED (blue) was observed to have peaking at 465 nm which was also shown in the study of Zach (2004).

From results obtained with experimental tests mentioned above, it was observed that LE-282 was working well in the range 200-750 nm. However, the challenging task of this study was to measure the PL, OSL and TL emission spectra of various samples relevant for dosimetry since PL, TL or OSL intensities of given samples were much

less bright when compared to test experiments mentioned above. With this purpose, initially PL emission spectra of beryllium oxide (BeO), aluminum oxide (Al_2O_3:C), calcium fluoride (CaF_2), gadolinium magnesium zinc pentaborate ($Gd(Mg,Zn)B_5O_{10}$:Ce,Mn) and zinc silicate:Mn (Zn_2SiO_4:Mn) were measured at 25 ^oC by exciting with 255 nm. As a result of these experiments, PL emission of BeO was observed at 380 nm as shown in the study of Pustovarov et al. (2001). Moreover, Muthe et al. (2008) reported the PL emission band of Al_2O_3:C was centered at 330 nm by using excitation wavelength in the range 220-270 nm. It was also observed as 330 nm when measured by LE-282. CaF_2 emission was observed around 340 nm; however, there was no similar experiment carried out under similar circumstances. Thus, only the study of Pandurangappa et al. (2011) may be referred where the PL emission of CaF_2 was reported at 396 nm when excited with 265 nm. Zn_2SiO_4:Mn emission was observed at 525 nm. Similarly, the studies of (Sohn et al., 1999; Zhenguo et al., 2003; Inoue et al., 2008, Parmar et al., 2009) were all explaining the same result. Finally, PL emission of $Gd(Mg,Zn)B_5O_{10}$:Ce,Mn was observed at 628 nm which acts in accordance with the one obtained by Marking and Snyder (2008) who invented red emitting manganese (Mn) and Cerium (Ce) co-activated $Gd(Mg,Zn)B_5O_{10}$:Ce,Mn. According to their invention, luminescence emission of phosphor was observed in the range 550-800 nm peaking at 630 nm.

Experiments carried on with the measurement of TL emission spectra of BeO and Al_2O_3:C and with OSL emission spectrum of Al_2O_3:C. Experiments were restricted only by those two samples since TL and OSL emission spectra of them had hardly been measured even though they had been the brightest ones. TL emission of BeO was observed at 335 nm when it was irradiated with 10 Gy and then heated to 200 ^oC. Using the same test procedure, when irradiated with 3 Gy and then heated to 140 ^oC, TL emission of Al_2O_3:C was obtained at 415 nm. In addition, according to the studies of (McKeever et al., 1995; Vij and Singh 1997), TL peak of BeO observed at 335 nm and also Rodriguez et al. (2011) reported that Al_2O_3:C has its TL peak at around 415 nm. Moreover, OSL emission of Al_2O_3:C was observed around 420 nm when irradiated with 160 Gy and then stimulated with 536 nm green LED. According to the study of Yukihara and McKeever (2006), it was found that Al_2O_3:C

had its OSL emission peak at 420 nm when irradiated with 200 Gy and stimulated with 532 nm laser source.

In summary, experiments mentioned above have shown that emission spectra of samples relevant for dosimetry can be obtained using the spectrometer developed for this purpose. Besides this, by considering the design and implementation of LE-282 emission spectrometer, one may enhance the device performance by improving the light collection unit. This will allow the measurement of weak TL and OSL signals from materials used for dating and dosimetry (such as quartz, feldspar and zircon). Another possibility can be the conversion of the device to a spectrophotometer with the addition of a light source to measure the transmittance or absorbance of samples.

REFERENCES

"An Introduction to Fluorescence Spectroscopy". 2000. PerkinElmer, Inc. Retrieved from http://physweb.bgu.ac.il/~bogomole/Books/An%20Introduction%20to%20Fluorescence%20Spectroscopy.pdf, last accessed on, 18.11.2011.

BAILIFF I.K., BOWMAN S.G.E., MOBBS S.F., AITKEN M.J., 1977. "The Photo-transfer Technique and Its Use in Thermoluminescence Dating". *Journal of Electrostatics*, **3**, 269-280.

BALL D.W., 2001. "The Basics of Spectroscopy". Bellingham, Washington: SPIE-International Society for Optical Engine.

BHATT, B.C., PAGE, P.S., RAWAT, R.S., DHABEKAR, B.S., MISRHA, D.R., 2008. "TL, OSL and PL Studies on Al_2O_3:Si,Ti Phosphor". *Radiat. Meas.* **43,** 327-331.

BLASSE G., GRABMAIER B.C., 1994. "Luminescent Materials". Heidelberg, Berlin: Springer-Verlag.

BOS A. J. J., WINKELMAN A. J. M., SIDORENKO A. V., 2002. "A TL/OSL Emission Spectrometer Extension of the RISØ READER". *Radiation Protection Dosimetry*, **101**, 111-114.

BØTTER-JENSEN L., McKEEVER S.W.S., WINTLE A.G., 2003. "Optically Stimulated Luminescence Dosimetry" Amsterdam, Netherlands: Elsevier Science B.V.

CALIBRATION SOURCES “HG-1 Mercury Argon Calibration Source”, Ocean Optics. Retrieved from http://www.oceanoptics.com/products/hg1.asp. Last accessed on, 12.01.2011.

CORNEY A., 1977. “Atomic and Laser Spectroscopy”. New York, USA: Oxford University Press Inc.

EICHMEIER J.A., THUMM M., 2008. “Vacuum Electronics Components and Devices” Heidelberg, Berlin: Springer-Verlag.

FISCHER R. E., TADIC-GALEB B., YODER P.R., 2008. “Optical System Design”. USA: The McGraw-Hill Companies, Inc.

FOX M., 2001. “Optical Properties of Solids”. New York, USA: Oxford University Press.

GAFT, M., REISFELD, R., PANCZER, G., 2005. “Luminescence Spectroscopy of Minerals and Materials”. Heidelberg, Berlin: Springer-Verlag.

HUANG X.Y., WANG J.X., YU D.C., YE S., ZHANG Q.Y., 2011. “Spectral Conversion for Solar Cell Efficiency Enhancement Using $YVO_4:Bi^{3+},Ln^{3+}$ (Ln=Dy, Er, Ho, Eu, Sm, and Yb) Phosphors”. *J. Appl. Phys*. **109**, 113526.

HUNTLEY D.J., GODFREY-SMITH D.I., THEWALT M.L.W., BERGER G.W., 1988. “Thermoluminescence Spectra of Some Mineral Samples Relevant to Thermoluminescence Dating”. *Journal of Luminescence*, **39**, 123-136.

INOUE Y., TOYODA T., MORIMOTO J., 2008. “Photoacoustic Spectra on Mn-Doped Zinc Silicate Powders by Evacuated Sealed Silica Tube Method”. *J Mater Sci*, **43**, 378–383.

IWAMOTO C., FUJIHARA S., 2009. “Fabrication and Optical Properties of NUV-Emitting SiO_2-SrB_4O_7:Eu^{2+} Glass-Ceramic Thin Films”. *Optical Materials*, 31, 1614-1619.

JACKSON J.H., HARRIS A.M., 1970. “The Fading of Optical Absorption Bands in TLD Lithium Fluoride”. *Physics letters A*, **29**, 423-424.

KRBETSCHEK, M.R., GÖTZE, J., DIETRICH, A., 1998. “Spectral Information from Minerals Relevant for Luminescence Dating.” *Radiation Measurements*, **27**, 695-748.

KUŞOĞLU-SARIKAYA, C., 2011. “Optically Stimulated Luminescence Studies on Natural Fluorites”. Master Thesis, Middle East Technical University, 90 pages, Ankara.

LERNER J.M., THEVENON A., 1988. “The Optics of Spectroscopy: A tutorial” Vol. 2.0, Jobin-Yvon: Instruments SA Inc.

MARKEY B.G., COLYOTT L.E., McKEEVER, S. W. S., 1997. “A New Flexible System for Measuring Thermally and Optically Stimulated Luminescence”. *Radiation Measurements*, **27**, 83-89.

MARKING G.A., SNYDER T.M., 2008. “Method of Making Red Emitting Borate Phosphor”. *World Intellectual Property Organization*, WO-2008/106313 A1.

McKEEVER, S. W. S., 1985. “Thermoluminescence of Solids”. New York, USA: Cambridge University Press.

McKEEVER S.W.S., MOSCOVITCH M., TOWNSEND P.D., 1995. “Thermoluminescence Dosimetry Materials: Properties and Uses”. Ashford, Kent, England: Nuclear Technology Pub.

MIERRY P.D., TINJOD F., CHENOT S., LANCEFIELD D., 2007. "Quantum Well Free Nitride Based UV LEDs Emitting at 380 nm". *phys. stat. sol. (c)*, **4**, No.1, 13-16.

MUTHE K.P., KULKARNI M.S., RAWAT N.S., MISHRA D.R., BHATT B.C., SINGH A., GUPTA S.K., 2008. "Melt Processing of Alumina in Graphite Ambient for Dosimetric Applications". *Journal of Luminescence*, **128**, 445–450.

NAKAMURA S., 2000. "InGaN-Based UV/Blue/Green LED and LD Structure". *Handbook of Thin Film Devices*, **2**, 225-263.

PALMER C., LOEWEN E., 2005. "Diffraction Grating Handbook". New York, USA: Newport Corporation.

PANDURANGAPPA C., LAKSHMINARASAPPA B.N., 2011. "Optical Absorption and Photoluminescence Studies in Gamma-Irradiated Nanocrystalline CaF_2". *J Nanomedic Nanotechnology*, **2**, 108.

PARMAR M.C., ZHUANG W.D., MURTHY K.V.R., HUANG X.W., HU Y.S., NATARAJAN V., 2009. "Role of SiO_2 in Zn_2SiO_4: Mn^{2+} Phosphor Used in Optoelectronic Materials". *Indian Journal of Engineering & Materials Sciences*, **16**, 185-187.

"Photomultiplier Tubes Basics and Applications (3rd edition)". 2007, Hamamatsu. Accessed on, 18.12.2011 and retrieved from http://sales.hamamatsu.com/assets/pdf/catsandguides/PMT_handbook-v3aE.pdf.

POOLTON N.R.J., BØTTER-JENSEN, L., WINTLE A.G., JAKOBSEN J., JØRGENSEN F., KNUDSEN K.L., 1994. "A Portable System for the Measurement of Sediment OSL in the Field". *Radiation Measurements*, **23**, 529-532.

PRAKASH I.N., BABU B., REDDY Ch.V., MURTY P.N., REDDY Y.P., RAO P.S., RAVIKUMAR R.V.S.S.N., 2011. "Spectroscopic Studies on Fe^{3+} and Mn^{2+} Doped SrB_4O_7 Glasses". *Physica B*, **406**, 3295-3298.

PUSTOVAROV V.A., IVANOV V.YU., KIRM M., KOROTAEV A.V., KRUZHALOV A.V., ZIMMERER G., ZININ E.I., 2001. "Time Resolved Luminescent VUV Spectroscopy of F- and F^+ Centers in Single BeO Crystals". *Nuclear Instruments and Methods in Physics Research A*, **470**, 353–357.

RIESER U., KRBETSCHEK M.R., STOLZ W., 1994. "CCD Camera Based High Sensitivity TL/OSL Spectrometer". *Radiation Measurements*, **23**, 523-528.

RIESER U., HABERMANN J., WAGNER G.A., 1999. "Luminescence Dating: A New High Sensitivity TL/OSL Emission Spectrometer". *Quaternary Science Reviews*, **18**, 311-315.

RODRIGUEZ M.G., DENIS G., AKSELROD B.S., UNDERWOOD T.H., YUKIHARA E.G., 2011. "Thermoluminescence, Optically Stimulated Luminescence and Radioluminescence Properties of Al2O3:C,Mg". *Radiation Measurements*, **46**, 1469-1473.

SKOOG, D. A., HOLLER, F. J., NIEMAN, T. A., 1998. "Principles of Instrumental Analysis". Thomson Learning, Inc.

SOHN K.S., CHO B., PARK H.D., 1999. "Photoluminescence Behavior of Manganese-Doped Zinc Silicate Phosphors". *J. Am. Ceram. Soc.,* **82**, 2779–2784.

TKACHENKO N.V., 2006. "Optical Spectroscopy". Amsterdam: Elsevier Science & Technology.

TOWNSEND P.D., LUFF B.J., 1994. "High Sensitivity Spectral Measurements". *Radiation Measurements*, **23**, 517.

VIJ, D.R., SINGH, N., 1997. "Thermoluminescence Dosimetric Properties of Beryllium Oxide". *Journal of materials.* **32,** 2791-2796.

YEN W.M., SHIONOYA S., YAMAMOTO H., 2007. "Phosphor Handbook 2nd edition". Boca Raton, FL: CRC Press/ Taylor and Franchis.

YUKIHARA, E.G., McKEEVER, S.W.S., 2006. "Spectroscopy and Optically Stimulated Luminescence of Al_2O_3:C using Time-Resolved Measurements". *J. Appl. Phys*. **100**, 083512.

ZACH R., 2004. "Color Stabilization of RGB LEDs in an LED Backlighting Example – Application Note". Opto Semiconductors, OSRAM. Retrieved from http://catalog.osramos.com/catalogue/catalogue.do?act=showBookmark&favOid=00000000000028b00010023. Last accessed on, 12.04.2011.

ZHENGUO J., KUN L., YONGLIANG S., ZHIZHEN Y., 2003. "Fabrication and Characterization of Mn-doped Zinc Silicate Films on Silicon Wafer". *Journal of Crystal Growth*, **255**, 353-356.

APPENDIX A

THE ELECTRONIC CONTROL UNIT

The electronic control unit is the heart of the LE-282. It carries the hardware and the firmware to control the monochromator and create necessary timing signals for data collection. The control unit is basically built around a microcontroller PIC 18F4550, stepper motor drivers and the necessary hardware around it. In this part wiring diagrams of electronic control unit are presented. All figures which are shown below correspond to different functions of electronic control unit of luminescence emission spectrometer (LE-282).

Figure A.1 shows the computer connection of 18F4550 with MAX232 board that is used to receive or transfer data from computer in accordance with RS-232 standard. All the control commands are passed via this interface.

Figure A.2 shows the input and output pins of bipolar motor driver unit using L298D (dual H-Bridge) chip and its wiring diagram related to connection with 18F4550 and bipolar motor (grating motor) on LE-282 and a DC voltage of 15V that is necessary to run the bipolar motor driver. The unit is connected to 15 V through two micro switches located at the mechanical limits of the grating drive mechanism (used as interlock) in order to shut down the power if the grating motor is out of control. Moreover 15V is dropped to 5V by a voltage divider network and also connected to RE0 pin of 18F4550. In addition, there is a relay placed in electronic control unit which is connected to the micro switches in parallel. If any of these switches is pushed, the power drop in RE0 pin is immediately enables the related interrupt routine in the firmware which then makes the relay switch closed and thus enables

back the power on bipolar motor driver unit and directs the grating to return back its home position by disabling the all previous processes.

A Darlington transistor array (ULN2803) is used to drive the unipolar motor of slit disk mounted on LE-282. Figure A.3 shows the wiring diagram of unipolar motor driver unit and its connection to 18F4550.

Figure A.4 shows the connection of optocouplers with 18F4550. As seen in Figure A.4, there are three optocouplers mounted on LE-282 which are controlled by 18F4550. Two of these optocouplers are used in control of grating motor. The third one is used for detecting the home position of the slit wheel.

Besides computer software, functions of luminescence measurement system are also monitored on a 2x16 character Liquid Crystal Display (LCD). Figure A.5 shows the related wiring diagram of LCD connection with 18F4550.

In DC measurement mode, which is used when measuring high luminescence signals, PMT output signal was conditioned by using a current to voltage converter and an amplifier with a gain of 50. Two operational amplifiers (OP-07) are used for this purpose. The amplified signal is transferred into ADC of 18F4550 where it was converted to digital signal. The related circuit diagram is shown in Figure A.6.

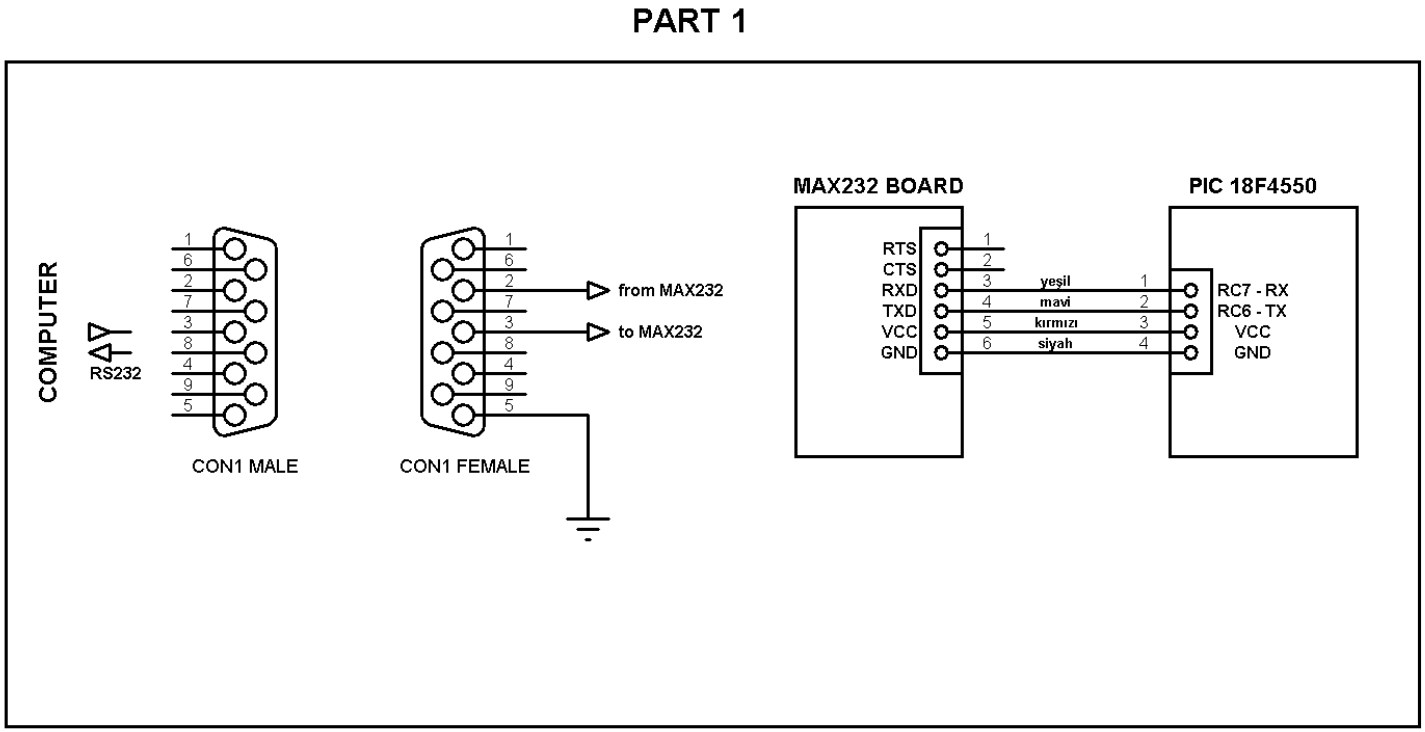

Figure A.1: Computer serial port and the related connection with 18F4550.

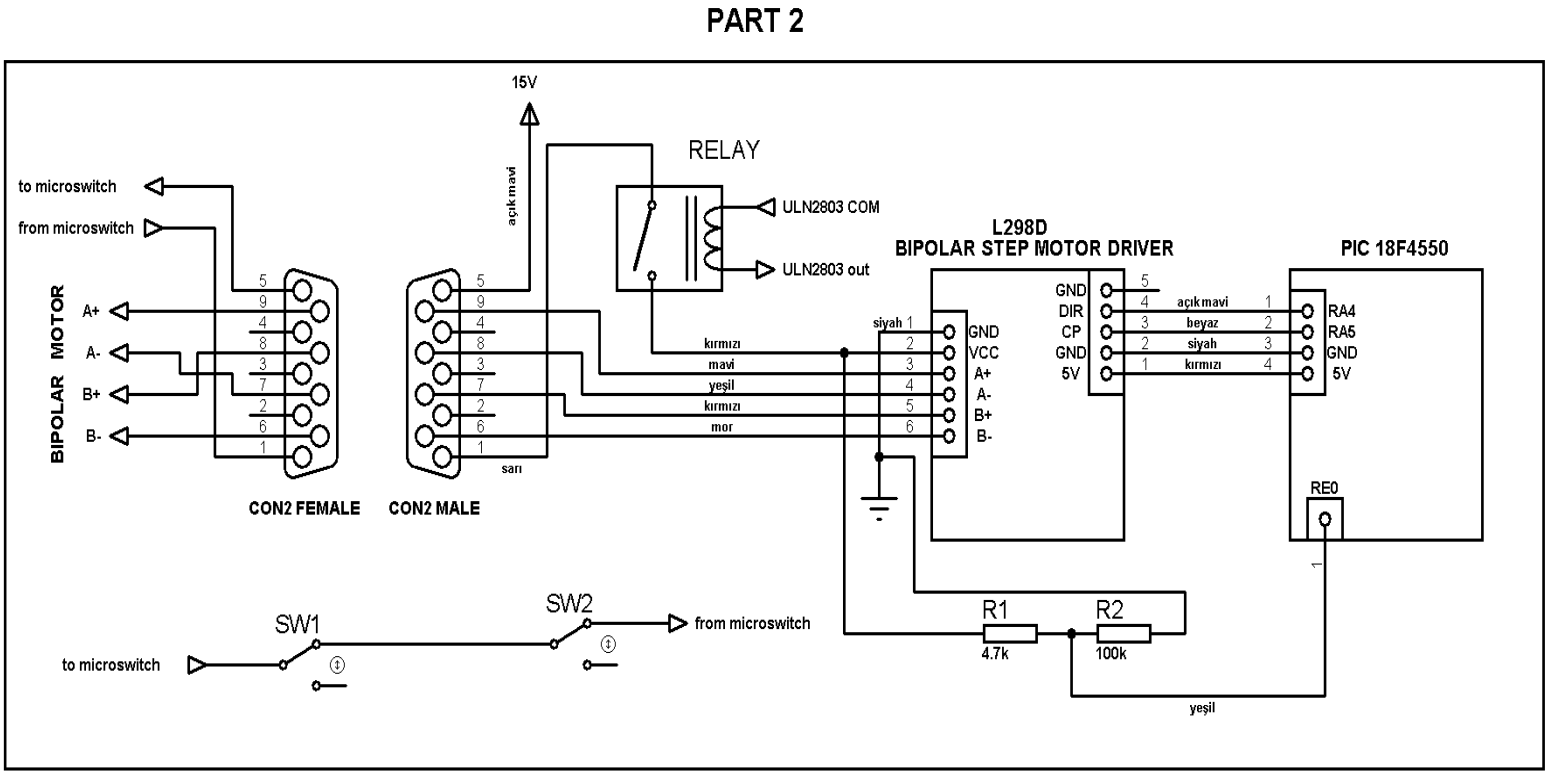

Figure A.2: Bipolar motor driver and its connection with 18F4550, relay, micro swithces and bipolar motor.

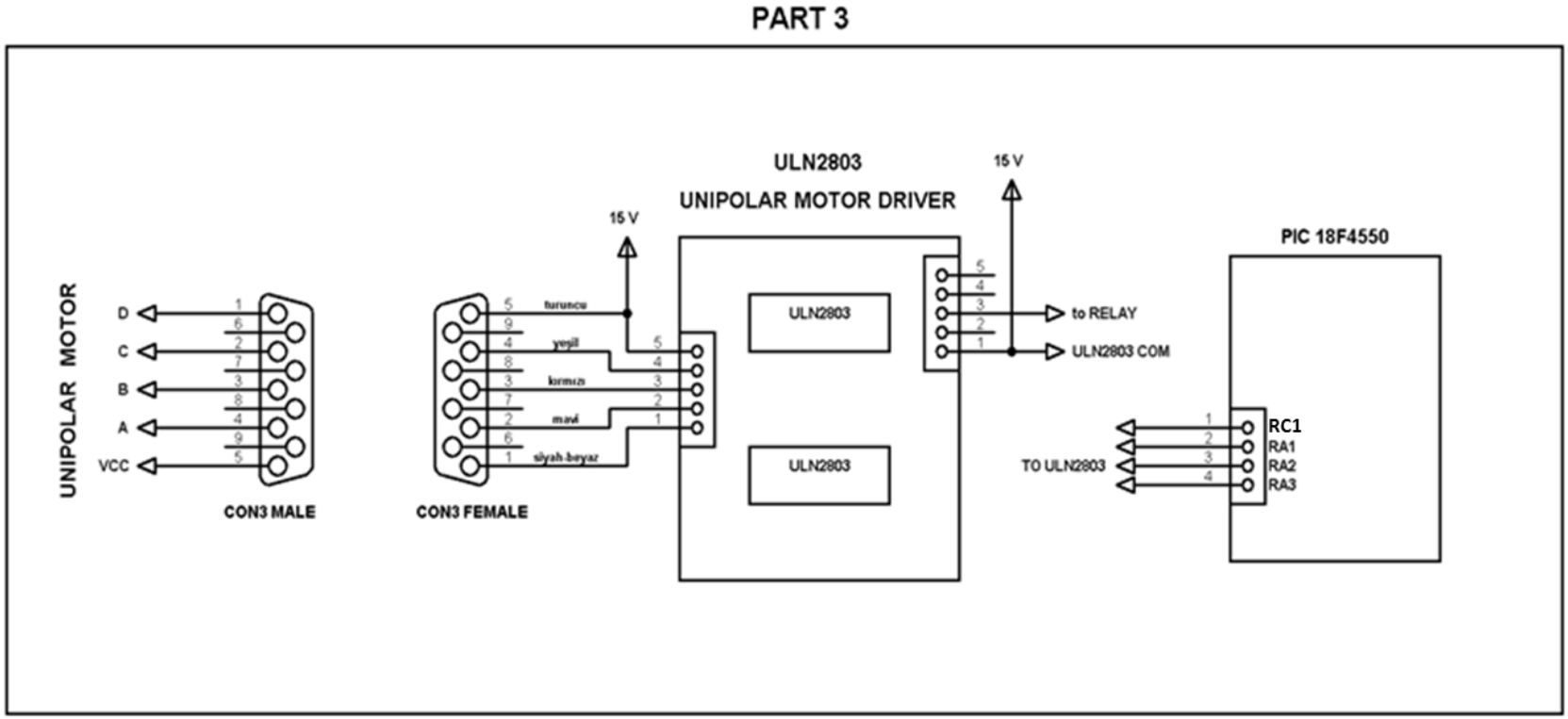

Figure A.3: Unipolar motor driver and its connection with 18F4550 and unipolar motor.

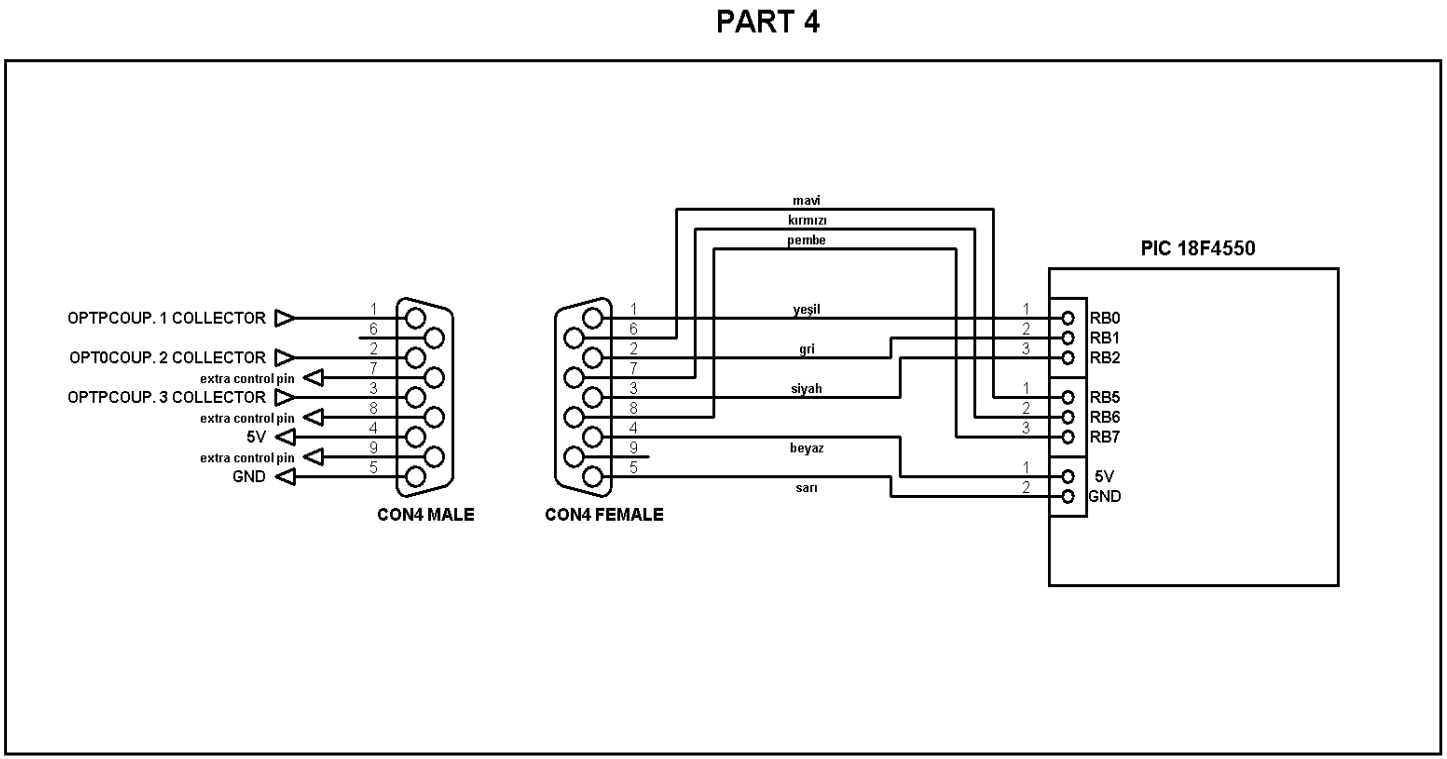

Figure A.4: Connection of optocouplers on LE-282 to 18F4550.

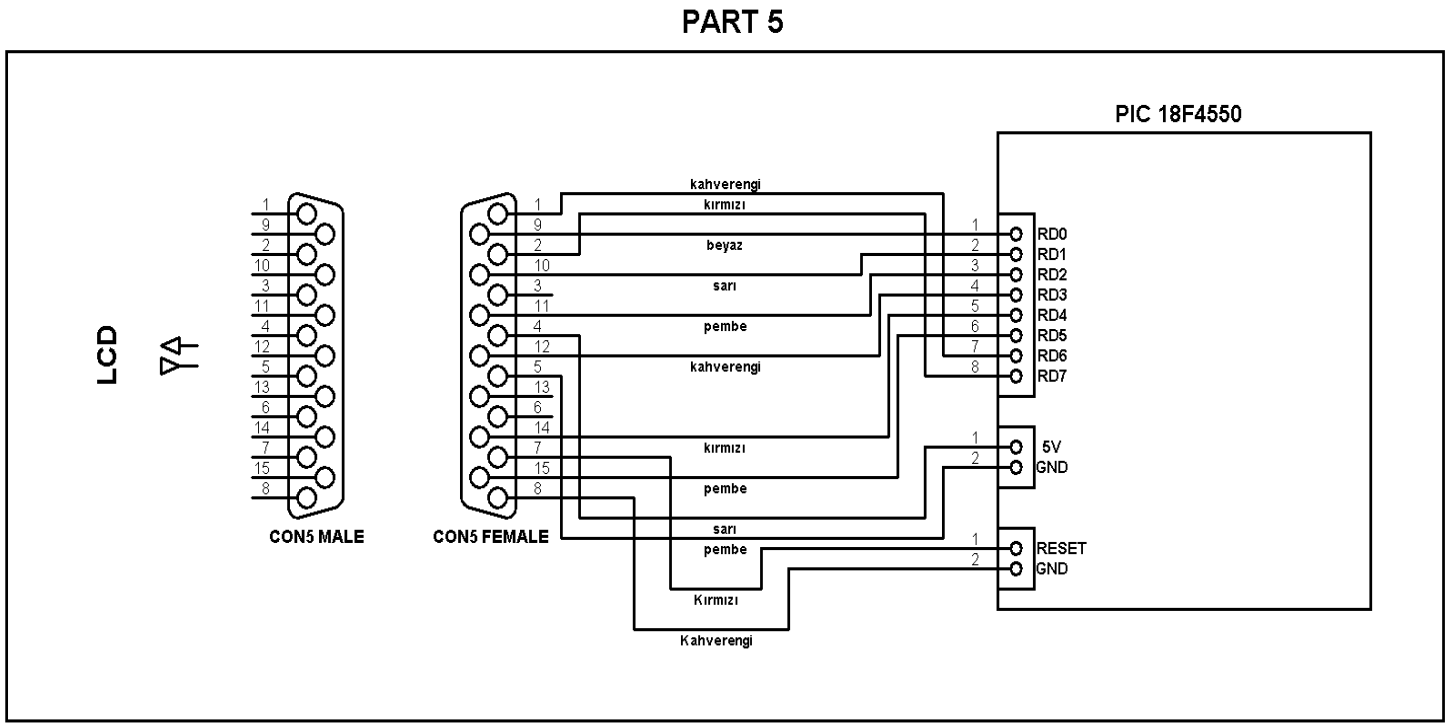

Figure A.5: Connection of LCD to 18F4550.

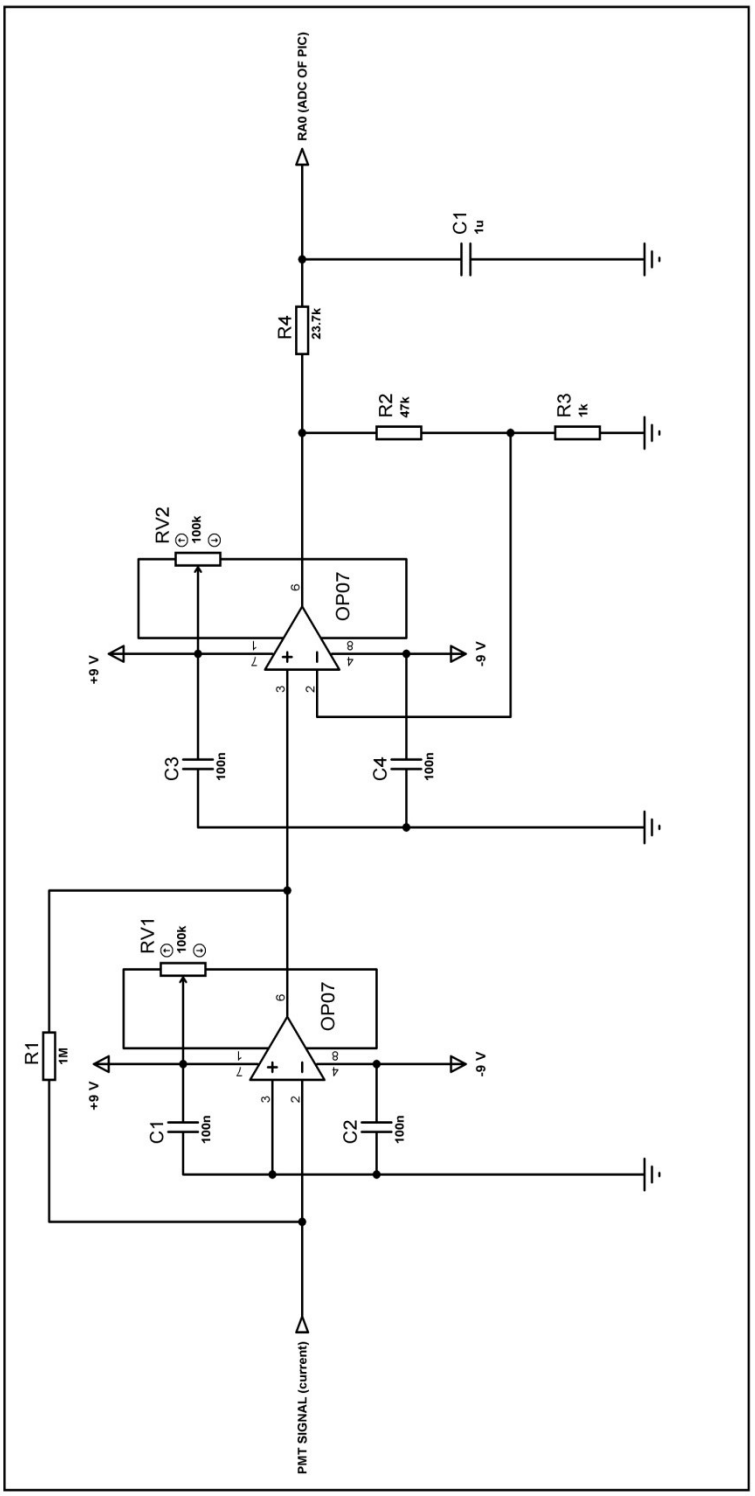

Figure A.6: PMT output signal amplifier circuit.

APPENDIX B

GENERAL VIEW OF THE LUMINESCENCE MEASUREMENT SYSTEM

In this section a general view of the luminescence emission spectrometer LE-282 and its components are given.

Figure B.1 shows the general view of the luminescence measurement system with all components and the computer interface.

Figure B.2 shows the internal view of Electronic Control Unit box with its components. However, 18V 1.5A DC power supply shown in the picture is no more used. 24V 4A power supply which is shown in Figure B.4 is used in place of it. Moreover, the related wiring diagrams of the components were given in Appendix A.

Top and side views (with the covers removed) of LE-282 are given in Figures B.3 and Figure B.4.

Calibration of the LE-282 and the PL experiments were performed using a light source which carries a halogen lamp (for the visible part) and a deuterium lamp (for the UV part). Although it was not mentioned in the text, such a light source was also constructed in the laboratory. For this purpose, a light source unit of an old spectrophotometer was used. This unit has a motor controlled spherical mirror to focus either deuterium or halogen lamp light to output port. This motor is controlled using a PIC 16F877A (Microchip) microcontroller. Lamp selection can be made either manually or using computer via RS-232 protocol.

In addition, the developed light source unit is a very comprehensive tool and thus suitable for use in many experiments. The related pictures of this unit are shown in Figure B.5 and Figure B.6. Moreover, as seen in Figure B.5, light source unit, sample holder, light collection unit and LE-282 are connected to each other via the sample holder and light collection optics.

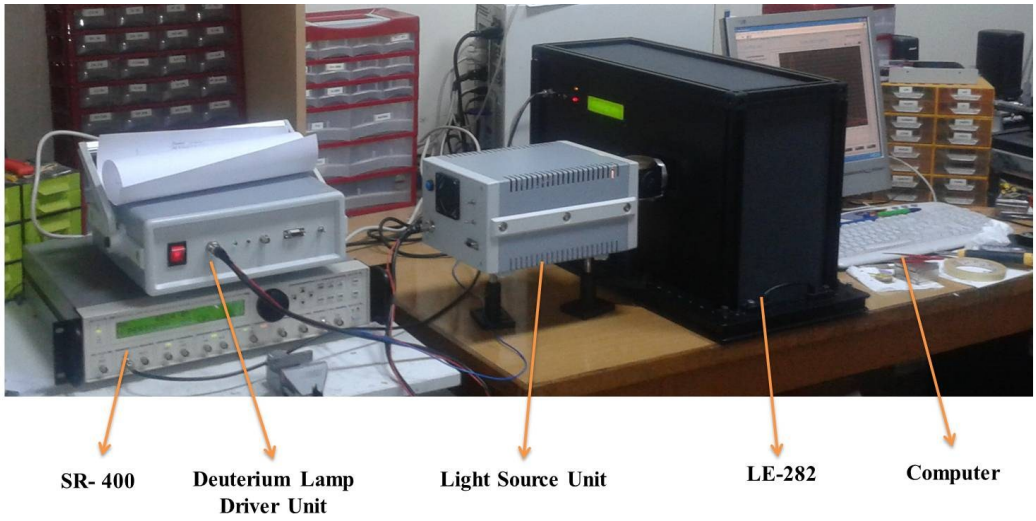

Figure B.1: General view of Luminescence Measurement System.

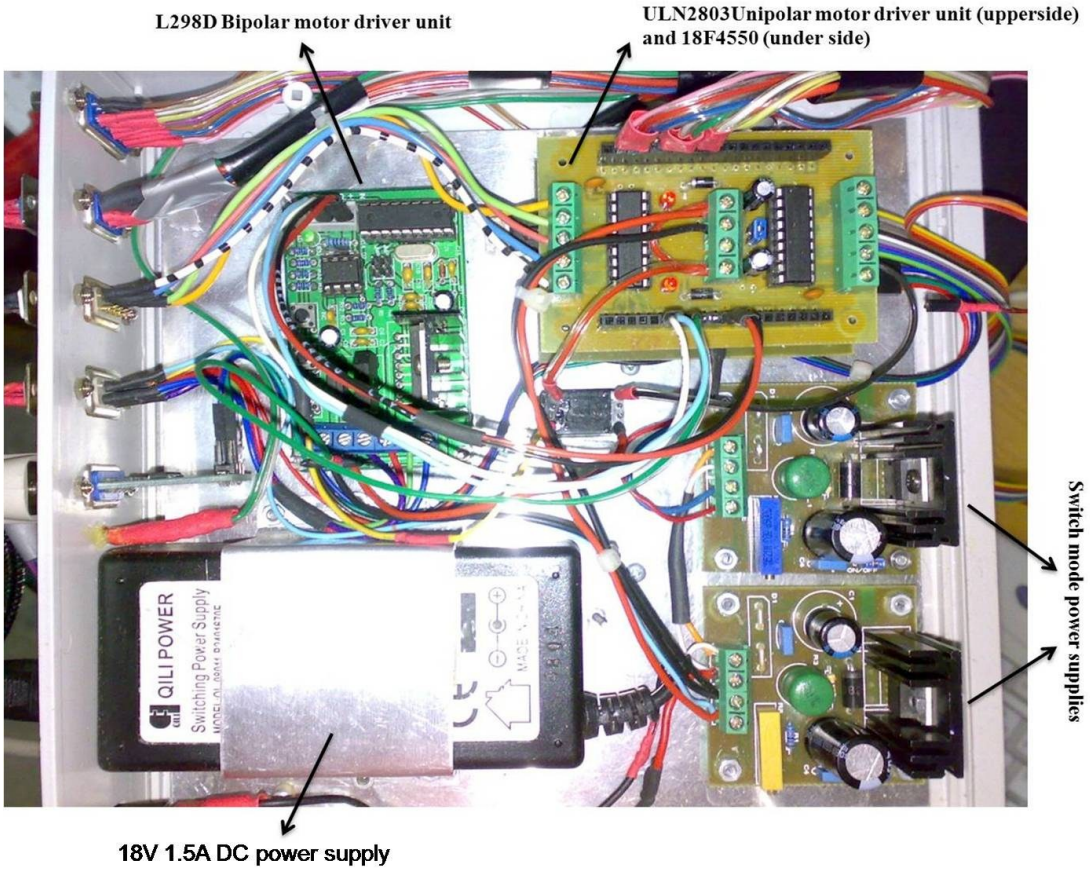

Figure B.2: Electronic Control Unit box. The main components are L298D Bipolar motor driver unit, ULN2803 Unipolar motor driver unit where pic 18F4550 is placed under it, switch mode power supplies. However, 18V 1.5A DC power supply shown in this picture is no more used. 24V 4A DC power supply is used in place of it.

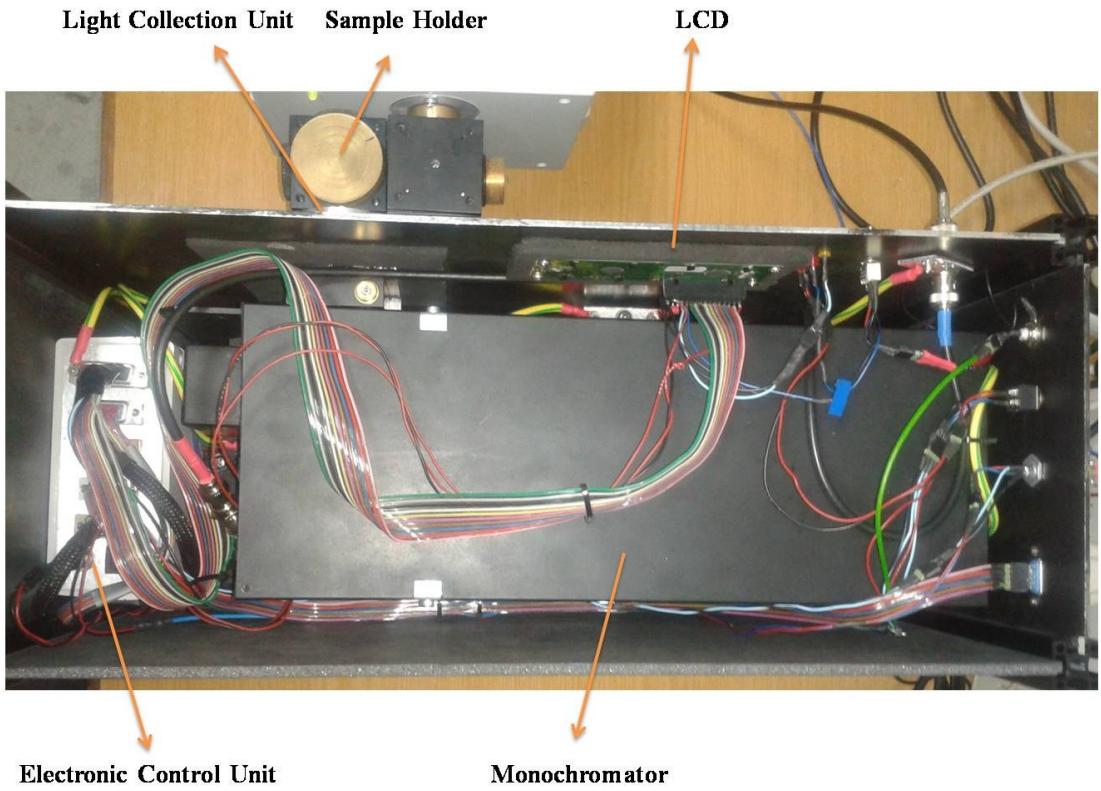

Figure B.3: Top view of LE-282. Electronic Control Unit, Light Collection Unit, Sample Holder, LCD and LE-282 are the components that can be seen from this view.

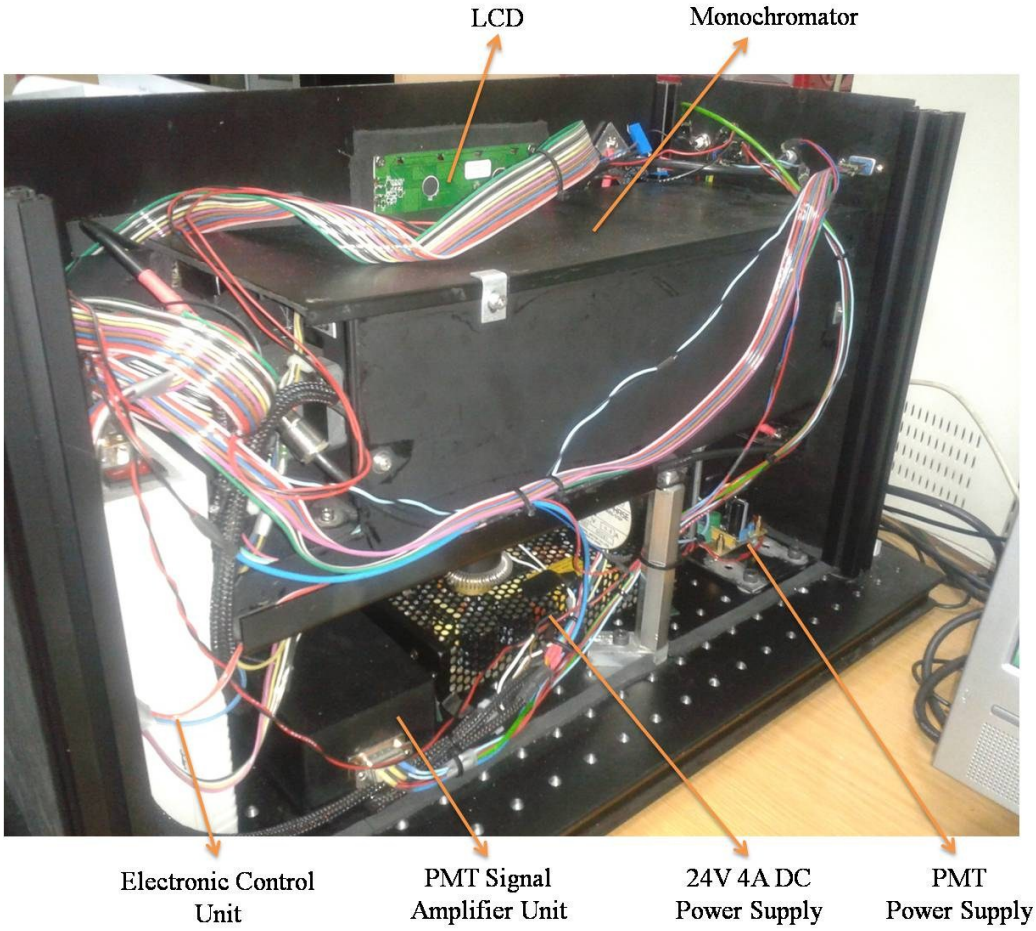

Figure B.4: Side view of LE-282. Electronic Control Unit, PMT Signal Amplifier Unit, LCD, 24V 4A DC Power Supply, PMT Power Supply and LE-282 are the components that can be seen from this view.

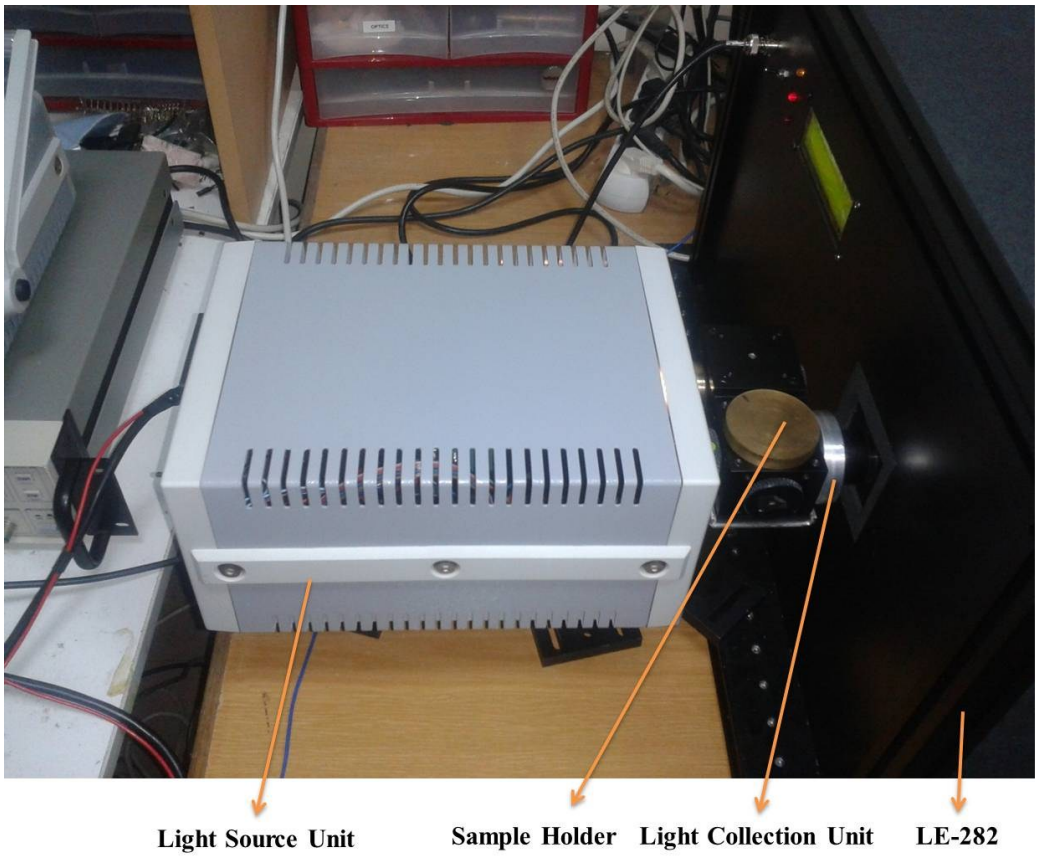

Figure B.5: Front view of LE-282 and Light Source Unit. They are connected to each other via the sample holder and light collection optics.

Figure B.6: The Light Source Unit and LE-282.